RH-12-2011

Dissertation for the degree of doctor of philosophy

# Holographic Models for Condensed Matter

Tobias Zingg


UNIVERSITY OF ICELAND

School of Engineering and Natural Sciences
Faculty of Physical Sciences
Reykjavík, September 2011

A dissertation presented to the University of Iceland, School of Engineering and Natural Sciences, in candidacy for the degree of doctor of philosophy

**Doctoral committee**

Prof. Lárus Thorlacius, advisor
University of Iceland and NORDITA (Nordic Institute for Theoretical Physics)

Prof. Þórður Jónsson
University of Iceland

Prof. Ragnar Sigurðsson
University of Iceland

**Opponents**

Assoc. Prof. Amanda W. Peet
University of Toronto

Assoc. Prof. Koenraad Schalm
Institute-Lorentz, University of Leiden

Holographic Models for Condensed Matter

Printed in Iceland by Háskólaprent
Science Institute Report RH-12-2011
ISBN 978-9979-9807-2-8

# Contents

# Abstract

Geometries with asymptotic Lifshitz scaling are conjectured to be duals to quantum critical systems that are invariant under anisotropic scaling. Black branes in these backgrounds obey standard thermodynamic relations which makes them suitable candidates to describe quantum critical physics at finite temperature. Several geometric and thermodynamic properties of these objects are investigated. A particularly intriguing result is that, by using a simple gravitational model, it is possible to qualitatively reproduce the behavior of the anomalous specific heat measured in certain heavy fermion alloys at critical doping. In the presence of a charged bulk scalar field, there is a phase transition to a superfluid condensate at low temperature, which was argued to be the stable ground state of these systems.

Electron stars can be thought of as charged fermionic siblings of neutron stars. These were conjectured as gravity duals of strongly interacting fermion systems. At finite temperature the electrons recede to form a cloud suspended over a black brane horizon. As temperature is raised, more and more charge is absorbed by the black brane. At a critical temperature, there is a third order phase transition to a configuration with just a charged black brane and no electron cloud. Transport properties of the system vary continuously over the whole temperature range.

# Ágrip (in Icelandic)

Tímarúm með Lifshitzskölun eru könnuð með þyngdarfræðilega lýsingu á fasabreytingum í huga. Varmafræði svarthola í slíku tímarúmi gefur innsýn í óvenjulega varmafræðilega eiginleika kerfa þar sem skammtafræðilegar fasabreytingar eiga sér stað. Mælingar sýna að ákveðnar málmblöndur þar sem virkur massi leiðnirafeinda er óvenju hár hafa hærri eðlisvarma en samræmist viðteknum fræðum um málma en í tiltölulega einföldum þyngdarfræðilíkönum með Lifshitzskölun má hinsvegar sjá sambærilega hegðun. Þyngdarfræðin lýsir jafnframt fasabreytingu yfir í ofurfljótandi ástand sem rök eru færð fyrir að sé stöðugt grunnástand kerfisins.

Einnig eru skoðaðar svonefndar rafeindastjörnur, sem eru lausnir á hreyfingarjöfnum rafhlaðins efnis í þyngdarfræði með neikvæðum heimsfasta, og könnuð nýleg tilgáta um að þær gefi þyngdarfræðilega lýsingu á rafeindakerfum þar sem víxlverkanir eru of sterkar til að hefðbundnum reikniaðferðum þéttefnisfræði verði við komið með góðu móti.

# Acknowledgements

First of all I would like to express my gratitude towards my advisor Lárus Thorlacius for his guidance, support and patience during the last four years.

My thanks also go to all with whom I successfully collaborated. Of those, I wish to attribute especial gratitude to my former fellow PhD student at the University of Iceland Erling Jóhann Brynjólfsson, as well as the NORDITA fellows Sean Nowling and Valentina Giangreco Marotta Puletti for many interesting and instructive discussions that helped me seeing things from new perspectives.

I also give special thanks to my doctoral committee, Ragnar Sigurðsson and Þórður Jónsson for all their work.

I acknowledge the hospitality at NORDITA, the Nordic Institute for Theoretical Physics, where I worked on my thesis since fall 2008.

This work was supported by the Eimskip Research Fund at the University of Iceland, the Icelandic Research Council and the Marie Curie Research Fund MRTN-CT-2004-005104.

Finally, I would like to express my gratitude to my family who have never ceased and probably never will cease showing me their support wherever I was heading and Katja Laura Seeliger who has been a perennial font of encouragement and delight ever since our paths intertwined.

# 1

# Introduction

Borrowing the term from optics, where a hologram denotes a picture that appears three-dimensional to the viewer, the holographic principle stands for the concept that a theory of quantum gravity on a space with a given dimension can be described by a field theory on a space with a lower number of dimensions. The origins of this concept of holography can be traced back to work pioneered in [1–5] where quantities like entropy and temperature were assigned to black holes in a way that the laws of thermodynamics could be extended to incorporate systems containing these exotic objects. A consequence of these definitions and considerations was the formulation of an entropy bound [6, 7]. To be more precise, it was found that the ratio of the entropy over the energy of a system must be bounded from above by an expression proportional to the radius of a sphere that encloses it. Furthermore, this bound happens to be saturated for the configuration of a single Schwarzschild black hole. If the entropy is interpreted as a measure of the number of microstates that give rise to the same macrostate, like it is in statistical mechanics or quantum theory, this has quite drastic consequences for any theory of quantum gravity. As a black hole represents the configuration with the highest possible energy density a gravitating system can have and the entropy of the aforementioned is proportional to the area of its horizon, the implication of the above mentioned bound is that the number of degrees of freedom of a quantum gravity system grows like the area of the surface containing it and not, as it would be intuitive for non-gravitating systems, like its volume. As such behavior would however be typical for a field theory defined on that hypersurface, the concept of the holographic principle was born. As mentioned above,

it states that the description of a volume of space is encoded on a boundary of the region.[1]

The cornucopia of ideas and interpretations that related the black hole entropy with microstates of quantum gravity theories like string theory or gave speculations how a dual field theory on a 'holographic screen' could be formulated are too multitudinous to be summarized here in detail. The publication that is essential for this thesis is [10], where a duality between certain types of M/string theories and superconformal Yang-Mills (SYM) theories was proposed. This marked the first explicit pairing of a theory of quantum gravity and a dual field theory on a 'holographic screen'. At the present day, this equivalence actually remains a conjecture and a thorough mathematical proof is still outstanding. Nevertheless, all investigations so far have just found arguments in favor of the validity of the duality between string theory on AdS spaces and conformal field theory. Furthermore, due to the rather explicit nature of the conjecture, it was possible to formulate a dictionary that allows to identify observables like correlation functions on both sides of the duality. This formulation is widely believed to also be valid in a more general setup, that is also for field theories that may not have Lorentz or conformal symmetry. By reversing the idea behind the holographic principle, i.e. instead of finding a field theory dual of a given quantum gravity theory, a quantum gravity theory is constructed that has a given gauge theory as dual, first attempts were made to apply the formalism of gauge/gravity to problems in condensed matter physics.

The new insights that may come from this are as follows. In condensed matter physics, field theories have proved to be a useful tool to describe the underlying processes in various systems. In many cases, however, correlation functions and other observables that give information about these systems are given by complicated expressions that can only be analyzed by Feynman rules and other perturbative methods. By construction, this approach is only applicable when the expansion parameter – which is often the strength of an interaction between fields – is small compared to other length scales in the system. Thus, a description of models that is governed by strong interaction is often beyond the range of accessibility of the prevalent methods in condensed matter physics. The gauge/gravity duality can shed new light on this because it provides a formalism that allows to map the task of finding correlation functions of strongly coupled fields to the analysis of initial and boundary value problems. These are still often enough highly non-trivial, but the mathematics behind them is well enough understood that it would allow, in theory, to use numerical methods to

[1] The first ideas were formulated in [8], for an overview see e.g. [9].

find the desired quantities up to the needed precision.

The content of this thesis is in the spirit of the last paragraph. It can be considered as a thought experiment that assumes the existence of a gauge/gravity duality and explores some uses of the formalism in the context of condensed matter physics. In section 2, some details about the dictionary between string theory on asymptotically AdS spacetimes and conformal field theories are summarized. Furthermore, it is described how this dictionary can be generalized in a way that allows it to be applied to more general class of spacetimes than AdS-like geometries. Section 3 gives a short introduction to quantum critical phenomena. These are rather novel features that were observed in experiments on various materials, particularly metal alloys, over the last decades that are not in accord with predictions from standard models in condensed matter physics like Landau Fermi liquids. So far, it has proved difficult to model the underlying physical processes of quantum critical materials with ordinary field theoretical methods. A conjectured gravitational dual to these systems are Lifshitz geometries which are introduced in section 4. Contrary to AdS geometries which lead to conformal scaling, Lifshitz geometries incorporate an anisotropic scaling between spacelike and timelike coordinates which is a more realistic scenario at a critical point. Finally, in section 5 so-called electron stars are investigated. These are solutions to the Einstein equations coupled to a fluid of fermions which are claimed to be dual to systems of strongly coupled fermions, where an approach by the current tools in field theory also poses a challenge in condensed matter physics.

The thesis is based on five research articles,

I *Holographic Superconductors with Lifshitz Scaling* by E.J. Brynjolfsson, U.H. Danielsson, L. Thorlacius and T. Zingg, published in the Journal of Physics A, volume 43 (2010),

II *Black Hole Thermodynamics and Heavy Fermion Metals* by E.J. Brynjolfsson, U.H. Danielsson, L. Thorlacius and T. Zingg, published in the Journal of High Energy Physics, volume 8 (2010),

III *Holographic models with anisotropic scaling* by E.J. Brynjolfsson, U.H. Danielsson, L. Thorlacius and T. Zingg, accepted for publication in Journal of Physics : Conference Series – *"6th International Symposium on Quantum Theory and Symmetries"* at the University of Kentucky, July 20 - 25, 2009,

IV *Holographic metals at finite temperature* by V.G.M. Puletti, S. Nowling, L. Thorlacius and T. Zingg, published in the Journal of High Energy Physics, volume 1 (2011),

V *Thermodynamics of Dyonic Lifshitz Black Holes* by T. Zingg, accepted for publication in the Journal of High Energy Physics in August 2011.

The results appearing in each of these papers are summarized in sections 4 and 5. The articles are attached at the end of the thesis with copyright permission from JHEP and IOP publishing.

# 2

# The gauge/gravity correspondence

This chapter gives a brief introduction to the conjectured AdS/CFT duality and an outline of the more general gauge/gravity correspondence. The approach chosen here is rather pragmatic and bottom-up, meaning that the emphasis is more on introducing the formalism used to make explicit calculations and less on how these concepts could be embedded into a string-theoretical framework or derived from first principles.

## 2.1 From AdS/CFT to AdS/CMT

The original conjecture of the AdS/CFT equivalence was made in [10] and has since spurred an overwhelming quantity of research exploring various aspects of this topic and also provided checks of its predictions – see e.g. [11] for a comprehensive overview.

The statement that is essential to this thesis is that a string theory on $\mathrm{AdS}_{d+1} \times Y$, where $Y$ is a $9-d$ dimensional manifold, is dual to a conformal field theory (CFT) on the boundary of $\mathrm{AdS}_{d+1}$ such that

$$\mathcal{Z}_{string} = \mathcal{Z}_{CFT} \ , \tag{2.1}$$

where $\mathcal{Z}$ denotes the partition function. The best studied example is type IIB string theory on $\mathrm{AdS}_5 \times \mathrm{S}^5$ which is dual to $\mathcal{N} = 4$ superconformal Yang-Mills (SYM) theory

with gauge group $SU(N)$. The parameters of these two theories are related by

$$4\pi g_s = g_{YM}^2 = \frac{\lambda}{N} \,, \tag{2.2}$$

$$\frac{R_{\mathrm{S}^5}^4}{l_s^4} = \frac{R_{\mathrm{AdS}_5}^4}{l_s^4} = 4\pi\lambda \,. \tag{2.3}$$

What makes these relations intriguing is that the regime $g_{YM} \ll 1$ and $\lambda \gg 1$ in SYM theory, which lies at the opposite end of $\lambda \ll 1$ where perturbation theory is applicable, corresponds to a string theory with $g_s \ll 1$ and a string length scale $l_s \ll R_{\mathrm{AdS}_5}$, which is exactly the regime where stringy effects are small and the theory reduces to supergravity. In this limit, the string partition function $\mathcal{Z}_{string}$ can be approximated by the value at the saddle point which is given by $\mathcal{S}_{sugra}$, the effective on-shell supergravity action,

$$\mathcal{Z}_{string} \simeq e^{-i\mathcal{S}_{sugra}} \,. \tag{2.4}$$

The significance of this relation becomes more clear when the definition of the generating functional for connected correlators $\mathcal{W}$ is recalled.[1] This functional has the property that the correlation function for given operators $\mathcal{O}_1, \ldots, \mathcal{O}_m$ with sources $J_1, \ldots, J_m$ is given by

$$\langle \mathcal{O}_1(x_1) \cdots \mathcal{O}_m(x_m) \rangle = (-i)^{m+1} \left. \frac{\delta^m W}{\delta J_1(x_1) \cdots \delta J_m(x_m)} \right|_{J=0} \,. \tag{2.5}$$

In particular, $\mathcal{Z} = e^{-i\mathcal{W}}$. Thus, from (2.1) and (2.4) follows

$$\mathcal{S}_{sugra} \simeq \mathcal{W} \,. \tag{2.6}$$

What has been suppressed in the formula above is how the sources in $\mathcal{W}$ enter $\mathcal{S}_{sugra}$, respectively $\mathcal{Z}_{string}$. This has been postulated as follows. If $\Phi$ is a field in the supergravity, respectively string theory, then it sources an operator $\mathcal{O}$ in the dual field theory through its boundary value, more precisely through $\phi^{(0)}$ defined as

$$\phi^{(0)} = \lim_{r \longrightarrow 0} r^{\kappa} \Phi \,, \tag{2.7}$$

where $r$ is a function that has a simple zero at the AdS boundary. The value of $\kappa$ is on the gravity side given by an expression that depends on mass $m$ and the spin of

[1] See any textbook about field theory, e.g. [12]

the field $\Phi$ and on the field theory side, $\kappa$ is related to the conformal dimension $\Delta$ of $\mathcal{O}$. For example, if $\Phi$ were a $p$-form on a $d+1$ dimensional asymptotically AdS manifold, these relations would be given by

$$m^2 = \kappa(\kappa + d) \,, \tag{2.8}$$

$$\Delta = d - p + \kappa \,. \tag{2.9}$$

Furthermore, if $g$ denotes the metric on this manifold, then a metric on the boundary can be assigned through

$$g^{(0)} = \lim_{r\to 0} r^2 g \,. \tag{2.10}$$

This is a result that was already established before the AdS/CFT conjecture in mathematics [13], when the concept of conformally compact spaces, which in physics correspond to asymptotically AdS spaces, was introduced. The name refers to the space being compactified by the addition of a boundary at infinity. Actually, on this boundary there exists not a uniquely defined metric but rather a conformal class of metrics, as any function $e^w r$ could be used in (2.10). Together with (2.7) this illustrates how the conformal invariance in the boundary field theory emerges [14].

The identification (2.6) also allows to explicitly calculate correlation functions [14–16] in the dual theory. Assuming the fields $\Phi_i$ have a standard kinetic term in the action $\mathcal{S}_{sugra}$ and no higher derivatives occur,

$$\langle \mathcal{O}_i \rangle \longleftrightarrow \Pi_i \,, \tag{2.11}$$

$$\langle \mathcal{O}_i \mathcal{O}_j \rangle \longleftrightarrow G_{ij} \,, \tag{2.12}$$

where $\Pi_i = *^{-1} \frac{\delta \mathcal{S}_{sugra}}{\delta \mathfrak{L}_n \Phi_i}$ denotes the conjugate momentum with respect to the normal derivative $\mathfrak{L}_n$ on the boundary and $G_{ij}$ stands for the bulk to boundary Green's function for the fields $\Phi_i$ and $\Phi_j$. Which Green's function, i.e. retarded or advanced, depends on the behavior of the field in the bulk, that is whether they describe ingoing or outgoing modes [16]. General $n$-point functions could also be calculated using (2.6), though they will depend on a more specific knowledge of the bulk interactions and are not as generic as one- or two-point functions. The stress-energy tensor of the dual field theory is sourced by the boundary metric (2.10) and therefore

$$\langle T_{\mu\nu} \rangle \longleftrightarrow \frac{\delta \mathcal{S}_{sugra}}{\delta g^{\mu\nu}} \,. \tag{2.13}$$

Similar to Green's functions of fields, the stress-energy tensor is determined by con-

ditions on the behavior of its source in the bulk. The metric $g_{\mu\nu}$ is assumed to either be regular or to have a black hole singularity that is enclosed by an event horizon. A temperature can be associated to the spacetime – and thus to the dual field theory – by Wick-rotating the time-coordinate and making it periodic such that the resulting Euclidean metric is regular. The temperature is then given by the inverse period length and if it becomes infinite, the temperature vanishes. If the metric describes a black hole, this procedure results in its Hawking temperature, i.e. the surface gravity on the event horizon.

What has been omitted in this section to avoid cluttering notation is that the identifications are again made after taking a limit in the same fashion as (2.7). Another issue is that the relations outlined here might need to be modified slightly to cancel divergences that can occur. This will be addressed later in section 2.4. Another issue that has not been addressed is that there could be more than one classical saddle point, in which case there needed to be a sum over multiple classical solution on the right hand side of (2.4). This means that a certain classical solution would not completely describe dual theory but just a certain phase of it. As the aim of this thesis is not to analyze the full phase diagram of a given field theory but to develop on certain models, this kind of phase transition will not be included in further considerations.

At first sight, the AdS/CFT duality seems a way to use the powerful methods developed in conformal field theory to obtain novel results in string theory, where it often can be difficult to make explicit calculations due to the sheer complexity of the theory. What however was realized soon thereafter was that by reversing the way of using the duality, AdS/CFT could also be used to get insight to issues in condensed matter physics that are difficult to address using standard tools of quantum field theory. Comprehensive reviews about the application of AdS/CFT duality for condensed matter physics, which nowadays is often referred to as the AdS/CMT correspondence, can be found in [17–20], an outline of this idea is as follows.

In field theory, the generating functional $\mathcal{W}$ is defined via a functional integral, often also called a Feynman integral. The understanding of these objects is not as far developed as integrals over finite-dimensional spaces, where they can be understood by the theory of the Lebesgue measure [21]. As a matter of fact, Feynman integrals are not even introduced by defining a measure on a functional space but by the definition of an integrator[2] that assigns a value to Gaussian integrals. In field theory, the standard action of a free field is of that type. A general action can then be analyzed by expanding in the couplings of the fields and using perturbative methods.

[2]See e.g. [22] for a mathematical treatment of this.

This also leads to a quite compact and useful formalism to derive Feynman rules. Though there are exceptions, like the spectrum of chiral primary operators that do not change as the coupling varies and have actually been used to check the AdS/CFT correspondence, most quantities depend rather strongly on the value of the coupling and a perturbative approach can in general not be expected to give useful results for strong coupling. This is an issue that has made it difficult to get an understanding of phenomena that involve strong interaction by using conventional field theoretical methods. What could shed new light on this is that for $\lambda \gg 1$, i.e. in the regime of strong interaction, the relation (2.6) holds. This allows to map the problem of calculating correlation functions via a complicated functional integral to the analysis of partial differential equations as (2.11) and (2.12) show. This is of course not a trivial task and explicit solutions are also sparse here, so obtaining an analytic result might be similarly difficult. Contrary to Feynman integrals, however, there exist powerful numerical algorithms to calculate approximate solutions to a partial differential equations up to any desired precision, and in applied physics this is often all that is needed to compare with experimental data.

## 2.2 The boundary of AdS space from a functional analytic point of view

In the original formulation of the AdS/CFT conjecture, the boundary of AdS space has a nice geometric interpretation as an object where the isometry group SO(2,$d$) of $\mathrm{AdS}_{d+1}$ acts as the conformal group. This is however very specific to AdS spaces and does not make obvious how a holographic screen for a more general class of spaces could be constructed. In order to get a notion that does not explicitly refer to the geometry of the space, the boundary will now be examined from a more functional analytic point of view. Therefore, the concept of a characteristic surface will be introduced briefly. A thorough treatment about this can be found in textbooks dealing with partial differential equations like [23, 24].

As an illustrative example a standard hyperbolic problem, the wave equation,

$$\Box y = 0 \,, \tag{2.14}$$

shall be considered. It should however be kept in mind that by means of the Cauchy-Kovalevskaya theorem and Holmgren's theorem the features that are introduced in the following are valid for a much more general class of partial differential equations.

With certain assumptions made about the metric coefficients, this even includes the Einstein equations.

In the context of PDEs, (2.14) itself is not the way in which the problem is posed. A standard formulation would be to consider a manifold $M$ and a submanifold $\chi \subset M$ with normal $n$ and considering the solution to

$$\begin{cases} \Box y &= 0 & \text{on} \quad M\,, \\ y &= y^{(0)} & \text{on} \quad \chi\,, \\ \mathfrak{L}_n y &= \eta^{(0)} & \text{on} \quad \chi\,. \end{cases} \tag{2.15}$$

The manifold $\chi$ is called a characteristic surface if prescribed boundary conditions $y^{(0)}$ and $\eta^{(0)}$ determine the solution $y$. If $\chi$ has a timelike normal vector field, (2.15) is often referred to as initial value problem and as boundary value problem if $\chi$ has a spacelike normal vector field.

In the case of the manifold being AdS, i.e. if the metric on $M$ was given by

$$ds^2 = -(1+r^2)dt^2 + r^2\Omega_{d-1} + \frac{dr^2}{1+r^2}\,, \tag{2.16}$$

with $\Omega_{d-1}$ denoting the metric on $\mathcal{S}^{d-1}$, it turns out that a characteristic surface cannot be timelike. This is illustrated in figure 2.1. The solution is determined in the region consisting of all lightlike geodesics emanating from $\chi$. Choosing initial data on a surface $t = const$, indicated by the green line in figure 2.1(a), will thus only determine the solution in the green shaded region which does not cover the whole space. It is however possible to prescribe initial data on a surface with $r = const$, indicated by the vertical blue line in 2.1(b), and this would determine the solution on the whole of AdS.

In boundary value problems on spaces with a radial coordinate $r$ it often turns out that the equation (2.14), when just regarded as an equation in $r$, is of Fuchsian type [25, 26] and has singularities at $r = 0$ and $r \longrightarrow \infty$. In fact, singularities can also occur at a finite value of $r$ if there is a caustic like an event horizon. For metric functions this would not be such a grave issue, as for many applications the metric is anyway assumed to have a black hole singularity that is hidden behind a horizon. For fields that are assumed to propagate on the background given by a metric, however,

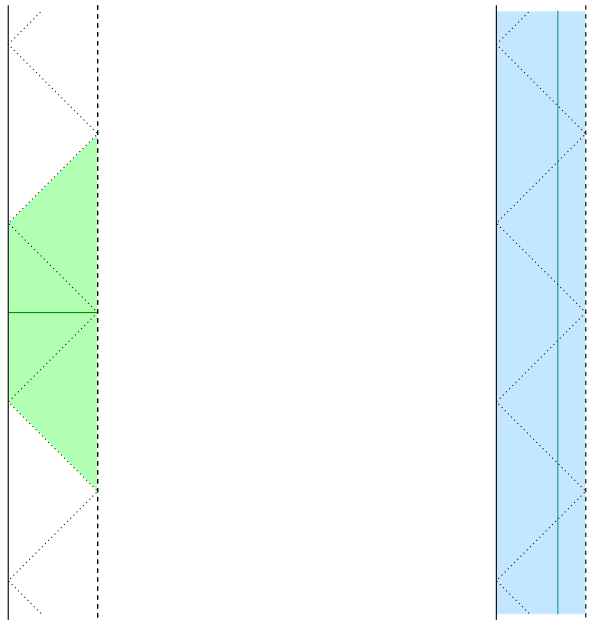


**Figure 2.1:** Penrose diagram of AdS space. Time $t$ is on the vertical axis and extends to infinity in each direction, the radial direction $r$ extends horizontally, between $r = 0$ represented by the solid vertical line and the AdS boundary at the dashed line. Each indicated triangular region corresponds to a patch that is conformal to Minkowski space. The horizontal green line in (a) is a surface $t = const$, boundary data prescribed here just determine the solution in the green shaded area. The vertical blue line in (b) is a surface with $r = const$. This is a characteristic surface as boundary data prescribed here determine the solution on the whole space.

it is often favorable to not pose the problem as in (2.15) but

$$\begin{cases} \Box y = 0 & \text{on} \quad M\,, \\ y = y^{(0)} \quad \text{or} \quad \mathfrak{L}_n y = \eta^{(0)} & \text{on} \quad \chi\,, \\ \lim\limits_{r\to r_s} f(r)(\partial_t - g(r)\partial_r)y = 0 & . \end{cases} \tag{2.17}$$

Here, either Dirichlet or Neumann boundary conditions are imposed – though also a mixed condition would be possible – and to make up for the missing second condition that determines a unique solution, a so-called radiation condition like in the last line of (2.17) is imposed. Depending on the sign of $g(r)$, this condition demands the solution to look like an ingoing or outgoing wave when approaching a singular point $r_s$. It is a boundary value problem along these lines, that serves as means to calculate

a holographic greens function as described in the previous section.

To summarize, the boundary of AdS can be considered as a characteristic surface that has been moved to spatial infinity. As the boundary is at a singular point with regard to the radial direction, some subtleties must be taken into account when taking this limit to obtain a well posed problem. This leads to the introduction of a scaling factor as in (2.7) and (2.10).

## 2.3 Outline of the gauge-gravity duality

A schematic idea of gauge-gravity duality can now be formulated by basically taking the terminology introduced in subsection 2.2 and leaving away any reference to the geometry of AdS space. It should be reminded that this section gives a summary of the basic idea of how fields and their conjugate momenta are translated to source and response in the dual field theory from a bottom up approach. This means that the focus is on presenting the formalism that is actually used to compute explicit expressions in the field theory from a gravitational dual, which is the subject of this thesis, whereas for details about the ideas on how this formalism can be derived from first principles or embedded into the framework of string theory it will be referred to the extensive literature on this subject – see e.g. [27, 28] and references therein.

Consider an action $\mathcal{S}_{cl}[\Phi] = \int_M \mathcal{L}[d\Phi, \Phi]$, where $\Phi = (e_A, \phi_i)$ stands collectively for a semi-orthonormal basis[3] $e_A$ and all other fields $\phi_i$ on some manifold $M$. Assume that there exists a submanifold $\chi \subset M$ with normal $n$ such that the problem of finding the classical solution,

$$\begin{cases} D_\Phi \mathcal{S} & = & 0 & \text{on} & M\,, \\ \Phi & = & \Phi^{(0)} & \text{on} & \chi\,, \\ *^{-1}\frac{\partial \mathcal{L}}{\partial(\mathfrak{L}_n \Phi)} & = & \Pi_\Phi = \Pi^{(0)} & \text{on} & \chi\,, \end{cases} \tag{2.18}$$

is well-posed, i.e. $\chi$ is a characteristic surface for (2.18). Take $\mathfrak{j}_i^{(0)} \subset \{\phi_i^{(0)}, \pi_i^{(0)}\}$ to be a set that contains half of the boundary values for the fields, denote by $\mathfrak{r}_i^{(0)}$ the other half and assume further that $\mathcal{S}_{cl}$ is an effective action resulting from taking the classical limit of a string theory – or any other theory of quantum gravity for that matter – with partition function $\mathcal{Z} = \mathcal{Z}[\mathfrak{j}_i^{(0)}]$. Then there exists a dual field theory

[3] The metric is given by $g_{\mu\nu} = \eta^{AB} e_{A\mu} e_{B\nu}$. Choosing to use $e_A$ instead of $g_{\mu\nu}$ is because the dual field theory is in general not expected to have Lorentz symmetry and it might be more convenient to use a formulation where certain directions can be treated separately – like the timelike $e_0$ in the Lifshitz model (cf. paper V) that is subject to a different scaling condition than spacelike directions.

defined on $\chi$ with partition function $\mathcal{Z}_{FT}$ such that

$$\mathcal{Z}[e_A^{(0)}, \mathfrak{j}_i^{(0)}] = \mathcal{Z}_{FT}[e_A^{(0)}, \mathfrak{j}_i^{(0)}] = e^{-iW[e_A^{(0)}, \mathfrak{j}_i^{(0)}]} , \tag{2.19}$$

where $\mathfrak{j}_i^{(0)}$ are interpreted as sources for operators $\mathcal{O}_i$. In the classical limit,

$$\mathcal{S}_{cl}[e_A^{(0)}, \mathfrak{j}_i^{(0)}] = W[e_A^{(0)}, \mathfrak{j}_i^{(0)}] , \tag{2.20}$$

where, by abuse of notation, $\mathcal{S}_{cl}[e_A^{(0)}, \mathfrak{j}_i^{(0)}]$ stands for the evaluation of $\mathcal{S}_{cl}$ on a solution of (2.18) that only has the boundary conditions imposed that are given by $e_A^{(0)}$ and $\mathfrak{j}_i^{(0)}$. As $W$ depends only on half of the boundary conditions, there must be constraints $C[\Phi_0, \Pi_0] = 0$. These come from replacing the missing half of boundary conditions (2.18) with conditions that impose regularity conditions on the global solution :

1. *The metric is either regular, or, if there exist singularities, they are enclosed by an event horizon.*

2. *Fields are subject to a radiation condition in the interior, respectively at the horizon.*

The surface gravity on the event horizon in condition 1. above determines the temperature in the dual field theory. The radiation condition 2. determines which Greens functions will be calculated in the dual field theory. The retarded (advanced) Greens functions $G_{ij}$ are obtained by demanding the fields to be regular for spacelike momenta and having an ingoing (outgoing) wave expansion for timelike momenta. The choice of $\mathfrak{j}_i^{(0)}$ determines the thermodynamic ensemble of the dual field theory and the scaling dimensions of the operators $\mathcal{O}_i$. Changing the choice of $\mathfrak{j}_i^{(0)}$ would correspond to a Legendre transformation. With this, in analogy to (2.11) and (2.12), one- and two-point functions are given by

$$\langle \mathcal{O}_i \rangle \quad \longleftrightarrow \quad \mathfrak{r}_i^{(0)} , \tag{2.21}$$

$$\langle \mathcal{O}_i \mathcal{O}_j \rangle \quad \longleftrightarrow \quad G_{ij} . \tag{2.22}$$

For similar reasons than for using a semi-orthonormal basis instead of a metric for a non-relativistic dual theory, it might also be more suitable to use a stress tensor complex, consisting of energy $\mathcal{E}$, energy flux $\mathcal{E}^j$, momentum $\mathcal{P}_A$ and spatial stress tensor $\Pi_A^j$, instead of a covariant stress-energy tensor. By defining the conjugate momenta $\tau_A = *^{-1}\eta_{AB}\frac{\partial \mathcal{L}}{\partial(\mathfrak{L}_n e_B)}$, setting $A = \{0, a\}$ and using $t$ to denote time in the

dual theory, relation (2.13) can then be rewritten as

$$\mathcal{E} \longleftrightarrow \tau_0(\partial_t)\,, \tag{2.23}$$

$$\mathcal{E}^j \longleftrightarrow \tau_0\Big|_{\partial_t^\perp}\,, \tag{2.24}$$

$$\mathcal{P}_A \longleftrightarrow \tau_A(\partial_t)\,, \tag{2.25}$$

$$\Pi^j_A \longleftrightarrow \tau_A\Big|_{\partial_t^\perp}\,. \tag{2.26}$$

As indicated earlier, the description above is rather schematic and leaves out several details. Like in the case of AdS, $e^{(0)}_A$, $\mathfrak{j}^{(0)}_i$ and $\mathfrak{r}^{(0)}_i$ on $\chi$ do not enter in the original form into the dual field theory but need to be rescaled, depending on the exact position of $\chi$ in $M$. Such things are however very specific to the particular model considered and cannot simply be written down in full generality. In fact, the ways in which a given manifold $M$ could be sliced, i.e. the ways in which $\chi$ could be embedded into $M$ are argued to be related to the renormalization group and/or field redefinitions in the dual field theory – see e.g. [29,30] for rather recent developments. For the purpose of this thesis, this will not be very relevant, as $\chi$ is always taken to be at spatial infinity and the rescaling will simply act to normalize the contributions which would diverge in this limit.

## 2.4 Holographic renormalization

In the considerations so far, a detail that has been omitted is the formulation of the action in way that it is well defined and finite on-shell. In many applications in physics this is not of special significance as the action is often just used as a formal tool to use a variational principle to obtain the equations of motion and the latter are actually the center of attention. To illustrate this, consider the Einstein-Hilbert action

$$\mathcal{S}_{EH} = -\int_M (R - 2\Lambda) v_M, \tag{2.27}$$

whose variation results in the Einstein equations. A solution of these equations must obey $R = \frac{2D}{D-2}\Lambda$ on a $D$-dimensional Manifold $M$, but when evaluating (2.27) on-shell, the integral would diverge if $M$ contained a non-compact direction. As general relativity is however defined by the Einstein equations and not directly by the evaluation of (2.27) itself, this is an issue of a merely formal nature. Contrary to this, in the application of the holographic dictionary the evaluation of the on-shell action

is an essential ingredient of the formalism and thus it is of utmost importance that divergent contributions to the action are cured. In physics, such a problem that an expression might actually be ill-defined and needs to be rewritten in a way that no divergences occur is not new and is often referred to by the euphemistic expression 'renormalization'. In the context of AdS/CFT, the redefinition of the action is known by the name holographic renormalization.[4] The procedure rather straightforward, but, as aptly worded in [32], becomes of 'forbidding complexity' when a higher number of dimensions or fields are involved. Thus, instead of presenting the procedure in full detail, this section is just devoted to give an outline of the concept of holographic renormalization.

The idea to make an ill-defined action $\mathcal{S} = \int \mathcal{L}$ finite on-shell can be traced back to an observation in classical mechanics. There it is well-known that an action $\mathcal{S}_\lambda = \int_M \mathcal{L}_\lambda$ with $\mathcal{L}_\lambda = \mathcal{L} - d\lambda$ would lead to the same equations of motion for any choice of $\lambda$. Hence, $\mathcal{S}$ can be considered as renormalized when $\lambda$ can be constructed such that $\mathcal{S}_\lambda$ is well-defined. To make more manifest which is the original Lagrangian that needs to be renormalized and which are the terms needed to make $\mathcal{S}$ well-defined, it is also possible – and done in practice – to write $\mathcal{S}_\lambda = \int_M \mathcal{L} - \int_{\partial M} \lambda$. The last term, $\int_{\partial M} \lambda$, is called the counterterm action. The complications in this procedure arise when constructing $\lambda$. In order to not interfere with the original setup, $\lambda$ should only depend on the fields that enter $\mathcal{L}$ and furthermore, the term $\int_{\partial M} \lambda$ should also preserve the symmetries of $\mathcal{S}$. In general, this construction is very hard to achieve unless an explicit solution of the equations of motion is known. It turns out, however, that an explicit form of $\lambda$ can be obtained by an iteration process that returns the final answer after a finite number of steps if $M$ is assumed to have a certain structure that can be outlined as follows. If there is a function $r$ such that all divergences in the metric and the fields occur as $r \longrightarrow 0$, then, in order to identify all divergences in $\mathcal{S}$ it might be sufficient to just know the solution up to a certain order in $r$. The details about this are of course very specific to the particular model considered. In the case of asymptotic AdS or Lifshitz spaces that are of relevance for this thesis, $r$ will be some kind of radial function that in a certain sense measures the distance to spatial infinity.

#### Example : scalar coupled to Einstein gravity

To illustrate the procedure of holographic renormalization and how a Legendre transformation changes the thermodynamic potential of the dual theory, the example of a

[4] For a comprehensive overview check [31] and references therein.

scalar field coupled to the Einstein theory of gravity is presented. The formal action is given by

$$\mathcal{S}^0 = -\int_M (R - 2\Lambda) v_M + \frac{1}{2}\int d\Phi \wedge *d\Phi + \frac{m^2}{2}\int \Phi^2 v_M \ , \tag{2.28}$$

where $v_M = *1$ denotes the volume form on the manifold $M$ and $\Phi$ is a scalar field. For concreteness, $\dim M = 4$ and $m^2 = -2$ is chosen, this means that the conformal dimension $\Delta_\Phi = 1$ and the cosmological constant $\Lambda = -3$. The equations of motion resulting from (2.28) are

$$R_{\mu\nu} - \frac{R}{2} g_{\mu\nu} + 3 g_{\mu\nu} = T^\Phi_{\mu\nu} \ , \tag{2.29}$$

$$\Box\Phi + 2\Phi = 0 \ , \tag{2.30}$$

where $T^\Phi_{\mu\nu}$ stands for the stress-energy tensor of the scalar field,

$$T^\Phi_{\mu\nu} = \frac{1}{2}\left( [d\Phi]_\mu [d\Phi]_\nu - \frac{1}{2}[d\Phi]^\kappa [d\Phi]_\kappa g_{\mu\nu} + \Phi^2 g_{\mu\nu} \right) \ . \tag{2.31}$$

The manifold $M$ is assumed to be asymptotically AdS, this allows to chose the parametrization of the metric as $ds^2 = \frac{1}{r^2}\left(dr^2 + g_{\mu\nu} dx^\mu dx^\nu\right)$ in the vicinity of spatial infinity which is located at $r = 0$. Plugging this into the equations of motion results in a power series expansion in $r$ for $g_{\mu\nu}$ and $\Phi$ after a longer calculation,

$$g_{\mu\nu} = g^{(0)}_{\mu\nu} + r^2 g^{(2)}_{\mu\nu} + r^3 \left( t^{(0)}_{\mu\nu} - \frac{2}{9}\phi^{(0)}\pi^{(0)} \right) + O(r^4) \ , \tag{2.32}$$

$$\Phi = r\phi^{(0)} + r^2 \pi^{(0)} + O(r^3) \ , \tag{2.33}$$

where the coefficients are subject to the relations

$$g^{(2)}_{\mu\nu} = -R[g^{(0)}]_{\mu\nu} + \frac{1}{8}\left( R[g^{(0)}] + \frac{1}{8}{\phi^{(0)}}^2 \right) g^{(0)}_{\mu\nu} \ , \tag{2.34}$$

$${t^{(0)}}^\kappa{}_\kappa = 0 \ . \tag{2.35}$$

In the above, ${g^{(0)}}^{\mu\nu}$ is used to raise indices, $R[g^{(0)}]_{\mu\nu}$ stands for the Ricci tensor of the metric $g^{(0)}_{\mu\nu}$ and $R[g^{(0)}] = R[g^{(0)}]^\kappa{}_\kappa$ for the corresponding Ricci scalar. Using this, it can be shown that the renormalized action,

$$\mathcal{S}^{ren} = \mathcal{S}^0 + \int_{\partial M} \left( 2K + 4 + R[\gamma] + \frac{1}{2} \right) v_{\partial M} \ , \tag{2.36}$$

where $K$ is the extrinsic curvature and $\gamma = \frac{g}{r^2}$ denotes the restriction of the metric to $\partial M$, is indeed finite on-shell. The holographic stress-energy tensor calculates to

$$\begin{aligned} \langle T^{\mu\nu} \rangle &= -\frac{2}{\sqrt{-\det g}} \frac{\delta \mathcal{S}^{ren}}{\delta g_{\mu\nu}} \\ &= 2K^{\mu\nu} + 2R[\gamma]^{\mu\nu} - \left( 2K + 4 + R[\gamma] + \frac{1}{2}\Phi^2 \right) g^{\mu\nu} \, . \end{aligned} \tag{2.37}$$

In a similar fashion, for the operator $\mathcal{O}_\Phi$ sourced by $\Phi$ follows

$$\begin{aligned} \langle \mathcal{O}_\Phi \rangle &= -\frac{1}{r^2\sqrt{-\det g}} \frac{\delta \mathcal{S}^{ren}}{\delta \Phi} \\ &= \frac{1}{r^2} \tilde{\Pi} \, , \end{aligned} \tag{2.38}$$

where $\tilde{\Pi} = \Pi_\Phi - \Phi$ is the renormalized conjugate momentum of $\Phi$. Thus, when $\partial M$ is moved towards spatial infinity,

$$\langle T_{\mu\nu} \rangle \overset{r\to 0}{\longrightarrow} 3t^{(0)}_{\mu\nu} + \frac{1}{3}\phi^{(0)}\pi^{(0)} g^{(0)}_{\mu\nu} \, , \tag{2.39}$$

$$\langle \mathcal{O}_\Phi \rangle \overset{r\to 0}{\longrightarrow} \pi^{(0)} \, . \tag{2.40}$$

In order to consider an ensemble with fixed $\delta\tilde{\Pi}$ instead of fixed $\delta\Phi$, the renormalized action must be changed to

$$\tilde{\mathcal{S}}^{ren} = \mathcal{S}^{ren} + \int_{\partial M} \tilde{\Pi}\, \Phi \, v_{\partial M} \, . \tag{2.41}$$

This represents a Legendre transformation of (2.36). In this theory, an operator $\mathcal{O}_{\tilde{\Pi}}$ with conformal weight $\Delta_{\tilde{\Pi}} = 2$ is associated with $\tilde{\Pi}$ such that

$$\langle \mathcal{O}_{\tilde{\Pi}} \rangle = \frac{1}{r}\Phi \, . \tag{2.42}$$

In the limit $r \longrightarrow 0$ then follows

$$\langle \mathcal{O}_{\tilde{\Pi}} \rangle \overset{r\to 0}{\longrightarrow} \phi^{(0)} \, . \tag{2.43}$$

If $\Omega = -TS^{ren,Eucl}$ and $\tilde{\Omega} = -T\tilde{\mathcal{S}}^{ren,Eucl}$ denote the free energies of the two theories above – which are calculated via the on-shell Euclidean action compactified on a circle of length $\frac{1}{T}$ – it follows from (2.41) that they are related by $\tilde{\Omega} = \Omega - \phi^{(0)}\pi^{(0)}$, which is exactly how a Legendre transformation changes the potential in thermodynamics.

# 3

# Quantum criticality

## 3.1 Critical points

A critical point denotes the value $g_c$ of a control parameter $g$ at which a transition between two different phases in a material can occur. The parameter $g$ can be thought of as any kind of external parameter of a system, e.g. pressure, field strength of an applied electric or magnetic field or the level of doping of a material. An observation that is called universality is that in a large class of systems several of their properties become independent of the dynamical details and are just characterized by so-called critical exponents when a critical point is approached. For example, the correlation length $\xi$ diverges as

$$\xi \propto |g - g_c|^{-\nu} , \tag{3.1}$$

where $\nu > 0$ is the dynamical exponent for $\xi$. Another important quantity is the dynamical critical exponent $z$, which relates the characteristic energy scale of the system $\Delta$ with $\xi$,

$$\Delta \propto \xi^{-z} . \tag{3.2}$$

As $\Delta$ is inversely proportional to the characteristic time $\tau$ of the system, this means that $\tau$ diverges as

$$\tau \propto \xi^{z} . \tag{3.3}$$

The divergence of $\xi$ and the vanishing of $\Delta$ indicate that there is no associated length or energy scale in the system and it becomes invariant under the rescaling

$$t \longrightarrow \lambda^z t, \qquad x \longrightarrow \lambda x \,, \tag{3.4}$$

which is often referred to as Lifshitz scaling.

## 3.2 Quantum critical phenomena

A quantum critical point refers to a continuous phase transition that occurs at the absolute zero of temperature. These phase transitions are not driven by thermal fluctuations as in classical thermodynamics, but by zero point quantum fluctuations due to Heisenberg's uncertainty principle. Though the quantum critical point is actually only defined at zero temperature, the physics at that point dominates regions away from it at finite temperature. This is due to the fact that the energy scale $\Delta$, the so-called mass gap which describes fluctuations away from the ground state, vanishes at $g = g_c$. When temperature $T$ is turned on, for regions where $\Delta < T$ the system does not know about these excited stated but is instead still described by the physics at $g = g_c$. Therefore, in the $g - T$ phase diagram of the material, schematically depicted in figure 3.1, a quantum critical region fans out that separates the two other phases. This region can basically be thought of as being described by the coupling $g = g_c$. Over the last decades, several measurements of materials near a quantum critical

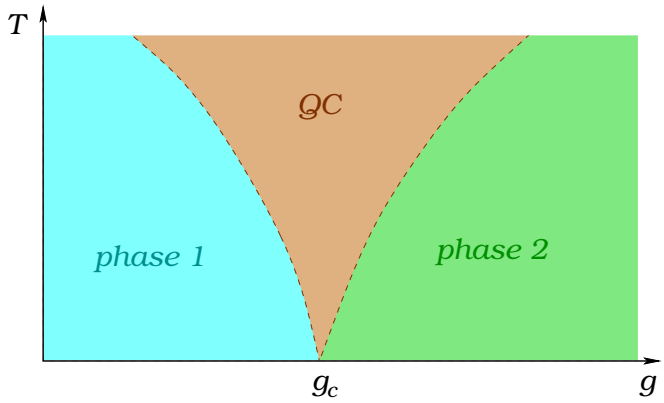


**Figure 3.1:** A schematic depiction of a phase diagram near a quantum critical point. Two phases are separated by a region which is described by the physics of the quantum critical point at $g = g_c$ at finite temperature.

point were made, see e.g. [33–36] to just name a few. These investigations brought features to light that could not be described by the prevalent models in condensed matter physics, like the Landau theory of Fermi liquids.

A prominent example of such materials would be heavy fermion metals, intermetallic compounds that containing elements with 4f or 5f electrons. The name originates from the fact that the conduction electrons below a a characteristic temperature behave as if they had an effective mass of 100-1000 times the mass of a free electron. The properties of these componds derive from the partly filled f-orbitals of rare earth or actinide ions which behave like localized magnetic moments. In a certain regime at low temperatures, heavy fermion metals can be described by Landau Fermi liquid theory via introducing quasiparticles which have the same charge and quantum numbers as electrons but a much higher effective mass. In this regime, the Sommerfeld ratio settles down to a constant and the electrical resistivity is quadratic in temperature. In measurements initiated by von Löhneysen *et al.* [33] it was found that certain heavy fermion compounds can become quantum critical at a certain level of doping. Several features in this quantum critical region, nowadays often referred to as strange metal phase, are very dissimilar from predictions made by Landau Fermi liquid theory. For example, the Sommerfeld ratio keeps growing continuously when lowering temperature and fits indicate that it obeys an inverse power or inverse power logarithmic law. Furthermore, the resistivity was also found to not be quadratic but linear in the temperature. This means that the strange metal phase must be a new type of electron liquid.

A strange metal phase is actually found in a variety of compound materials, including unconventional superconductors like pnictide or cuprate superconductors. These materials are not adequately described by BCS theory or Bogolyubov's theory. An illustration of a typical phase diagram for a cuprate high-temperature superconductor is shown in figure 3.2, it shows the appearance of a superconducting 'dome' and a phase with anomalous metallic behavior. It should be noted though, that these features are not exclusive to cuprates and have also been observed in a variety of other materials, including several heavy fermion compounds. It is hypothesized that the strange metal phase, and even the superconducting regime, are governed by a quantum critical point hidden beneath the dome [37, 38] – though the appearance of the latter could be suppressed by applying a strong magnetic field.

The strange metal phase as well as unconventional high-temperature superconductivity are novel features that still leave a lot of open questions about the underlying physical process. Some phenomenological models, like marginal fermi liquids, were

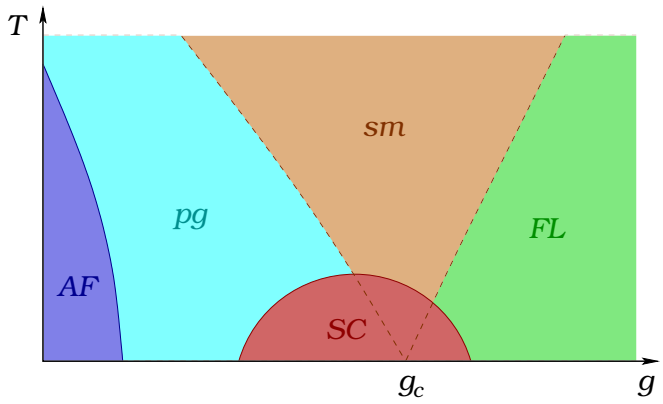


**Figure 3.2:** A schematic depiction of a phase diagram for a cuprate. A strange metal region (sm) separates the Fermi liquid phase (FL) from a phase called pseudogap (pg). The strange metal phase is believed to be governed by a quantum critical point $g_c$ which is covered by a superconducting dome (SC). At low doping and temperature, the cuprate becomes antiferromagnetic (AF).

developed in solid state physics that were able to reproduce certain features of high-temperature superconductors. Despite this success, the modelling of non-Fermi liquid behavior is still in its infancy and at the present day there is no widely accepted theory that explains all of their properties.

As these systems are governed by strongly correlated electrons, it stands to reason that they correspond to a region in parameter space where a holographic description via a gravitational dual is feasible. In the next chapters, Lifshitz geometries and electron stars are introduced which both were conjectured as a gravitational dual description of a material in a non-Fermi liquid phase that is governed by a quantum critical point.

# 4

# Lifshitz holography

Though it was never written down by Lifshitz himself, the metric

$$\frac{ds^2}{L^2} = -\frac{dt^2}{r^{2z}} + \frac{dx^2}{r^2} + \frac{dr^2}{r^2} \,, \tag{4.1}$$

which is invariant under the Lifshitz scaling (3.4) when also scaling $r \longrightarrow \lambda r$, is nowadays often referred to as Lifshitz-metric, as a homage to his contributions to the theory of critical points and phase transitions [39]. Despite (4.1) was already found in [40], it not was conjectured as a model for a gravitational dual to a field theory that is invariant under (3.4) until [41], which put it in the focus of much research in the time thereafter. It would take too much space to summarize all contributions made on this field, but some of the pioneering work was done in [42], where black holes in asymptotically Lifshitz spacetimes were introduced, the treatise in [43, 44] that allowed for a setup with arbitrary dimension and critical exponent $z$, [45] where the thermodynamic properties of these system were analyzed and [46], where after a thorough investigation of systems with Lifshitz scaling also first ideas were presented, how the gravitational model could be embedded into a string-theoretical framework.

The significance of metrics with asymptotic anisotropic scaling in the context of gauge/gravity duality should not be underestimated. With regard to construct gravitational duals to quantum critical systems which are invariant under Lifshitz scaling in the UV limit, such metrics seem more relevant than asymptotically AdS spacetimes which just incorporate conformal scaling $z = 1$. Furthermore, as the majority of the work in the gauge/gravity duality had a focus on AdS/CFT and

explicit examples of string theories with their dual non-conformal field theories are not at hand, the similarities of asymptotically Lifshitz spacetimes with asymptotically AdS spacetimes provide a starting point to generalize known results to a larger class of applications.

### Summary of published results

The work on this thesis began in I, where an earlier study of Lifshitz black holes [42, 44, 47] was continued. In a first part, the global structure of static asymptotic Lifshitz black holes was studied. By a general argument, it was shown that they contain a null curvature singularity, which was in agreement with the fistful of known exact solutions. In a second part, a Maxwell gauge field and a charged scalar were added to the black hole. This allowed for a phase transition at a critical temperature where the scalar field forms a condensate, indicating a superfluid phase that can also lead to superconductivity as in the case $z = 1$.[1] This construction could be relevant for solid state physics, where superconducting systems at Lifshitz points are known [51].

In the subsequent publications II and III, several properties of Lifshitz black holes were further investigated. In the absence of a condensate, the zero temperature limit is an equivalent of an extremal AdS-RN black brane, i.e. a configuration with vanishing surface gravity but non-zero entropy. It was shown that the coupling of the system to the scalar field remedies this and leads to a ground state with vanishing entropy, indicating that this configuration is stable. An intriguing result was that the simple gravitational model investigated was able to qualitatively reproduce the non-Fermi liquid behavior of the Sommerfeld ratio observed in some heavy fermion alloys at critical doping [35, 52], i.e. an unbounded growth when the temperature goes to zero.

Finally, in V some aspects that were omitted in previous studies of Lifshitz models were examined. By an investigation of the asymptotic expansion near spatial infinity, a holographic renormalization procedure was presented that allowed thermodynamic potentials to be defined for dyonic Lifshitz black holes – carrying both electric and magnetic charge – in such a way that standard thermodynamic relations hold. This extended the work in [45, 53] and confirmed that the thermodynamic treatment of charged Lifshitz black holes in previous publications was justified. The paper also provided an analysis of magnetic properties. In contrast to AdS black holes which are always diamagnetic, Lifshitz black holes were shown to allow for paramagnetic behavior in certain regions of the parameter space.

[1] See [48–50].

### Ongoing and future research

During the work on this thesis, some further aspects of Lifshitz models were investigated. These have not been published so far but some of them were reported on at various conferences.

One observation was that the extremal Lifshitz black brane has a near horizon geometry which is $\mathrm{AdS}_2 \times \mathbb{R}^{n-2}$, analogous to the extremal AdS-RN black brane. This suggests that many aspects of the near horizon analysis in [54] can be carried over to Lifshitz geometries, though a thorough treatment of this was postponed in favor of other projects.

The anomalous Sommerfeld ratio was also calculated in the presence of a scalar condensate and was found to be discontinuous at the phase transition. This behavior was qualitatively in agreement with results from measurements made in heavy fermion compounds in the transition to a superconducting state [55].

There is also an ongoing project that deals with the probing of systems with anisotropic scaling by free fermions along the lines of the pioneering work in [54, 56, 57] and an analysis of the single fermion spectral function. Preliminary results here indicate that many features resemble those previously obtained in asymptotic AdS spacetimes. In the same project, transport properties of Lifshitz systems are investigated. Some new technical issues arise in the computations, but the results here are also qualitatively similar to those in AdS backgrounds.

Another direction that could be pursued now that the holographic renormalization and thermodynamic properties of these systems are better understood, would be to fix a certain value of $z$ and scan through all remaining parameters to find the full phase diagram of the system, in an analogous fashion to [58] where such an investigation was made for $z = 1$. This could illustrate which configuration – i.e. anisotropic or isotropic scaling or the presence of a condensate – would minimize the free energy depending on the value of the parameters that determine the thermodynamic ensemble of the dual field theory.

# 5

# Electron stars

Electron stars were introduced in [59] and were conjectured as gravity duals for systems with strongly interacting fermions. The motivation behind this was to obtain a holographic model that incorporates an electromagnetic and gravitational backreaction on the internal bulk geometry. The name electron star was chosen as an analogy to the concept of a neutron star in astrophysics, which is described via a solution of the Einstein equations coupled to a perfect fluid [60,61]. An electron star is similarly constructed, but with the difference that the fluid is assumed to be charged and the equation of state is modeled after zero temperature Fermi statistics. Thus, the star can in a certain sense be seen as a mean field description of an electron fluid where local features and interactions were coarse-grained such that the resulting model is described through its pressure, charge density, energy density and the four-velocity of its current. The construction also neglects local effects of gravitational or electromagnetic interactions in the equation of state, which is a valid and fairly natural assumption in a parameter regime where the action describing this model is assumed to be the classical gravitational effective action of an underlying string theory in the 'probe brane' limit [59]. Outside this parameter regime the groundstate for a holographic fermion system is described by other configurations [62].

Investigations showed that the UV region of electron star models are AdS, but in the IR they exhibit Lifshitz scaling with a non-universal dynamical critical exponent $z$ that depends on the couplings of the model, indicating the emergence of non-Fermi liquid behavior. In rather recent developments, these objects were also shown to contain other features that are characteristic for fermionic systems, like Kosevich-

Lifshitz quantum oscillations [63] and a series of Fermi surfaces such that the Luttinger count is satisfied [64].

### Summary of published results

In IV, the original model of [59] was generalized to non-zero temperatures. This was achieved by constructing a configuration where an electron cloud is suspended over the horizon of a AdS-RN black brane whose charge has the same sign, such that electrostatic repulsion balances the gravitational attraction. In the limit of vanishing temperature the radius of the horizon recedes to zero and the original electron star is recovered. In this limit, the free energy smoothly approaches the value of the electron star. By considering the scalar curvature, it was also demonstrated how Lifshitz scaling emerges in the interior of the electron cloud and gives rise to the Lifshitz IR geometry of the electron star. With rising temperature, the black hole absorbs more and more charge from the electron cloud and at a certain point there is a phase transition to a AdS-RN black hole with no electron cloud. By considering how the free energy varies with temperature it was shown that this transition is of third order and that the electron cloud configuration is thermodynamically preferred below the critical temperature. Transport properties of the system were also investigated and it was found that the conductivity interpolates smoothly between the zero temperature electron star and the pure AdS-RN configuration.

Some of these results overlapped with independent work in [65].

### Ongoing and future research

In an ongoing project whose results will be submitted for published in the not too distant future, electron stars are investigated for signs of a sharp Fermi surface that do not depend on external probes. A way to do this is to search for non-analyticities in current-current correlation functions in the shear channel[1] that give rise to Friedel-like oscillations. However, a first investigation of this correlation function did not reveal any such features. In hindsight, this may not be too surprising when it is recalled that Friedel oscillations occur in systems possessing a sharp Fermi surface where the internal degrees of freedom are subject to a polarization process. In the setup of an electron star, the bulk fermion fluid is modeled as an ideal fluid that is void of any internal features that could be polarized by the appearance of fluctuations in the gauge field. It can be speculated that this may be remedied when the description of

[1] This is technically simpler than investigating the sound channel, but it is expected that both channels should capture similar features.

the bulk fermion fluid was generalized in a way that incorporates more of the local features that perished in the process of coarse-graining to an ideal fluid.

A more positive result that came from calculating correlation functions in the shear channel was that the numerical results suggest that all quasi-normal modes are restricted to the lower half of the complex frequency plane, as it is the case for an AdS background [66]. This indicates that fluctuations around the electron star configuration do not cause instabilities.

# 6

# Conclusions

Though the concept of holography in string theory and its mathematical formulation is still at the level of conjecture, the analysis of holographic models has so far not encountered any insurmountable obstacles. Encouraged by the success of the AdS/CFT conjecture in supersymmetric systems, these ideas have been extended to systems with less symmetry. The results obtained here were rather encouraging to continue investigations of these models as several of their properties were found to be in accord with condensed matter theory or experiments.

This thesis made a contribution towards a holographic description of quantum critical phenomena and strongly interacting fermion systems. A major lesson learned from the investigation on Lifshitz models is that with a slight modification, many results known from the AdS/CFT duality can be carried over to a holographic description of quantum critical systems that are invariant under anisotropic scaling in the UV. This clarified several issues about how to formulate a holographic dictionary for a non-conformal non-relativistic gauge/gravity duality. An intriguing byproduct of this analysis was the qualitative agreement of predictions of these models with actual experimental data. Also, a better understanding of several properties of the recently proposed electron star models was developed. They seem promising candidates to obtain a holographic description of a Fermi surface for strongly correlated electron systems, but many aspects of this remain to be investigated in future work.

The models presented in this thesis are able to capture qualitative features of quantum critical systems. Nonetheless, they are not yet developed to a level of detail where they could actually be used to fit experimental data and there is still much

work to be done to fully establish holography as a tool for condensed matter physics. Noting that after almost one and a half decade after its formulation even the original AdS/CFT correspondence still remains a conjecture, it seems likely that there is a long way ahead until this dream can finally be seen to come true.

# Bibliography


[1] J. D. Bekenstein, *Black holes and the second law*, *Nuovo Cim. Lett.* **4** (1972) 737–740.

[2] J. D. Bekenstein, *Black holes and entropy*, *Phys. Rev.* **D7** (1973) 2333–2346.

[3] J. D. Bekenstein, *Generalized second law of thermodynamics in black hole physics*, *Phys. Rev.* **D9** (1974) 3292–3300.

[4] S. Hawking, *Black hole explosions*, *Nature* **248** (1974) 30–31.

[5] S. Hawking, *Particle Creation by Black Holes*, *Commun.Math.Phys.* **43** (1975) 199–220.

[6] C. R. Stephens, G. 't Hooft, and B. F. Whiting, *Black hole evaporation without information loss*, *Class. Quant. Grav.* **11** (1994) 621–648, [gr-qc/9310006].

[7] J. D. Bekenstein, *Universal upper bound on the entropy-to-energy ratio for bounded systems*, *Phys. Rev. D* **23** (Jan, 1981) 287–298.

[8] G. 't Hooft, *Dimensional reduction in quantum gravity*, gr-qc/9310026.

[9] R. Bousso, *The holographic principle*, *Rev. Mod. Phys.* **74** (2002) 825–874, [hep-th/0203101].

[10] J. M. Maldacena, *The large N limit of superconformal field theories and supergravity*, *Adv. Theor. Math. Phys.* **2** (1998) 231–252, [hep-th/9711200].

[11] O. Aharony, S. S. Gubser, J. M. Maldacena, H. Ooguri, and Y. Oz, *Large N field theories, string theory and gravity*, *Phys. Rept.* **323** (2000) 183–386, [hep-th/9905111].

[12] M. E. Peskin and D. V. Schroeder, *An Introduction to Quantum Field Theory*. Westview Press, USA, 1995.

[13] C. Fefferman and C. Robin Graham, *Conformal Invariants*, in *Elie Cartan et les mathématiques d'aujourd'hui*, Astérisque, pp. 95–116, Société Mathématique de France, Paris, June, 1985. hors série.

[14] E. Witten, *Anti-de Sitter space and holography*, *Adv. Theor. Math. Phys.* **2** (1998) 253–291, [hep-th/9802150].

[15] S. S. Gubser, I. R. Klebanov, and A. M. Polyakov, *Gauge theory correlators from non-critical string theory*, *Phys. Lett.* **B428** (1998) 105–114, [hep-th/9802109].

[16] D. T. Son and A. O. Starinets, *Minkowski-space correlators in AdS/CFT correspondence : Recipe and applications*, *JHEP* **09** (2002) 042, [hep-th/0205051].

[17] J. McGreevy, *Holographic duality with a view toward many-body physics*, 0909.0518.

[18] S. A. Hartnoll, *Lectures on holographic methods for condensed matter physics*, *Class. Quant. Grav.* **26** (2009) 224002, [0903.3246].

[19] S. Sachdev, *Condensed matter and ads/cft*, 1002.2947v1.

[20] S. A. Hartnoll, *Horizons, holography and condensed matter*, 1106.4324.

[21] H. L. Lebesgue, *Intégrale, longueur, aire*. PhD thesis, Université Henri Poincaré Nancy, France, 1902.

[22] P. Cartier and C. DeWitt-Morette, *A new perspective on Functional Integration*, *J. Math. Phys* (May, 1995) 2237, [funct-an/9602005].

[23] R. Courant and D. Hilbert, *Methoden der mathematischen Physik*, vol. XII of *Die Grundlehren der mathematischen Wissenschaften*. Verlag Justus Springer, Berlin, 1924.

[24] R. Courant and D. Hilbert, *Methoden der mathematischen Physik II*, vol. XLVII of *Die Grundlehren der mathematischen Wissenschaften*. Verlag Justus Springer, Berlin, 1937.

[25] I. L. Fuchs, *Zur Theorie der linearen Differentialgleichungen mit veränderlichen Coefficienten.*, *J. reine angew. Math.* **66** (1866) 121–160.

[26] I. L. Fuchs, *Zur Theorie der linearen Differentialgleichungen mit veränderlichen Coefficienten. (Ergänzungen zu der im $66^{sten}$ Bande dieses Journals enthaltenen Abhandlung).*, *J. reine angew. Math.* **68** (1868) 354–385.

[27] G. T. Horowitz and J. Polchinski, *Gauge/gravity duality*, gr-qc/0602037. To appear in 'Towards Quantum Gravity'. Edited by Daniele Oriti. Cambridge University Press.

[28] J. Polchinski, *Introduction to Gauge/Gravity Duality*, 1010.6134.

[29] I. Heemskerk, J. Penedones, J. Polchinski, and J. Sully, *Holography from Conformal Field Theory*, *JHEP* **0910** (2009) 079, [0907.0151].

[30] I. Heemskerk and J. Polchinski, *Holographic and Wilsonian Renormalization Groups*, *JHEP* **06** (2011) 031, [1010.1264].

[31] K. Skenderis, *Lecture notes on holographic renormalization*, *Class. Quant. Grav.* **19** (2002) 5849–5876, [hep-th/0209067].

[32] I. Papadimitriou and K. Skenderis, *AdS / CFT correspondence and geometry*, hep-th/0404176.

[33] H. V. Löhneysen, T. Pietrus, G. Portisch, H. G. Schlager, A. Schröder, M. Sieck, and T. Trappmann, *Non-Fermi-liquid behavior in a heavy-fermion alloy at a magnetic instability*, *Physical Review Letters* **72** (May, 1994) 3262–3265.

[34] S. R. Julian, C. Pfleiderer, F. M. Grosche, N. D. Mathur, G. J. McMullan, A. J. Diver, I. R. Walker, and G. G. Lonzarich, *The normal states of magnetic d and f transition metals*, *Journal of Physics Condensed Matter* **8** (Nov., 1996) 9675–9688.

[35] G. R. Stewart, *Non-Fermi-liquid behavior in d- and f-electron metals*, *Rev. Mod. Phys.* **73** (2001) 797–855.

[36] S. A. Grigera, R. S. Perry, A. J. Schofield, M. Chiao, S. R. Julian, G. G. Lonzarich, S. I. Ikeda, Y. Maeno, A. J. Millis, and A. P. Mackenzie, *Magnetic Field-Tuned Quantum Criticality in the Metallic Ruthenate $Sr_3Ru_2O_7$*, *Science* **294** (Oct., 2001) 329–332.

[37] D. M. Broun, *What lies beneath the dome?*, *Nature Physics* **4** (2008), no. 3 170–172.

[38] J. Zaanen, *A Modern, but way too short history of the theory of superconductivity at a high temperature*, 1012.5461.

[39] E. M. Lifshitz, *On the Theory of Second-Order Phase Transitions I and II*, *Zh. Eksp. Teor. fiz* **11** (1941) 255 and 269.

[40] P. Koroteev and M. Libanov, *On Existence of Self-Tuning Solutions in Static Braneworlds without Singularities*, *JHEP* **02** (2008) 104, [0712.1136].

[41] S. Kachru, X. Liu, and M. Mulligan, *Gravity Duals of Lifshitz-like Fixed Points*, *Phys. Rev.* **D78** (2008) 106005, [0808.1725].

[42] U. H. Danielsson and L. Thorlacius, *Black holes in asymptotically Lifshitz spacetime*, *JHEP* **03** (2009) 070, [0812.5088].

[43] M. Taylor, *Non-relativistic holography*, 0812.0530.

[44] G. Bertoldi, B. A. Burrington, and A. Peet, *Black Holes in asymptotically Lifshitz spacetimes with arbitrary critical exponent*, *Phys. Rev.* **D80** (2009) 126003, [0905.3183].

[45] G. Bertoldi, B. A. Burrington, and A. W. Peet, *Thermodynamics of black branes in asymptotically Lifshitz spacetimes*, *Phys. Rev.* **D80** (2009) 126004, [0907.4755].

[46] S. A. Hartnoll, J. Polchinski, E. Silverstein, and D. Tong, *Towards strange metallic holography*, *JHEP* **04** (2010) 120, [0912.1061].

[47] R. B. Mann, *Lifshitz Topological Black Holes*, *JHEP* **06** (2009) 075, [0905.1136].

[48] S. S. Gubser, *Breaking an Abelian gauge symmetry near a black hole horizon*, *Phys. Rev.* **D78** (2008) 065034, [0801.2977].

[49] S. A. Hartnoll, C. P. Herzog, and G. T. Horowitz, *Building a Holographic Superconductor*, *Phys. Rev. Lett.* **101** (2008) 031601, [0803.3295].

[50] S. A. Hartnoll, C. P. Herzog, and G. T. Horowitz, *Holographic Superconductors*, *JHEP* **12** (2008) 015, [0810.1563].

[51] A. I. Buzdin and M. L. Kulić, *Unusual behavior of superconductors near the tricritical Lifshitz point*, *Journal of Low Temperature Physics* **54** (Feb., 1984) 203–213.

[52] H. v. Löhneysen, A. Rosch, M. Vojta, and P. Wolfle, *Fermi-liquid instabilities at magnetic quantum phase transitions*, *Rev.Mod.Phys.* **79** (2007) 1015–1075.

[53] S. F. Ross and O. Saremi, *Holographic stress tensor for non-relativistic theories*, *JHEP* **0909** (2009) 009, [0907.1846].

[54] T. Faulkner, H. Liu, J. McGreevy, and D. Vegh, *Emergent quantum criticality, Fermi surfaces, and $AdS_2$*, *Phys.Rev.* **D83** (2011) 125002, [0907.2694].

[55] R. Vollmer, A. Faißt, C. Pfleiderer, H. v. Löhneysen, E. D. Bauer, P.-C. Ho, V. Zapf, and M. B. Maple, *Low-Temperature Specific Heat of the Heavy-Fermion Superconductor $PrOs_4Sb_{12}$*, *Phys. Rev. Lett.* **90** (Feb, 2003) 057001.

[56] H. Liu, J. McGreevy, and D. Vegh, *Non-Fermi liquids from holography*, 0903.2477.

[57] M. Cubrovic, J. Zaanen, and K. Schalm, *String Theory, Quantum Phase Transitions and the Emergent Fermi-Liquid*, *Science* **325** (2009) 439–444, [0904.1993].

[58] G. T. Horowitz and B. Way, *Complete Phase Diagrams for a Holographic Superconductor/Insulator System*, *JHEP* **1011** (2010) 011, [1007.3714].

[59] S. A. Hartnoll and A. Tavanfar, *Electron stars for holographic metallic criticality*, *Phys. Rev.* **D83** (2011) 046003, [1008.2828].

[60] R. C. Tolman, *Static solutions of Einstein's field equations for spheres of fluid*, *Phys.Rev.* **55** (1939) 364–373.

[61] J. Oppenheimer and G. Volkoff, *On Massive neutron cores*, *Phys.Rev.* **55** (1939) 374–381.

[62] M. Cubrovic, Y. Liu, K. Schalm, Y.-W. Sun, and J. Zaanen, *Spectral probes of the holographic Fermi groundstate: dialing between the electron star and AdS Dirac hair*, 1106.1798.

[63] S. A. Hartnoll, D. M. Hofman, and A. Tavanfar, *Holographically smeared Fermi surface: Quantum oscillations and Luttinger count in electron stars*, *Europhys. Lett.* **95** (2011) 31002, [1011.2502].

[64] S. A. Hartnoll, D. M. Hofman, and D. Vegh, *Stellar spectroscopy: Fermions and holographic Lifshitz criticality*, 1105.3197.

[65] S. A. Hartnoll and P. Petrov, *Electron star birth: A continuous phase transition at nonzero density*, *Phys.Rev.Lett.* **106** (2011) 121601, [1011.6469].

[66] M. Edalati, J. I. Jottar, and R. G. Leigh, *Shear Modes, Criticality and Extremal Black Holes*, *JHEP* **1004** (2010) 075, [1001.0779].

# Papers

# Paper I

IOP PUBLISHING JOURNAL OF PHYSICS A: MATHEMATICAL AND THEORETICAL

J. Phys. A: Math. Theor. **43** (2010) 065401 (18pp) doi:10.1088/1751-8113/43/6/065401

# Holographic superconductors with Lifshitz scaling

**E J Brynjolfsson[1], U H Danielsson[2], L Thorlacius[1,3] and T Zingg[1,3]**

[1] University of Iceland, Science Institute, Dunhaga 3, IS-107 Reykjavik, Iceland
[2] Institutionen för fysik och astronomi, Uppsala Universitet, Box 803, SE-751 08 Uppsala, Sweden
[3] NORDITA, Roslagstullsbacken 23, SE-106 91 Stockholm, Sweden

E-mail: erlingbr@hi.is, ulf.danielsson@physics.uu.se, lth@nordita.org and zingg@nordita.org

Received 4 September 2009, in final form 12 December 2009
Published 19 January 2010
Online at stacks.iop.org/JPhysA/43/065401

**Abstract**
Black holes in asymptotically Lifshitz spacetime provide a window onto finite temperature effects in strongly coupled Lifshitz models. We add a Maxwell gauge field and charged matter to a recently proposed gravity dual of (2+1)-dimensional Lifshitz theory. This gives rise to charged black holes with scalar hair, which correspond to the superconducting phase of holographic superconductors with $z > 1$ Lifshitz scaling. Along the way we analyze the global geometry of static, asymptotically Lifshitz black holes at the arbitrary critical exponent $z > 1$. In all known exact solutions there is a null curvature singularity in the black hole region, and, by a general argument, the same applies to generic Lifshitz black holes.

PACS numbers: 11.25.Tq, 04.70.−s, 64.70.Tg, 74.20.Mn

(Some figures in this article are in colour only in the electronic version)

## 1. Introduction

A holographic superconductor [1, 2] is dual to an asymptotically AdS spacetime with a charged black hole carrying scalar hair. It is a theoretical construction where a superconducting phase transition in a strongly coupled system is studied via the AdS/CFT correspondence [3]. Having a black hole places the system at finite temperature, the black hole charge gives rise to a chemical potential in the dual theory, and the scalar field hair signals the condensation of a charged operator in the dual theory. Without a chemical potential all temperatures are equivalent due to the underlying conformal symmetry and there can be no phase transition. With a chemical potential, on the other hand, a new scale is introduced that allows for a phase transition at some critical temperature.

The black holes in question are found as solutions of AdS gravity coupled to a Maxwell gauge field and matter in the form of a charged scalar. Black holes that are neutral under the

  

Maxwell field do not develop any hair. Near a charged black hole, however, the gauge field sourced by the black hole couples to the charged scalar and induces a negative mass squared sufficient for condensation provided the temperature is low enough. It was observed in [4] that even a neutral scalar can lead to condensation below a non-zero critical temperature due to the existence of a new and effectively lower Breitenlohner–Freedman bound [5] near the horizon of a low temperature, near extremal, AdS–Reissner–Nordström black hole. See [6] and [7] for recent reviews of holographic superconductivity.

In the present paper we show that similar phenomena can occur in a theory exhibiting Lifshitz scaling:

$$t \to \lambda^z t, \qquad \mathbf{x} \to \lambda \mathbf{x}, \tag{1.1}$$

with $z \neq 1$. Models with scaling of this type have, for example, been used to model the quantum critical behavior in strongly correlated electron systems [8–11]. Our starting point is the model proposed by Kachru *et al* [12] for the holographic study of strongly coupled (2+1)-dimensional systems with Lifshitz scaling. While this model in itself does not support a phase transition to a superconductor it turns out that a relatively simple extension does.

A quantum critical point exhibiting dynamical scaling of the form (1.1) has a gravitational dual description in terms of a spacetime metric of the form

$$\mathrm{d}s^2 = L^2 \left( -r^{2z}\,\mathrm{d}t^2 + \frac{\mathrm{d}r^2}{r^2} + r^2\,\mathrm{d}^2\mathbf{x} \right), \tag{1.2}$$

which is invariant under the transformation

$$t \to \lambda^z t, \qquad r \to \frac{r}{\lambda}, \qquad \mathbf{x} \to \lambda \mathbf{x}\,. \tag{1.3}$$

Here $L$ is a characteristic length scale and the coordinates $(t, r, x^1, x^2)$ are taken to be dimensionless. Critical points with $z > 1$ are often said to be non-relativistic. This can be motivated by considering null geodesics at fixed $r = r_0$ in the Lifshitz background (1.2). Along such a geodesic one finds that $(\mathrm{d}\mathbf{x}/\mathrm{d}t)^2 = r_0^{2z-2}$ and so for $z > 1$ the effective speed of light in the boundary theory diverges as $r_0 \to \infty$.

In [12] it was shown how the fixed point geometry (1.2), with $z > 1$, can be obtained from an action coupling (3+1)-dimensional gravity with a negative cosmological constant to Abelian two- and three-form field strengths:

$$S = \int \mathrm{d}^4x\sqrt{-g}(R - 2\Lambda) - \frac{1}{2}\int *F_{(2)} \wedge F_{(2)} - \frac{1}{2}\int *H_{(3)} \wedge H_{(3)} - c\int B_{(2)} \wedge F_{(2)}, \tag{1.4}$$

with $H_{(3)} = \mathrm{d}B_{(2)}$ and the cosmological constant and the coupling between the form fields given by $\Lambda = -\frac{z^2+z+4}{2L^2}$ and $c = \frac{\sqrt{2z}}{L}$. The equations of motion for the form fields can be written as

$$d * F_{(2)} = -cH_{(3)}, \qquad d * H_{(3)} = -cF_{(2)}, \tag{1.5}$$

and the Einstein equations are

$$G_{\mu\nu} + \Lambda g_{\mu\nu} = \tfrac{1}{2}\big(F_{\mu\lambda}F_{\nu}^{\ \lambda} - \tfrac{1}{4}g_{\mu\nu}F_{\lambda\sigma}F^{\lambda\sigma}\big) + \tfrac{1}{4}\big(H_{\mu\lambda\sigma}H_{\nu}^{\ \lambda\sigma} - \tfrac{1}{6}g_{\mu\nu}H_{\lambda\sigma\rho}H^{\lambda\sigma\rho}\big). \tag{1.6}$$

Black holes in this (3+1)-dimensional gravity theory were considered in [13], where numerical black hole solutions were found at $z = 2$ and used to study finite temperature effects in the dual (2+1)-dimensional system. Related work on Lifshitz black holes can be found in [14], where topological black holes with hyperbolic horizons were included, and in

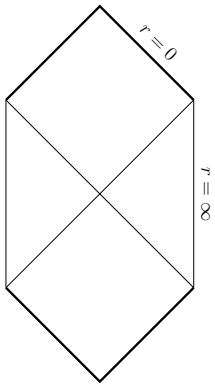


**Figure 1.** Conformal diagram for a Lifshitz black hole. The thick lines denote null curvature singularities.

[15, 16], where black holes at general values of $z$ were considered[4]. These Lifshitz black holes carry a charge that couples to the two-form field strength $F_{(2)}$, but they are in many respects more analogous to AdS–Schwarzschild black holes than charged AdS–Reissner–Nordström black holes. In particular, since the black hole charge cannot be varied independently of the black hole area, there is only a one-parameter family of black hole solutions for a given value of $z$.

We will see below that without additional ingredients the underlying Lifshitz symmetry prevents the system from undergoing phase transitions. We therefore extend the system to include a Maxwell field, with field strength $\mathcal{F}_{(2)}$, and a scalar field $\psi$ that is charged under the new gauge field but neutral under the original Lifshitz fields $F_{(2)}$ and $H_{(3)}$. This turns out to be sufficient in order to observe a superconducting phase transition characterized by Lifshitz scaling with $z > 1$. In our modified theory, it is the Maxwell field $\mathcal{F}_{(2)}$ that corresponds to physical electromagnetism while the original Lifshitz gauge fields are viewed as an auxiliary construction, whose only role is to modify the asymptotic symmetry of the geometry from AdS to Lifshitz.

The plan of the rest of the paper is as follows. We begin in section 2 with a brief review of Lifshitz black holes in the model (1.4). We extend previous treatments by considering the global geometry, including the black hole interior. In those cases where an exact solution is known, we find a null curvature singularity at $r = 0$ and a Carter–Penrose diagram as shown in figure 1. We show that a null singularity is generic for black holes in this model. In section 3 we generalize the model to include an additional Maxwell field. We exhibit a family of exact solutions at $z = 4$, which describe Lifshitz black holes that are charged under the new Maxwell field and obtain numerical solutions for charged black holes at other values of $z > 1$. These black holes can be viewed as the Lifshitz analog of AdS–Reissner–Nordström black holes. In section 4 we further extend the model by adding a charged scalar field and look for the black hole instability that signals the onset of superconductivity. Finally, we conclude with some final remarks in section 5.

[4] Black hole solutions in other gravity models exhibiting Lifshitz scaling have been considered in [17–19].

## 2. Lifshitz black holes revisited

The action (1.4) is known to have spherically symmetric static black hole solutions of the form

$$\mathrm{d}s^2 = L^2\left( - r^{2z} f(r)^2\, \mathrm{d}t^2 + \frac{g(r)^2}{r^2}\, \mathrm{d}r^2 + r^2(\mathrm{d}\theta^2 + \chi(\theta)^2\, \mathrm{d}\varphi^2)\right), \tag{2.1}$$

with

$$\chi(\theta) = \begin{cases} \sin\theta & \text{if} \quad k = 1, \\ \theta & \text{if} \quad k = 0, \\ \sinh\theta & \text{if} \quad k = -1, \end{cases}$$

where $k = +1, 0, -1$ corresponds to a spherical, flat and hyperbolic horizon, respectively. An asymptotically Lifshitz black hole with a non-degenerate horizon has $f(r),\ g(r) \to 1$ as $r \to \infty$ and a simple zero of both $f(r)^2$ and $g(r)^{-2}$ at the horizon $r = r_0$.

### *2.1. Exact solutions and global extensions*

Several families of numerical solutions of this general form have been found [13–15] along with a couple of isolated exact black hole solutions. These are a $z = 2$ topological black hole with a hyperbolic horizon [14]:

$$f(r) = \frac{1}{g(r)} = \sqrt{1 - \frac{1}{2r^2}}, \tag{2.2}$$

and a $z = 4$ black hole [15]:

$$f(r) = \frac{1}{g(r)} = \sqrt{1 + \frac{k}{10r^2} - \frac{3k^2}{400r^4}}, \tag{2.3}$$

with $k = \pm 1$. The $k = +1$ case has a spherical horizon while $k = -1$ corresponds to a topological black hole with a hyperbolic horizon. When we extend the system to include an additional Maxwell gauge field (see section 3 below) we will see that the exact $z = 4$ solution (2.3) is a special case of a one-parameter family of exact solutions in the extended theory.

We start our discussion by working out the global geometry of the exact $z = 2$ topological black hole (2.2) and constructing the associated conformal diagram. In order to study the interior geometry of a black hole, one looks for coordinates that are non-singular at the black hole horizon and allow the solution to be extended into the black hole. The first step is to transform to a tortoise coordinate $r_*$ for which

$$\mathrm{d}s^2 = L^2\left(r^4\left(1 - \frac{1}{2r^2}\right)(-\mathrm{d}t^2 + \mathrm{d}r_*^2) + r^2(\mathrm{d}\chi^2 + \sinh^2\chi\, \mathrm{d}\varphi^2)\right). \tag{2.4}$$

Here $r$ is to be viewed as a function of $r_*$ determined via

$$\frac{\mathrm{d}r}{\mathrm{d}r_*} = r^3\left(1 - \frac{1}{2r^2}\right), \tag{2.5}$$

which integrates to

$$r = \frac{1}{\sqrt{2}\sqrt{1 - \exp(r_* - r_*^\infty)}}. \tag{2.6}$$

As usual, the tortoise coordinate $r_*$ goes to $-\infty$ at the horizon but note that it goes to a finite value in the $r \to \infty$ asymptotic region. This is easily seen to be a generic feature of asymptotically Lifshitz black holes for any $z > 1$.

Next we form the null combinations $v = t + r_*$, $u = t - r_*$ and perform a conformal reparametrization

$$\begin{aligned} v &\to V = \exp\left[\tfrac{1}{2}(v - r_*^\infty)\right], \\ u &\to U = -\exp\left[-\tfrac{1}{2}(u + r_*^\infty)\right], \end{aligned} \tag{2.7}$$

which brings the metric into the form

$$\mathrm{d}s^2 = L^2(-4r^4\,\mathrm{d}U\,\mathrm{d}V + r^2(\mathrm{d}\theta^2 + \sinh^2\theta\,\mathrm{d}\varphi^2)). \tag{2.8}$$

In these coordinates the geometry is manifestly nonsingular at the event horizon and the solution can be extended to $r < 1/\sqrt{2}$.

In general, when extending a black hole solution through a non-degenerate horizon, the required conformal reparametrization is of the form

$$\begin{aligned} v &\to V = \alpha \exp(\kappa v), \\ u &\to U = -\alpha \exp(-\kappa u), \end{aligned} \tag{2.9}$$

where $\alpha$ is an arbitrary constant and $\kappa$ is the surface gravity of the black hole in question. The surface gravity determines the Hawking temperature, $T_H = \frac{\kappa}{2\pi}$, and it is easily checked by other means that $T_H = \frac{1}{4\pi}$ is the correct value for the $z = 2$ black hole in (2.2). We have chosen the value of the constant $\alpha$ in (2.7) such that $UV \to -1$ in the $r \to \infty$ asymptotic limit.

The $z = 2$ topological black hole has a curvature singularity at $r = 0$, which can for example be seen by computing the Ricci scalar[5]

$$R = \frac{1}{r^2 L^2}(1 - 22\,r^2). \tag{2.10}$$

It follows from

$$-UV = 1 - \frac{1}{2r^2} \tag{2.11}$$

that $r \to \infty$ corresponds to $UV \to -1$ and $r \to 0$ to $UV \to \infty$. The Carter–Penrose conformal diagram[6] in figure 1 is then obtained by writing

$$V = \tan\frac{\pi P}{2}, \qquad U = \tan\frac{\pi Q}{2}. \tag{2.12}$$

The $z = 4$ case can be dealt within a similar manner. There is a null curvature singularity at $r = 0$ and the tortoise coordinate for a $z = 4$ black hole is given by

$$r_* - r_*^\infty = \frac{1}{2b_1(b_1 + b_2)} \log\left(1 - \frac{b_1}{r^2}\right) + \frac{1}{2b_2(b_1 + b_2)} \log\left(1 + \frac{b_2}{r^2}\right), \tag{2.13}$$

with $b_1 = \frac{1}{20}(2|k| - k)$ and $b_2 = \frac{1}{20}(2|k| + k)$. The change of coordinates to

$$V = \exp[b_1(b_1 + b_2)(v - r_*^\infty)], \qquad U = -\exp[-b_1(b_1 + b_2)(u + r_*^\infty)] \tag{2.14}$$

renders the metric nonsingular at the horizon:

$$\mathrm{d}s^2 = L^2\left(-\frac{r^8}{\kappa^2}\left(1 + \frac{b_2}{r^2}\right)^{1 - \frac{b_1}{b_2}}\,\mathrm{d}U\,\mathrm{d}V + r^2(\mathrm{d}\theta^2 + \chi^2(\theta)\,\mathrm{d}\varphi^2)\right). \tag{2.15}$$

[5] The fixed point geometry (1.2) is also singular at $r = 0$ but in a relatively mild way. All scalar invariants constructed from the Riemann tensor are finite but tidal effects between neighboring null geodesics diverge as $r \to 0$. See for example [6].

[6] We refer to figure 1 as a conformal diagram but it should be kept in mind that the boundary at $r \to \infty$ is in fact not conformally flat due to the asymmetric scaling of the spatial and time directions in asymptotically Lifshitz spacetime.

The Hawking temperature of these $z = 4$ black holes is

$$T_H = \frac{1}{200\pi}(2-k), \tag{2.16}$$

and the Ricci scalar is given by

$$R = \frac{1}{L^2}\left(\frac{9k^2}{200r^4} - \frac{3k}{5r^2} - 54\right). \tag{2.17}$$

There is a null curvature singularity at $r \to 0$ and the conformal diagram is that of figure 1. In section 2.3 below, we present a general argument that this conformal diagram applies to all black hole solutions of the system of equations (1.5)–(1.6).

### *2.2. Lifshitz black holes at general $z > 1$*

The exact solutions offer a glimpse at the parameter space of Lifshitz black holes at isolated points. More generic solutions can be obtained numerically. We are interested in the global geometry including the black hole interior. For this we take our cue from the extension of the exact solution described above and write the metric in the form

$$\mathrm{d}s^2 = L^2[-\mathrm{e}^{2\rho(v,u)}\,\mathrm{d}v\,\mathrm{d}u + \mathrm{e}^{-2\phi(v,u)}(\mathrm{d}\theta^2 + \chi(\theta)^2\,\mathrm{d}\varphi^2)]. \tag{2.18}$$

The notation is descended from two-dimensional gravity and allows the field equations to be written in a relatively economical way. With this ansatz the metric is characterized by two field variables, $\rho$ and $\phi$, which determine the local scale of the $v, u$ plane and the scale of the transverse two-manifold, respectively. The null coordinates $v, u$ are related to the $t, r$ coordinates in (2.1) via $v = t + r_*$, $u = t - r_*$, with the tortoise coordinate $r_*$ given by

$$r_* - r_*^\infty = -\int_r^\infty \frac{\mathrm{d}\tilde{r}}{\tilde{r}^{z+1}}\frac{g(\tilde{r})}{f(\tilde{r})}. \tag{2.19}$$

The Lifshitz fixed point geometry (1.2) has $f(r) = g(r) = 1$ and in that case

$$r_* = r_*^\infty - \frac{1}{z\,r^z}. \tag{2.20}$$

More generally, we see from (2.19) that $r_*$ goes to a finite value asymptotically for any Lifshitz spacetime, for which $f(r), g(r) \to 1$ as $r \to \infty$.

#### *2.2.1. The equations of motion.*

With the following ansatz for the form fields:

$$F_{(2)} = L\,f_{vu}(v,u)\,\mathrm{d}v \wedge \mathrm{d}u, \tag{2.21}$$

$$H_{(3)} = L^2(h_v(v,u)\,\mathrm{d}v - h_u(v,u)\,\mathrm{d}u) \wedge \mathrm{d}\theta \wedge \chi(\theta)\,\mathrm{d}\varphi, \tag{2.22}$$

their field equations (1.5) become

$$-\partial_v(\mathrm{e}^{-2\rho-2\phi} f_{vu}) = \sqrt{\frac{z}{2}}\,h_v, \tag{2.23}$$

$$\partial_u(\mathrm{e}^{-2\rho-2\phi} f_{vu}) = \sqrt{\frac{z}{2}}\,h_u, \tag{2.24}$$

$$-\partial_v(\mathrm{e}^{2\phi}h_u) + \partial_u\,(\mathrm{e}^{2\phi}h_v) = \sqrt{2z}\,f_{vu}. \tag{2.25}$$

These can in turn be re-expressed as a single second-order equation,

$$\partial_v\partial_u\tilde{f} + \partial_v\phi\partial_u\tilde{f} + \partial_u\phi\partial_v\tilde{f} + \frac{z}{2}\,\mathrm{e}^{2\rho}\tilde{f} = 0, \tag{2.26}$$

where we have defined

$$\tilde{f} \equiv \mathrm{e}^{-2\rho-2\phi} f_{vu}. \tag{2.27}$$

The equations of motion for $\phi$ and $\rho$ are obtained from (1.6):

$$-\partial_v\partial_u\phi + 2\partial_v\phi\partial_u\phi + \frac{k}{4}\,\mathrm{e}^{2\rho+2\phi} + \frac{(z^2+z+4)}{8}\,\mathrm{e}^{2\rho} - \frac{1}{4}\tilde{f}^2\,\mathrm{e}^{2\rho+4\phi} = 0, \tag{2.28}$$

$$-\partial_v\partial_u\rho + \partial_v\phi\partial_u\phi + \frac{k}{4}\,\mathrm{e}^{2\rho+2\phi} - \frac{1}{2}\tilde{f}^2\,\mathrm{e}^{2\rho+4\phi} + \frac{1}{2z}\,\mathrm{e}^{4\phi}\partial_v\tilde{f}\partial_u\tilde{f} = 0. \tag{2.29}$$

The conformal reparametrization (2.9) will render the metric nondegenerate at the horizon. The form of the field equations remains the same in the $V, U$ coordinate system with a transformed conformal factor:

$$\mathrm{e}^{2\rho(v,u)} = (-\kappa^2 UV)\,\mathrm{e}^{2\rho(V,U)}. \tag{2.30}$$

We now adapt a simple numerical method, which was originally developed for the study of two-dimensional black holes [20], to the case at hand. We introduce a new spatial variable

$$s \equiv -UV \tag{2.31}$$

and restrict our attention to static configurations. The field equations become

$$0 = s\tilde{f}'' + \tilde{f}' + 2s\phi'\tilde{f}' - \frac{z}{2}\tilde{f}\,\mathrm{e}^{2\rho}, \tag{2.32}$$

$$0 = s\phi'' + \phi' - 2s\phi'^2 + \frac{k}{4}\,\mathrm{e}^{2\rho+2\phi} + \frac{(z^2+z+4)}{8}\,\mathrm{e}^{2\rho} - \frac{1}{4}\tilde{f}^2\,\mathrm{e}^{2\rho+4\phi}, \tag{2.33}$$

$$0 = s\rho'' + \rho' - s\phi'^2 + \frac{k}{4}\,\mathrm{e}^{2\rho+2\phi} - \frac{1}{2}\tilde{f}^2\,\mathrm{e}^{2\rho+4\phi} - \frac{s}{2z}\,\mathrm{e}^{4\phi}\tilde{f}'^2, \tag{2.34}$$

where primes denote derivatives with respect to $s$.

The Lifshitz geometry (1.2) is given by

$$\tilde{f} = \sqrt{\frac{z(z-1)}{2}}r^2, \qquad \mathrm{e}^{-\phi} = r, \qquad \kappa^2 s\,\mathrm{e}^{2\rho(s)} = r^{2z}, \tag{2.35}$$

with $r(s)$ is obtained from (2.20) and (2.31). The horizon at $r = 0$ is singular and as a result $\kappa$ can take any value in the Lifshitz geometry. The $z = 2$ topological black hole has $\tilde{f} = r^2$ with $r(s) = 1/\sqrt{2(1-s)}$, while the $z = 4$ black holes turn out to have $\tilde{f} = \sqrt{6}\big(r^2 + \frac{k}{20}\big)$, with $r(s)$ obtained via $\frac{\mathrm{d}r}{\mathrm{d}r_*} = r^5\big(1 + \frac{k}{10r^2} - \frac{3}{400r^4}\big)$ and (2.31).

*2.2.2. Numerical solutions.* The event horizon is at $s = 0$ and $s$ is negative inside the black hole. With the assumption of a regular horizon we can read off the following relations among initial values at $s = 0$:

$$\phi'(0) = \frac{1}{4}\left(-k\,\mathrm{e}^{2\phi(0)} - \frac{(z^2+z+4)}{2} + \tilde{f}(0)^2\,\mathrm{e}^{4\phi(0)}\right)\mathrm{e}^{2\rho(0)}, \tag{2.36}$$

$$\tilde{f}'(0) = \frac{z}{2}\,\tilde{f}(0)\,\mathrm{e}^{2\rho(0)}, \tag{2.37}$$

$$\rho'(0) = \frac{1}{2}\left(-\frac{k}{2}\,\mathrm{e}^{2\phi(0)} + \tilde{f}(0)^2\,\mathrm{e}^{4\phi(0)}\right)\mathrm{e}^{2\rho(0)}. \tag{2.38}$$

These initial values can now be used to start a numerical integration of the system (2.32)–(2.34) from near $s = 0$, either outward toward $s > 0$ or into the black hole interior at $s < 0$. Inequivalent solutions are parametrized by $\phi(0)$ and $\tilde{f}(0)$. The $\phi(0)$ initial value gives the value of the area coordinate at the horizon through the relation $r = \mathrm{e}^{-\phi}$ and $\tilde{f}(0)$ determines the magnitude of the radial two-form field at the horizon. A shift of $\rho(0)$ amounts to a global rescaling of the $s$ coordinate and does not affect the geometry.

As discussed in [13], $\phi(0)$ and $\tilde{f}(0)$ cannot be varied independently while preserving the asymptotically Lifshitz character of the geometry. In the $z = 2$ case considered in that paper, there is a zero mode of the linearized system of equations near the Lifshitz fixed point, which must be set to zero for the system to approach the fixed point geometry (1.2) as $r \to \infty$. This requires a fine-tuning of parameters which uniquely determines $\tilde{f}(0)$ in terms of $\phi(0)$ or vice versa. In [15], it was shown that at $z > 2$, the zero mode is replaced by a power-law growing mode which must be set to zero to obtain an asymptotically Lifshitz geometry. The question was more subtle at $z < 2$ where instead there is a mode with a weak power-law fall-off but a finite energy argument [15, 21] may be employed to conclude that this mode must also be set to zero[7].

With the variables that we are using here there is a simple criterion to identify the subset of initial values $\phi(0)$ and $\tilde{f}(0)$ that led to asymptotically Lifshitz black holes for any value of $z > 1$. We already learned from (2.19) that the numerical integration toward $s > 0$, i.e. toward the asymptotic region, will terminate at a finite value $s = s_\infty$. We also know that $\mathrm{e}^{2\rho(v,u)} \to r^{2z}$, as $r \to \infty$ for asymptotically Lifshitz geometry. For a given $\phi(0)$ we tune $\tilde{f}(0)$ until the combination $\rho(s) + z\phi(s)$ goes to a finite value in the limit $s \to s_\infty$. Furthermore, through the transformation rule (2.30) for the conformal factor we can read off the Hawking temperature of the black hole:

$$T_H = \frac{\kappa}{2\pi} = \frac{1}{2\pi\sqrt{s_\infty}} \lim_{s\to s_\infty} \mathrm{e}^{-\rho(s)-z\phi(s)}, \tag{2.39}$$

once we have fine-tuned the initial data to give a finite limit. This method works the same way for both $z > 2$ and $z < 2$. Although the unwanted mode is slowly decaying as a function of $r$ when $r \to \infty$ in the $z < 2$ case, it has a growing amplitude as a function of $s$ due to the rapid growth of $\frac{\mathrm{d}r}{\mathrm{d}r_*}$ as $s \to s_\infty$.

A numerical solution for both the exterior and interior geometry can now be obtained by separately integrating toward positive and negative $s$, using the same fine-tuned initial data, and then patching the two solutions together across $s = 0$. Figure 2 shows a numerical black hole solution at $z = 4$ obtained in this manner. The curvature singularity is at $s \to -\infty$ in these coordinates and the numerical evaluation will break down before it is reached.

### *2.3. Global geometry of generic Lifshitz black holes*

We now give an argument that the conformal diagram in figure 1 applies to a generic Lifshitz black hole solution that has a single non-degenerate horizon and is obtained from the action (1.4), for some value of $z > 1$. To do that, one examines the asymptotic behavior of solutions to the system of equations (2.32)–(2.34) near the singularity, i.e. as $s \to -\infty$. The structure of the equations restricts the asymptotic behavior to one of two types. The first type has

$$\text{I:} \quad \mathrm{e}^{\phi} = (-s)^{\alpha}\,\mathrm{e}^{\phi_0} + \cdots, \quad \mathrm{e}^{\rho} = (-s)^{-\alpha-1/2}\,\mathrm{e}^{\rho_0} + \cdots, \quad \tilde{f} = (-s)^{-2\alpha} f_0 + \cdots, \tag{2.40}$$

[7] By the energy argument of [15], a second mode of the linearized system should also be set to zero in the $z < 2$ case, leading to at best a discrete spectrum of Lifshitz black holes at $z < 2$. This condition is too strong, indicating a problem with the background subtraction used in [15]. An alternative definition of the energy of asymptotically Lifshitz solutions, based on boundary counterterms, recently appeared in [21] for which only a single mode needs to be fine-tuned away in order to have finite energy at $z < 2$.

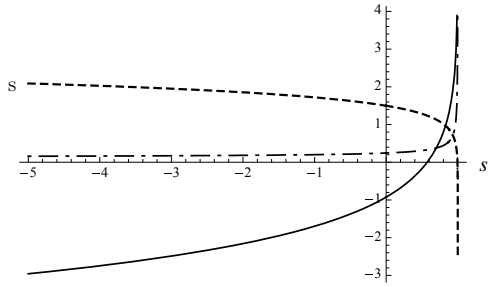


**Figure 2.** Numerical solution for a $z = 4$ Lifshitz black hole with $\rho$ solid, $\phi$ dashed and $f$ dot-dashed. The horizon is at $s = 0$ and $r \to \infty$ corresponds to $s \to 1$.

where $\alpha$, $\phi_0$, $\rho_0$ and $f_0$ are non-universal constants. The assumption that $r \to 0$ as $s \to -\infty$ amounts to the requirement $\alpha > 0$ but otherwise these constants are unrestricted *a priori*[8].

With $\alpha > 0$ the last term in (2.32), the last two terms in (2.33) and the next to last term in (2.34) are sub-leading for this type of solution. The remaining terms in (2.32) cancel automatically at leading order, while (2.33) and (2.34) are satisfied at leading order if

$$\frac{k}{8}\,\mathrm{e}^{2\rho_0+2\phi_0} = -\alpha^2, \qquad f_0^2\,\mathrm{e}^{4\phi_0} = \frac{z}{2}. \tag{2.41}$$

It follows that this type of asymptotic behavior can only be realized in a $k = -1$ geometry. It can be easily checked that the $z = 2$ topological black hole solution is of this type with $\alpha = \frac{1}{2}$.

The other possible behavior near the singularity is

$$\text{II:} \qquad \mathrm{e}^{\phi} = (-s)^{\beta}\,\mathrm{e}^{\phi_0} + \cdots, \qquad \mathrm{e}^{\rho} = (-s)^{-2\beta-1/2}\,\mathrm{e}^{\rho_0} + \cdots, \qquad \tilde{f} = f_0 + \cdots,$$
$$\tilde{f}' = (-s)^{-2\beta-1} f_1 + \cdots, \tag{2.42}$$

with $\beta > 0$. In this type of solution the last term in (2.32), the fourth and fifth terms in (2.33) and the fourth term in (2.34) are subleading as $s \to -\infty$. The remainder of (2.32) is automatically satisfied at leading order, while (2.33) and (2.34) require

$$\frac{f_0^2}{8}\,\mathrm{e}^{2\rho_0+4\phi_0} = \beta^2, \qquad f_1^2 = \frac{3z}{4} f_0^2\,\mathrm{e}^{2\rho_0}. \tag{2.43}$$

This time around there is no restriction on the value of $k$. The exact $z = 4$ black hole solutions fall into this category, with $\beta = \frac{3}{8}$ in the $k = 1$ case and $\beta = \frac{1}{8}$ in the $k = -1$ case.

The Ricci scalar diverges in the $s \to -\infty$ limit. For type I solutions, the leading behavior is $R = \frac{1}{L^2 r^2} + \cdots$, while for type II solutions we find $R = \frac{3 f_0^2}{L^2 r^4} + \cdots$. The curvature singularity at $r \to 0$ is always null. This follows immediately from the fact that

$$\mathrm{e}^{2\rho} \to 0, \qquad \text{as} \quad s \to -\infty, \tag{2.44}$$

for both allowed types of asymptotic behavior. As a result, the conformal diagram in figure 1 describes generic asymptotically Lifshitz black holes with a single non-degenerate horizon that are obtained from the action (1.4).

In the notation used in [13], appropriately continued to inside the horizon, a type I solution has $f \propto r^{1-z}$, $g \propto r^2$, $h \propto 1$ and $j \propto r^{-1}$, for small $r$. The corresponding limiting behavior of a solution of type II is $f \propto r^{2-z}$, $g \propto r^2$, $h \propto r^{-2}$ and $j \propto r^{-2}$.

[8] We note that our argument assumes that $r \to 0$ as $s \to -\infty$ and does not preclude the existence of solutions with a smooth inner horizon at which $r \to r_-$ as $s \to -\infty$ for some finite $r_- > 0$. On the other hand, none of the known exact solutions at $z > 1$ have such an inner horizon.

## 3. Charged Lifshitz black holes

We wish to extend the notion of a holographic superconductor to systems with Lifshitz scaling. In order to do this, we need to introduce some additional ingredients to the gravity model that we have been considering. As it stands, the model has only a single characteristic length scale and does not support a superconducting transition, or any other phase transition for that matter. If we want to make phase transitions possible, we need to introduce a new scale into the problem. This can be seen explicitly as follows. The gravitational dual of a holographic superconductor is a charged plane-symmetric black hole with hair [4], so for this application we work with $k = 0$ geometries of the form

$$\mathrm{d}s^2 = L^2[-\mathrm{e}^{2\rho(v,u)}\,\mathrm{d}v\,\mathrm{d}u + \mathrm{e}^{-2\phi(v,u)}(\mathrm{d}x^2 + \mathrm{d}y^2)]. \tag{3.1}$$

The plane-symmetric black hole geometry has a scaling symmetry, which is absent for spherical or hyperbolic horizons. The metric is invariant under a global rescaling of the planar coordinates $x, y \to e^{\alpha}x, e^{\alpha}y$ accompanied by a uniform shift $\phi \to \phi + \alpha$ while keeping $\rho$, $v$ and $u$ unchanged. On the other hand, such a shift changes the Hawking temperature (2.39). Since different non-zero Hawking temperatures can be mapped into each other by scale transformations they are all physically equivalent in this system and there cannot be any phase transitions. Another way to state this is that in a scale invariant theory at finite temperature there is no other length scale apart from that defined by the temperature itself and therefore different temperatures must be physically equivalent.

There are different ways to add another length scale to the Lifshitz system. We chose to do this by letting our black holes carry an electric charge, which couples to a Maxwell field $\mathcal{F}_{(2)}$. This corresponds to introducing a non-zero charge density into the dual field theoretic system [4] and adds a term to the action

$$S_{\mathcal{F}} = -\frac{1}{2}\int *\mathcal{F}_{(2)} \wedge \mathcal{F}_{(2)}, \tag{3.2}$$

which has the same form as the kinetic term of $F_{(2)}$ and contributes in same way to the field equations. Introducing a new gauge field may, at first sight, appear to be an unnecessary complication given that the model already has a two-form field strength, $F_{(2)}$, and a three-form field strength, $H_{(3)}$, which couples to the two-form field and could be viewed as a form of charged matter. While such an interpretation could in principle be pursued, we find it more useful to consider $F_{(2)}$ and $H_{(3)}$ as auxiliary fields, that only couple to gravity, and whose only role is to give rise to gravitational backgrounds with Lifshitz scaling. We are then free to separately include the physical electromagnetic field $\mathcal{F}_{(2)}$ and introduce charged matter that couples to it but not to the Lifshitz form fields. The manner in which we construct our holographic superconductors with Lifshitz scaling is analogous to the corresponding construction for the $z = 1$ case in [4]. In fact, in the limit $z \to 1$, our system reduces to the one considered by those authors and we have used this to check our numerical algorithm against known results for $z = 1$.

Writing

$$\mathcal{F}_{(2)} = L\, p_{vu}(v,u)\,\mathrm{d}v \wedge \mathrm{d}u, \tag{3.3}$$

the Maxwell equations for $\mathcal{F}_{(2)}$ reduce to

$$\partial_v(\mathrm{e}^{-2\rho-2\phi}p_{vu}) = 0 = \partial_u(\mathrm{e}^{-2\rho-2\phi}p_{vu}). \tag{3.4}$$

The general solution can be written as

$$p_{vu} = Q\,\mathrm{e}^{2\rho+2\phi}, \tag{3.5}$$

and has a simple interpretation as the Coulomb field of a point charge. Now consider a black hole with charge $Q$ in the $s$ variable. Since the new gauge field does not couple directly to the original Lifshitz gauge fields, the field equation for $\tilde{f}$ (2.32) remains unchanged while equations (2.33) and (2.34) pick up terms involving the black hole charge[9]:

$$0 = s\phi'' + \phi' - 2s\phi'^2 + \frac{k}{4}\,\mathrm{e}^{2\rho+2\phi} + \frac{(z^2+z+4)}{8}\,\mathrm{e}^{2\rho} - \frac{1}{4}(\tilde{f}^2+Q^2)\,\mathrm{e}^{2\rho+4\phi}, \tag{3.6}$$

$$0 = s\rho'' + \rho' - s\phi'^2 + \frac{k}{4}\,\mathrm{e}^{2\rho+2\phi} - \frac{1}{2}(\tilde{f}^2+Q^2)\,\mathrm{e}^{2\rho+4\phi} - \frac{s}{2z}\,\mathrm{e}^{4\phi}\,\tilde{f}'^2. \tag{3.7}$$

The field equations can be numerically integrated as before and we will present some numerical results below, but before that we present some exact solutions. In the first example we recover the well-known AdS–Reissner–Nordström solution as a special case with $z = 1$ and $\tilde{f} = 0$. This provides a check of the formalism. The remaining examples are new and describe one-parameter families of charged Lifshitz black holes at $z = 4$.

### *3.1. AdS–RN black holes at $z = 1$*

The AdS–Reissner–Nordström solution at $z = 1$ describes an electrically charged black hole in asymptotically AdS spacetime. In the variables we are using, it is given by

$$\mathrm{e}^{2\rho(r_*)} = r^2 + k - \frac{1}{r}\left(r_h^3 + kr_h + \frac{Q^2}{r_h}\right) + \frac{Q^2}{r^2}, \tag{3.8}$$

with $k = +1, 0, -1$ for a spherical, flat or hyperbolic horizon at $r = r_h$. The relationship between the area and tortoise coordinates is

$$\frac{\mathrm{d}r}{\mathrm{d}r_*} = r^2 + k - \frac{1}{r}\left(r_h^3 + kr_h + \frac{Q^2}{r_h}\right) + \frac{Q^2}{r^2}, \tag{3.9}$$

and the Lifshitz gauge field $\tilde{f}$ is everywhere vanishing. It can be easily checked that

$$\mathrm{e}^{2\rho(s)} = \frac{1}{\kappa^2 s}\,\mathrm{e}^{2\rho(r_*)}, \qquad \mathrm{e}^{-\phi(s)} = r, \tag{3.10}$$

with $s = \mathrm{e}^{2\kappa(r_*-r_*^\infty)}$ is a solution of equations (3.6) and (3.7) with $\tilde{f} = 0$.

The Hawking temperature

$$T_H = \frac{1}{4\pi}\left(3r_h + \frac{k}{r_h} - \frac{Q^2}{r_h^3}\right) \tag{3.11}$$

goes to zero as the charge approaches the extremal value for a given horizon area:

$$T_H \to 0 \qquad \text{as} \quad Q^2 \to Q^2_{\text{ext}} = 3r_h^4 + kr_h^2, \tag{3.12}$$

as shown in figure 3.

### *3.2. Exact solutions for charged black holes at $z = 4$*

Numerical work is required in order to explore the full parameter range of asymptotically Lifshitz black hole solutions at $z > 1$ but exact solutions are useful, even if they only apply in special cases. We have found a family of exact charged black hole solutions for $z = 4$, which

[9] For completeness we allow for $k \neq 0$ in the field equations but we are primarily interested in the $k = 0$ case for the application to holographic superconductors.

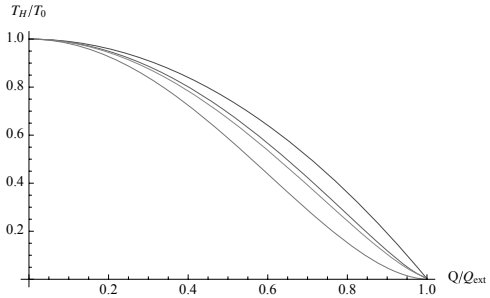


**Figure 3.** The Hawking temperature of charged black holes with $r_h = 1, k = +1$ for $z = 4, 2, \frac{3}{2}, 1$ from bottom to top. The temperature is normalized to the temperature of the corresponding uncharged black hole while the charge is normalized to the corresponding extremal charge. The curve for $z = 1$ is plotted from the analytic expression (3.11) while the $z > 1$ curves are obtained from numerical solutions.

generalize the isolated $z = 4$ solutions discussed in section 2.1. In the notation of equations (2.2)–(2.3) the metric is given by

$$f(r) = \frac{1}{g(r)} = \sqrt{1 + \frac{k}{10r^2} - \frac{3k^2}{400r^4} - \frac{Q^2}{2r^4}}, \tag{3.13}$$

with $k = +1, 0, -1$. The metric reduces to the $z = 4$ solutions of section 2.1 when $Q = 0$ and $k = \pm 1$ while the $Q = 0, k = 0$ case reduces to the $z = 4$ Lifshitz fixed point geometry.

The tortoise coordinate is given by equation (2.13) with

$$b_1 = \sqrt{\frac{k^2}{100} + \frac{Q^2}{2}} - \frac{k}{20}, \tag{3.14}$$

$$b_2 = \sqrt{\frac{k^2}{100} + \frac{Q^2}{2}} + \frac{k}{20}. \tag{3.15}$$

The change to $U, V$ coordinates in (2.14) leads to a metric of the form (2.15), with the new values of $b_1$ and $b_2$, which is nonsingular at the horizon. The Lifshitz gauge field can be obtained by inserting the $\rho(s)$ and $\phi(s)$ read off from (3.13) into (3.6) and solving for $\tilde{f}(s)$. One finds that $\tilde{f} = \sqrt{6}\left(r^2 + \frac{k}{20}\right)$ is independent of the black hole charge $Q$.

The Hawking temperature is $T_H = \frac{\kappa}{2\pi}$ with

$$\kappa = Q^2 + \frac{k^2}{50} - \frac{k}{10}\sqrt{\frac{k^2}{100} + \frac{Q^2}{2}}. \tag{3.16}$$

The $k = 0$ metric has $b_1 = b_2$ and takes a particularly simple form in $U, V$ coordinates:

$$\mathrm{d}s^2 = L^2\left(-\frac{r^8}{Q^2}\,\mathrm{d}U\,\mathrm{d}V + r^2(\mathrm{d}\theta^2 + \theta^2\,\mathrm{d}\varphi^2)\right). \tag{3.17}$$

In this case the horizon is at $r = \frac{Q}{\sqrt{2}}$ and the Hawking temperature is $T_H = \frac{Q^2}{2\pi}$, both of which go to zero in the $Q \to 0$ limit.

Returning to the more general exact solution in (3.13), the Ricci scalar is given by

$$R = \frac{1}{L^2}\left(\frac{3Q^2}{r^4} + \frac{9k^2}{200r^4} - \frac{3k}{5r^2} - 54\right) \tag{3.18}$$

and is singular at $r \to 0$. The curvature singularity is null and the conformal diagram remains the same as in figure 1. In particular, unlike ordinary Reissner–Nordström black holes, these charged Lifshitz black holes do not have an inner horizon away from the singularity at $r \to 0$. The general analysis from section 2.3 of the asymptotic behavior near the singularity can be extended to the case of charged Lifshitz black holes. They exhibit type II behavior with the replacement $f_0^2 \to f_0^2 + Q^2$ in equation (2.42).

### *3.3. Numerical charged black hole solutions*

The field equations with the additional Maxwell field included were presented earlier in equations (2.32), (3.6) and (3.7). The initial values giving a smooth horizon at $s = 0$ are modified as follows by a non-vanishing black hole charge:

$$\phi'(0) = \frac{1}{4}\left(-k\,\mathrm{e}^{2\phi(0)} - \frac{(z^2+z+4)}{2} + (\tilde{f}(0)^2 + Q^2)\,\mathrm{e}^{4\phi(0)}\right)\mathrm{e}^{2\rho(0)}, \tag{3.19}$$

$$\rho'(0) = \frac{1}{2}\left(-\frac{k}{2}\,\mathrm{e}^{2\phi(0)} + (\tilde{f}(0)^2 + Q^2)\,\mathrm{e}^{4\phi(0)}\right)\mathrm{e}^{2\rho(0)} \tag{3.20}$$

$$\tilde{f}'(0) = \frac{z}{2}\,\tilde{f}(0)\,\mathrm{e}^{2\rho(0)}. \tag{3.21}$$

For any given value of $z > 1$, there is a two-parameter family of asymptotically Lifshitz black hole solutions. If we take the charge $Q$ and $\phi(0)$ as independent parameters then $\tilde{f}(0)$ needs to be fine-tuned in order to obtain the correct asymptotic behavior as $s \to s_\infty$. Changing the value of $\rho(0)$ amounts to a global rescaling of the $s$ coordinate and does not change the geometry.

The numerical integration proceeds in the same way as before and plots of numerical solutions are qualitatively similar to figure 2. The existence of a new length scale in the system can be seen in the Hawking temperature obtained from (2.39) for black holes with different $Q$ keeping the area coordinate at the horizon fixed. Figure 3 shows the black hole temperature as a function of $Q$ for several values of $z$. All the black holes have $\phi(0) = 0$. In order to facilitate comparison, the temperature of all the black holes for a given $z$ is normalized to the Hawking temperature of a $Q = 0$ black hole with the same value of $z$ and similarly the charge is normalized to the extremal charge of black holes with the given value of $z$.

## 4. Coupling to charged matter

The final ingredient is a scalar field $\psi$, which is charged under the new gauge field $\mathcal{F}_{(2)}$ but neutral under the original Lifshitz fields $F_{(2)}$ and $H_{(3)}$. This allows our black holes to grow scalar hair and, under certain conditions, the black hole hair corresponds to the condensation of a charged operator at low temperatures in the dual field theory. The overall picture is quite similar to the one obtained for the charged AdS black holes in [4] and extends the notion of a holographic superconductor to systems that exhibit Lifshitz scaling with $z > 1$.

### *4.1. Charged scalar field*

The scalar field action is given by

$$S_\psi = -\frac{1}{2}\int \mathrm{d}^4x\sqrt{-g}(g^{\mu\nu}(\partial_\mu\psi^* + \mathrm{i}q\mathcal{A}_\mu\psi^*)(\partial_\nu\psi - \mathrm{i}q\mathcal{A}_\nu\psi) + m^2\psi^*\psi), \tag{4.1}$$

where $\mathcal{A}_\mu$ are the components of a one-form potential for the two-form field strength $\mathcal{F}_{(2)}$ and $q$ is the charge of $\psi$. There is an analog in this system of the Breitenlohner–Freedman bound [5] on the allowed mass of the scalar field:

$$L^2 m^2 > -\frac{(z+2)^2}{4}. \tag{4.2}$$

The requirement that the corresponding Euclidean action be finite places restrictions on the asymptotic behavior of the scalar field as $r \to \infty$. This was worked out in detail for the $z = 2$ case in [12][10] and, since the analysis carries over to general $z > 1$ in a straightforward way, we merely summarize some results without going into details.

The scalar field equation obtained from (4.1) has two independent solutions $\psi(x^\mu) = c_+\psi_+(x^\mu) + c_-\psi_-(x^\mu)$ that have the asymptotic form

$$\psi_\pm(x^\mu) \to r^{-\Delta_\pm}\tilde{\psi}_\pm(\tau, \theta, \varphi) + \cdots, \tag{4.3}$$

at large $r$, where

$$\Delta_\pm = \frac{z+2}{2} \pm \sqrt{\left(\frac{z+2}{2}\right)^2 + m^2 L^2}. \tag{4.4}$$

If the mass squared satisfies

$$L^2 m^2 > 1 - \left(\frac{z+2}{2}\right)^2, \tag{4.5}$$

then only $\psi_+$ falls off sufficiently rapidly as $r \to \infty$ and the scalar field has the boundary condition

$$\psi(x^\mu) \to r^{-\Delta_+}\left(\tilde{\psi}_+(\tau, \theta, \varphi) + O\left(\frac{1}{r^2}\right)\right). \tag{4.6}$$

The scalar field is then dual to an operator of dimension $\Delta_+ > \frac{z}{2} + 2$.

If, on the other hand, the mass squared is in the range

$$1 - \left(\frac{z+2}{2}\right)^2 > L^2 m^2 > -\left(\frac{z+2}{2}\right)^2, \tag{4.7}$$

then both $\psi_+$ and $\psi_-$ have sufficiently rapid falloff and there is a choice of two different quantizations for the scalar field. In one case the scalar field is asymptotic to $\psi_+$ and dual to an operator of dimension $\Delta_+$ with $\frac{z}{2} + 1 < \Delta_+ < \frac{z}{2} + 2$. In the other case the scalar field is asymptotic to $\psi_-$ and dual to an operator of dimension $\Delta_-$ with $\frac{z}{2} < \Delta_- < \frac{z}{2} + 1$.

In our numerical calculations we set the scalar mass squared to

$$L^2 m^2 = \frac{1}{4} - \left(\frac{z+2}{2}\right)^2 \tag{4.8}$$

which is inside the range where there is a choice of two boundary theories. This value leads to convenient values for the operator dimensions, $\Delta_\pm = \frac{z+2}{2} \pm \frac{1}{2}$. Nonlinear descendants of the leading scalar field modes are suppressed by $O\left(\frac{1}{r^2}\right)$ at $r \to \infty$ and this choice of mass squared ensures that the first descendant of $\psi_-$ falls off faster than $\psi_+$.

[10] The discussion in [12] was in turn based on earlier work on symmetry breaking in the context of the AdS/CFT correspondence [22].

### *4.2. Lifshitz black holes with scalar hair*

We will look for static spherically symmetric black hole solutions using a metric of the form (2.18). We make the gauge choice

$$\mathcal{A} = L(a_v \, \mathrm{d}v + a_u \, \mathrm{d}u), \tag{4.9}$$

with $a_v = a_u \equiv a$. In this gauge, the Maxwell equations for static configurations imply the equation

$$\psi^* \frac{\mathrm{d}\psi}{\mathrm{d}r_*} - \psi \frac{\mathrm{d}\psi^*}{\mathrm{d}r_*} = 0, \tag{4.10}$$

which implies, in turn, that the phase of $\psi$ is constant and we can take the scalar field to be real valued. The remaining non-trivial Maxwell equation is

$$\frac{\mathrm{d}}{\mathrm{d}r_*}\left(\mathrm{e}^{-2\rho-2\phi}\frac{\mathrm{d}a}{\mathrm{d}r_*}\right) + q^2L^2\psi^2\,\mathrm{e}^{-2\phi}a = 0, \tag{4.11}$$

which agrees with (3.4) if $q = 0$, i.e. when $\psi$ is a neutral scalar field that does not act as a source for the Maxwell field.

The next step is to write equations for static configurations using the $s$ variable, in which the metric is non-degenerate at the horizon. Since $a$ is a component of a one-form potential, it transforms under a change of coordinates:

$$a(r_*) = \frac{\mathrm{d}s}{\mathrm{d}r_*}a(s) = 2\kappa \, s \, a(s). \tag{4.12}$$

It follows that the potential vanishes at the horizon in tortoise coordinates as long as it remains a smooth function there in the $s$ variable. The Maxwell equation becomes

$$\frac{\mathrm{d}}{\mathrm{d}s}\left(\mathrm{e}^{-2\rho-2\phi}\left(a + s\frac{\mathrm{d}a}{\mathrm{d}s}\right)\right) + \frac{q^2L^2}{4}\psi^2\,\mathrm{e}^{-2\phi}a = 0, \tag{4.13}$$

and for a smooth horizon at $s = 0$ the initial data must satisfy

$$-a'(0) + a(0)(\rho'(0) + \phi'(0)) = \frac{q^2L^2}{8}\psi(0)^2 a(0)\,\mathrm{e}^{2\rho(0)}. \tag{4.14}$$

The value of $a(0)$ is a free parameter that determines the black hole charge. To see this, we note that for $q = 0$ we have $a + sa' = \frac{Q}{4}\,\mathrm{e}^{2\phi+2\rho}$, with $Q$ the black hole charge, and in this case

$$a(0) = \frac{Q}{4}\,\mathrm{e}^{2\phi(0)+2\rho(0)}. \tag{4.15}$$

If there is a non-vanishing scalar field with $q \neq 0$, then the solution of the Maxwell equation will no longer be a simple Coulomb field but we are nevertheless free to write $a(0)$ the same way as in (4.15) and the constant $Q$ can still be interpreted as the total charge inside the black hole.

The scalar field equation in the $s$ variable is

$$0 = s\psi'' + \psi' - 2s\phi'\psi' + 4sq^2L^2a^2\psi - \frac{m^2L^2}{4}\,\mathrm{e}^{2\rho}\psi, \tag{4.16}$$

with the following condition on initial data at a smooth horizon:

$$\psi'(0) = \frac{m^2L^2}{4}\,\mathrm{e}^{2\rho(0)}\psi(0). \tag{4.17}$$

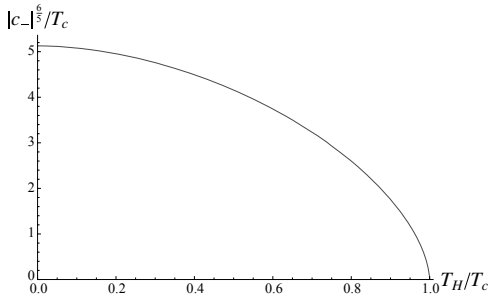


**Figure 4.** Holographic superconductivity at $z = 3/2$. The graph shows the condensate in the $\mathcal{O}_-$ theory as a function of temperature normalized to the critical temperature.

The equation for $\tilde{f}$ remains unchanged but the remaining two field equations get contributions from the scalar action:

$$0 = s\phi'' + \phi' - 2s\phi'^2 + \frac{k}{4}\,\mathrm{e}^{2\rho+2\phi} + \frac{(z^2+z+4)}{8}\,\mathrm{e}^{2\rho} - \frac{1}{4}\tilde{f}^2\,\mathrm{e}^{2\rho+4\phi} - 4(a + s\,a')^2\,\mathrm{e}^{-2\rho} - \frac{m^2L^2}{16}\,\mathrm{e}^{2\rho}\psi^2, \tag{4.18}$$

$$0 = s\rho'' + \rho' - s\phi'^2 + \frac{k}{4}\,\mathrm{e}^{2\rho+2\phi} - \frac{1}{2}\tilde{f}^2\,\mathrm{e}^{2\rho+4\phi} - \frac{s}{2z}\,\mathrm{e}^{4\phi}\,\tilde{f}'^2 - 8(a + s\,a')^2\,\mathrm{e}^{-2\rho} + \frac{s}{4}\psi'^2 - sq^2L^2a^2\psi^2, \tag{4.19}$$

and the conditions on the initial data become

$$\phi'(0) = \frac{1}{4}\left(-k\,\mathrm{e}^{2\phi(0)} - \frac{(z^2+z+4)}{2} + (\tilde{f}(0)^2 + Q^2)\,\mathrm{e}^{4\phi(0)} + \frac{m^2L^2}{4}\psi(0)^2\right)\mathrm{e}^{2\rho(0)}, \tag{4.20}$$

$$\rho'(0) = \frac{1}{2}\left(-\frac{k}{2}\,\mathrm{e}^{2\phi(0)} + (\tilde{f}(0)^2 + Q^2)\,\mathrm{e}^{4\phi(0)}\right)\mathrm{e}^{2\rho(0)}. \tag{4.21}$$

For given values of $z$, $k$, $q$ and $m^2$ there is now a three-parameter family of smooth initial values for the dynamical fields at the horizon given by $Q$, $\psi(0)$ and $f(0)$. As before, the initial data must be fine-tuned to obtain an asymptotically Lifshitz geometry and we take the black hole charge $Q$ and the value of the scalar field at the horizon $\psi(0)$ as independent parameters.

### *4.3. Superconducting phase*

In order to study black hole geometries that are dual to a holographic superconductor we set $k = 0$. For a given value of $z$ we set the scalar mass squared to the value in (4.8) and select a value for the scalar field charge $q$. We then find numerical black hole solutions with scalar hair for a range of $Q$ and $\psi(0)$ and study the asymptotic large $r$ behavior of the scalar hair in each case. The signal of a superconducting condensate in one or the other boundary theory is to have either

$$c_+ = 0 \qquad \text{and} \qquad \langle\mathcal{O}_-\rangle = c_- \neq 0 \tag{4.22}$$

or

$$c_- = 0 \qquad \text{and} \qquad \langle \mathcal{O}_+ \rangle = c_+ \neq 0. \tag{4.23}$$

The curve of vanishing $c_+$ ($c_-$) in the $Q$ versus $\psi(0)$ plane can be tracked, tabulating the value of $c_-$ ($c_+$) as a function of the black hole temperature along the way. Figure 4 shows the result of this procedure for hairy Lifshitz black holes at $z = 3/2$ for the scalar field charge $q = 1$. There is clear evidence of condensation in the corresponding boundary theory. Analogous results are obtained for other values of $q$ and more general $z > 1$ but we defer a more detailed study of the parameter space to [23].

## 5. Conclusions

In this paper we have given a holographic description of superconductors with Lifshitz scaling. The key ingredient is a family of black holes with scalar hair in an asymptotically Lifshitz space time. These black holes are interesting in their own right, and we have studied their geometry in detail uncovering several intriguing properties, including the presence of null singularities. Our work is an extension of the previous work on Lifshitz black holes in [13–15].

As in the case of the more conventional holographic superconductors at $z = 1$, see [1, 2], our black holes need to be equipped with additional charges in order for a phase transition to a superconducting phase to occur. We provide such a construction and show how a charged scalar in this background condenses at a critical temperature, indicating a superconducting phase.

Our results demonstrate that phase transitions leading to superconductivity at low temperature, can be given a holographic description also for Lifshitz points. Such superconductors are known from solid state physics, see e.g. [24], and we hope that our results will be useful for further studies of these systems. Some of their properties are different from usual superconductors, and it would be interesting to see whether this has a holographic counterpart.

## Acknowledgments

This work was supported in part by the Göran Gustafsson foundation, the Swedish Research Council (VR), the Icelandic Research Fund, the University of Iceland Research Fund, and the Eimskip Research Fund at the University of Iceland.

## References

[1] Gubser S S 2008 Breaking an Abelian gauge symmetry near a black hole horizon *Phys. Rev.* D **78** 065034 (arXiv:0801.2977 [hep-th])

[2] Hartnoll S A, Herzog C P and Horowitz G T 2008 Building a holographic superconductor *Phys. Rev. Lett.* **101** 031601 (arXiv:0803.3295 [hep-th])

[3] Maldacena J M 1998 The large N limit of superconformal field theories and supergravity *Adv. Theor. Math. Phys.* **2** 231
Maldacena J M 1999 *Int. J. Theor. Phys.* **38** 1113 (arXiv:hep-th/9711200)

[4] Hartnoll S A, Herzog C P and Horowitz G T 2008 Holographic superconductors *J. High Energy Phys.* JHEP0812(2008)015 (arXiv:0810.1563 [hep-th])

[5] Breitenlohner P and Freedman D Z 1982 Stability in Gauged extended supergravity *Ann. Phys.* **144** 249

[6] Hartnoll S A 2009 Lectures on holographic methods for condensed matter physics *Class. Quantum Grav.* **26** 224002 (arXiv:0903.3246 [hep-th])

[7] Herzog C P 2009 Lectures on holographic superfluidity and superconductivity *J. Phys. A: Math. Theor.* **42** 343001 (arXiv:0904.1975 [hep-th])

[8] Rokhsar D S and Kivelson S A 1988 Superconductivity and the quantum hard-core dimer gas *Phys. Rev. Lett.* **61** 2376
[9] Ardonne E, Fendley P and Fradkin E 2004 Topological order and conformal quantum critical points *Ann. Phys.* **310** 493 (arXiv:cond-mat/0311466)
[10] Fradkin E, Huse D A, Moessner R, Oganesyan V and Sondhi S L 2004 Bipartite Rokhsar–Kivelson points and Cantor deconfinement *Phys. Rev.* B **69** 224415 (arXiv:cond-mat/0311353)
[11] Vishwanath A, Balents L and Senthil T 2004 Quantum criticality and deconfinement in phase transitions between valence bond solids *Phys. Rev.* B **69** 224416 (arXiv:cond-mat/0311085)
[12] Kachru S, Liu X and Mulligan M 2008 Gravity duals of Lifshitz-like fixed points *Phys. Rev.* D **78** 106005 (arXiv:0808.1725 [hep-th])
[13] Danielsson U H and Thorlacius L 2009 Black holes in asymptotically Lifshitz spacetime *J. High Energy Phys.* JHEP0903(2009)070 (arXiv:0812.5088 [hep-th])
[14] Mann R B 2009 Lifshitz topological black holes *J. High Energy Phys.* JHEP0906(2009)075 (arXiv:0905.1136 [hep-th])
[15] Bertoldi G, Burrington B A and Peet A 2009 Black holes in asymptotically Lifshitz spacetimes with arbitrary critical exponent *Phys. Rev.* D **80** 126003 (arXiv:0905.3183 [hep-th])
[16] Bertoldi G, Burrington B A and Peet A W 2009 Thermodynamics of black branes in asymptotically Lifshitz spacetimes *Phys. Rev.* D **80** 126004 (arXiv:0907.4755 [hep-th])
[17] Taylor M 2008 Non-relativistic holography arXiv:0812.0530 [hep-th]
[18] Azeyanagi T, Li W and Takayanagi T 2009 On string theory duals of Lifshitz-like fixed points *J. High Energy Phys.* JHEP0906(2009)084 [arXiv:0905.0688 [hep-th]]
[19] Pang D W 2009 A note on black holes in asymptotically Lifshitz spacetime arXiv:0905.2678 [hep-th]
[20] Birnir B, Giddings S B, Harvey J A and Strominger A 1992 Quantum black holes *Phys. Rev.* D **46** 638 (arXiv:hep-th/9203042)
[21] Ross S F and Saremi O 2009 Holographic stress tensor for non-relativistic theories *J. High Energy Phys.* JHEP0909(2009)009 (arXiv:0907.1846 [hep-th])
[22] Klebanov I R and Witten E 1999 AdS/CFT correspondence and symmetry breaking *Nucl. Phys.* B **556** 89 (arXiv:hep-th/9905104)
[23] Brynjolfsson E J, Danielsson U H, Thorlacius L and Zingg T 2009 in preparation
[24] Buzdin A I and Kulic M L 1984 Unusual behaviour of superconductors near the tricritical Lifshitz point *J. Low Temp. Phys.* **54** 203

# Paper II

JHEP

Published for SISSA by Springer

Received: *May 4, 2010*
Revised: *June 30, 2010*
Accepted: *July 14, 2010*
Published: *August 5, 2010*



# Black hole thermodynamics and heavy fermion metals

**E.J. Brynjolfsson,**[a] **U.H. Danielsson,**[b] **L. Thorlacius**[a,c] **and T. Zingg**[a,c]

[a] *University of Iceland, Science Institute, Dunhaga 3, IS-107 Reykjavik, Iceland*
[b] *Institutionen för fysik och astronomi, Uppsala Universitet, Box 803, SE-751 08 Uppsala, Sweden*
[c] *NORDITA, Roslagstullsbacken 23, SE-106 91 Stockholm, Sweden*

*E-mail:* erlingbr@hi.is, ulf.danielsson@physics.uu.se, lth@nordita.org, zingg@nordita.org

Abstract: Heavy fermion alloys at critical doping typically exhibit non-Fermi-liquid behavior at low temperatures, including a logarithmic or power law rise in the ratio of specific heat to temperature as the temperature is lowered. Anomalous specific heat of this type is also observed in a simple class of gravitational dual models that exhibit anisotropic scaling with dynamical critical exponent $z > 1$.

Keywords: Gauge-gravity correspondence, Black Holes

ArXiv ePrint: 1003.5361



doi:10.1007/JHEP08(2010)027

## Contents



JHEP08(2010)027

## 1 Introduction

Heavy fermion systems exhibit very interesting thermodynamic properties at low temperature. The Sommerfeld ratio of the specific heat to temperature at low $T$ is very large in these materials indicating an effective mass for the electrons near the Fermi surface that can be orders of magnitude larger than the free electron mass, hence the term heavy fermions. In low-temperature experiments on certain heavy fermion alloys at critical doping the Sommerfeld ratio does not settle down to a constant, as it would for a conventional Fermi liquid, but continues to rise as the temperature is lowered [1]. This behavior has also been observed in systems at near-critical doping by tuning external parameters such as pressure or magnetic field [1, 2]. The non-Fermi-liquid behavior of the specific heat is attributed to strongly correlated physics, governed by an underlying quantum critical point (see [3–5] for reviews of heavy fermion systems) but a detailed understanding of quantum critical metals remains a key problem in theoretical physics [6].

The last few years have seen increased interest in developing dual gravity models for strongly interacting systems in condensed matter physics (see [7–11] for recent reviews). While the gravitational approach has found a number of interesting applications it should be emphasized that its ultimate relevance to real condensed matter systems remains speculative. The original AdS/CFT conjecture [12], for which there is by now strong evidence, relates maximally supersymmetric 3+1 dimensional Yang-Mills gauge theory with a large number of colors to supergravity on a ten dimensional $AdS_5 \times S_5$ spacetime. In condensed matter physics one is instead interested in systems without supersymmetry where the validity of a gravitational dual description is a more open question. Furthermore, the large

number of colors plays a key role in the supersymmetric gauge theory context in justifying the use of large-scale classical geometry on the gravitational side of the duality and it is at present unclear what the corresponding formal limit would be for the strongly coupled condensed matter systems that one wants to model. These are important issues to settle but in the present paper we pursue a more modest goal of identifying yet another physical effect that can be phenomenologically modeled by a relatively simple dual gravitational system.

Gravity duals have one or more additional spatial dimensions compared to the field theory in question. Finite temperature effects are studied by having a black hole in the higher-dimensional spacetime and when the black hole is electrically charged the Hawking temperature and the black hole charge provide competing energy scales that can lead to interesting dynamics. We will consider quantum critical points in three spatial dimensions that are characterized by a scaling law,

$$t \to \lambda^z t, \qquad \vec{x} \to \lambda \vec{x}\,, \tag{1.1}$$

where the dynamical critical exponent $z$ is in general different from 1. We are particularly interested in quantum phase transitions in heavy fermion alloys where the metal goes from being paramagnetic to being antiferromagnetic as the level of doping or some other external control parameter is varied [1, 2]. Theoretical work based on a lattice Kondo model suggests that the associated quantum critical point exhibits anisotropic scaling with a non-universal dynamical critical exponent that can be fitted by comparison to experimental data [13]. In particular, it was found that $z \approx 2.7$ for the critically doped heavy fermion alloy $CeCu_{5.9}Au_{0.1}$, whose anomalous specific heat was reported in [1].

In [14] it was conjectured that a strongly coupled system at a fixed point governed by anisotropic scaling of this form could be modeled by a gravity theory in a so called Lifshitz spacetime with the metric,[1]

$$ds^2 = L^2 \left( -r^{2z} dt^2 + r^2 d\vec{x}^2 + \frac{dr^2}{r^2} \right), \tag{1.2}$$

which is invariant under the transformation

$$t \to \lambda^z t, \quad \vec{x} \to \lambda \vec{x}, \quad r \to \frac{r}{\lambda}\,. \tag{1.3}$$

Here $L$ is a characteristic length scale, which will determine the magnitude of the negative cosmological constant in the gravity model, and $(t, \vec{x}, r)$ are dimensionless coordinates in the higher dimensional spacetime. The finite temperature physics of such a system is then encoded into the geometry of a black hole, which is asymptotic to the Lifshitz spacetime (1.2).

In this paper we continue our study of asymptotically Lifshitz black holes from [16, 17] placing an emphasis on their thermodynamic properties. We compute the specific heat of charged asymptotically Lifshitz black holes as a function of temperature, keeping the charge density in the dual field theory fixed. At high $T$ the thermodynamic behavior of the dual system is governed by the symmetries of the quantum critical point leading to

[1] See [15] for early work on gravitational backgrounds with anisotropic scaling.



JHEP08(2010)027

a temperature dependence of the specific heat of the form $C \sim T^{3/z}$. This is a direct consequence of scaling and we find the same result in the gravity dual using black hole thermodynamics.

At low $T$, we observe a crossover in the black hole thermodynamics indicating non-trivial collective effects in the dual field theory. For $z = 1$ our system reduces to the thermodynamics of the well-known AdS-RN black branes. In this case, the specific heat divided by $T$ goes to a constant value in the limit of low temperature, which is the same behavior as seen in a conventional Fermi liquid. This result was obtained previously in [18], where it was interpreted as evidence for the presence of a Fermi surface in the dual system. It was noted in [18], however, from a holographic computation of transport properties that the low-energy effective theory near the Fermi surface cannot be that of weakly interacting fermions. Non-Fermi-liquid behavior has also been observed in spectral functions of probe fermions coupled to the $z = 1$ system [19, 20].

For a non-trivial dynamical critical exponent $z > 1$ the black brane thermodynamics calculation is more involved and we have to rely more heavily on numerical computations. Interestingly, we find qualitatively different behavior in this case. The Sommerfeld ratio $C/T$ now continues to rise as we go to lower temperatures, which is indeed the behavior observed in critically doped heavy fermion systems. The ability of gravity models with Lifshitz scaling to capture this non-Fermi-liquid aspect of real quantum critical metals is interesting and is the main result of the present paper.

## 2 The holographic model

The application that we have in mind involves a dual field theory in three spatial dimensions and accordingly the gravity dual is defined on a 4+1 dimensional spacetime to accommodate an emergent extra dimension. Most of our results carry over to other dimensions in a straightforward fashion. In particular, similar conclusions can be drawn about planar systems with $d = 2$.

We work with a 4+1 dimensional version of the holographic model of Kachru et al. [14], as formulated by Taylor [21], and with a Maxwell gauge field added, as in [17]. The bulk classical action for the gravitational sector consists of two parts,

$$S = S_{\text{Einstein-Maxwell}} + S_{\text{Lifshitz}}\,. \tag{2.1}$$

The first term is the usual action of $4 + 1$ dimensional Einstein-Maxwell gravity with a negative cosmological constant,

$$S_{\text{Einstein-Maxwell}} = \int \mathrm{d}^5x\sqrt{-g}\,\left(R - 2\Lambda - \frac{1}{4}F_{\mu\nu}F^{\mu\nu}\right). \tag{2.2}$$

This is followed by a term involving a massive vector field,

$$S_{\text{Lifshitz}} = -\int \mathrm{d}^5x\sqrt{-g}\,\left(\frac{1}{4}\mathcal{F}_{\mu\nu}\mathcal{F}^{\mu\nu} + \frac{c^2}{2}\mathcal{A}_\mu\mathcal{A}^\mu\right), \tag{2.3}$$

whose sole purpose is to provide backgrounds with anisotropic scaling of the form (1.3). We refer to this auxiliary vector field, which only couples to gravity, as the Lifshitz vector



JHEP08(2010)027

field. The original gravity model of [14] was 3+1-dimensional and anisotropic scaling was obtained by including a pair of coupled two- and three-form field strengths. Upon integrating out the three-form field strength, the remaining two-form becomes a field strength of a massive vector and in this form the model is easily extended to general dimensions [21].

The equations of motion obtained from the action (2.1) consist of the Einstein equations, the Maxwell equations, and field equations for the Lifshitz vector,

$$G_{\mu\nu} + \Lambda g_{\mu\nu} = T^{\text{Maxwell}}_{\mu\nu} + T^{\text{Lifshitz}}_{\mu\nu}\,, \tag{2.4}$$

$$\nabla_\nu F^{\nu\mu} = 0\,, \tag{2.5}$$

$$\nabla_\nu \mathcal{F}^{\nu\mu} = c^2 \mathcal{A}^\mu\,, \tag{2.6}$$

with the energy momentum tensors of the Maxwell and Lifshitz vector fields given by

$$T^{\text{Maxwell}}_{\mu\nu} = \frac{1}{2}(F_{\mu\lambda}F_\nu^{\ \lambda} - \frac{1}{4} g_{\mu\nu} F_{\lambda\sigma}F^{\lambda\sigma}), \tag{2.7}$$

$$T^{\text{Lifshitz}}_{\mu\nu} = \frac{1}{2}(\mathcal{F}_{\mu\lambda}\mathcal{F}_\nu^{\ \lambda} - \frac{1}{4} g_{\mu\nu} \mathcal{F}_{\lambda\sigma}\mathcal{F}^{\lambda\sigma}) + \frac{c^2}{2}(\mathcal{A}_\mu\mathcal{A}_\nu - \frac{1}{2} g_{\mu\nu}\mathcal{A}_\lambda\mathcal{A}^\lambda). \tag{2.8}$$

The Lifshitz fixed point geometry (1.2) is a solution of the equations of motion provided the characteristic length scale $L$ is related to the cosmological constant $\Lambda$ via

$$\Lambda = -\frac{z^2 + 2z + 9}{2L^2}\,, \tag{2.9}$$

the mass of the Lifshitz vector field is fine-tuned to $c = \sqrt{3z}/L$, and the Lifshitz vector field has the background value

$$\mathcal{A}_t = \sqrt{\frac{2(z-1)}{z}} L\, r^z\,, \qquad \mathcal{A}_{x_i} = \mathcal{A}_r = 0\,. \tag{2.10}$$

The Maxwell field vanishes in the Lifshitz background, $A_\mu = 0$.

Although we do not do it here, it is straightforward to couple matter to this system. Including a scalar field, for instance, leads to an instability at low $T$ giving rise to holographic superconductors with Lifshitz scaling [17]. It is also interesting to include a coupling to a bulk Dirac spinor and obtain fermion spectral functions along the lines of [19, 20, 22]. We find that the spectral functions in the $z > 1$ theory exhibit many of the same features as in the asymptotically AdS bulk spacetime considered in these earlier works, including peaks at certain values of momentum and frequency, but there are also important differences. In particular, the would be quasiparticle peaks are less sharply defined than their $z = 1$ counterparts.[2]

## 3 Charged black branes

In order to study finite temperature effects in the dual strongly coupled field theory we look for static black brane solutions of the equations of motion (2.4)–(2.6) which are asymptotic

[2] Work in progress.



JHEP08(2010)027

to the Lifshitz fixed point solution (1.2). We consider a 4+1 dimensional metric of the form

$$ds^2 = L^2 \left( -r^{2z} f(r)^2 dt^2 + r^2 d\vec{x}^2 + \frac{g(r)^2}{r^2} dr^2 \right) , \tag{3.1}$$

for which the non-vanishing components of the vielbein can be taken to be

$$e^0_t = L\, r^z f(r)\,, \quad e^1_{x_1} = \ldots = e^3_{x_3} = L\, r\,, \quad e^4_r = L\, \frac{g(r)}{r}\,. \tag{3.2}$$

An asymptotically Lifshitz black brane with a non-degenerate horizon has a simple zero of both $f(r)^2$ and $g(r)^{-2}$ at the horizon, which we take to be at $r = r_0$, and $f(r)$, $g(r) \to 1$ as $r \to \infty$. It is straightforward to generalize this ansatz to include black holes with a spherical horizon or topological black holes with a hyperbolic horizon but it is the flat horizon case (3.1) that is of direct interest for the gravitational dual description of a strongly coupled $3+1$ dimensional field theoretic system.

In a static electrically charged black brane background the Maxwell gauge field and the Lifshitz vector can be chosen to be of the form

$$A_M = \{\alpha(r), 0, \ldots, 0\}\,; \qquad \mathcal{A}_M = \sqrt{\frac{2(z-1)}{z}} \{a(r), 0, \ldots, 0\}\,, \tag{3.3}$$

where the corresponding coordinate frame components are given by $A_\mu = e^M_\mu A_M$ and $\mathcal{A}_\mu = e^M_\mu \mathcal{A}_M$.

### 3.1 Field equations for static configurations

The Maxwell equations and the equations of motion for the Lifshitz vector can be written in first-order form,

$$\frac{r}{f}\frac{d}{dr}\left(f\,\alpha\right) = -z\,\alpha + g\,\beta, \tag{3.4}$$

$$r\frac{d}{dr}\left(r^3\beta\right) = 0, \tag{3.5}$$

$$\frac{r}{f}\frac{d}{dr}\left(f\,a\right) = -z\,a + z\,g\,b, \tag{3.6}$$

$$r\frac{d}{dr}\left(r^3 b\right) = 3r^3 g\,a, \tag{3.7}$$

where $\beta$ and $b$ are defined via (3.4) and (3.6) respectively. The Maxwell equation (3.5) trivially integrates to

$$\beta(r) = \frac{\rho}{r^3}\,, \tag{3.8}$$

where the integration constant $\rho$ is proportional to the world-volume electric charge density of the black brane, which in turn is identified with the charge density in the dual field theory by the standard AdS/CFT dictionary [23, 24], as explained in detail in [25].

The Einstein equations reduce to the following pair of first-order differential equations

$$\frac{r}{g}\frac{dg}{dr} = \frac{g^2}{3}\left[\frac{(z-1)}{2}\left(3a^2 + zb^2\right) - \frac{(z^2+2z+9)}{2} + \frac{\rho^2}{4r^6}\right] + 2\,, \tag{3.9}$$

$$\frac{r}{f}\frac{df}{dr} = \frac{g^2}{3}\left[\frac{(z-1)}{2}\left(3a^2 - zb^2\right) + \frac{(z^2+2z+9)}{2} - \frac{\rho^2}{4r^6}\right] - z - 1. \tag{3.10}$$

The Lifshitz fixed point solution is given by $\alpha = \rho = 0$ and $f = g = a = b = 1$.

To bring out the underlying scale invariance of the model we rewrite the field equations using $u = \log(r/r_0)$ instead of $r$ and introduce the scale invariant ratio $\tilde{\rho} \equiv \rho/r_0^d$. The remaining Maxwell equation (3.4) and the equations of motion of the Lifshitz field (3.6) and (3.7) reduce to

$$\dot{\alpha} + \frac{\dot{f}}{f}\alpha = -z\alpha + \tilde{\rho}e^{-3u}g\,, \tag{3.11}$$

$$\dot{a} + \frac{\dot{f}}{f}a = -za + zgb\,, \tag{3.12}$$

$$\dot{b} = -3b + 3ga\,, \tag{3.13}$$

where $\dot{} \equiv \frac{d}{du}$. The Einstein equations (3.9) and (3.10) can similarly be rewritten

$$\frac{\dot{g}}{g} = \frac{g^2}{6}\left[(z-1)\left(3a^2+zb^2\right) + \frac{\tilde{\rho}^2}{2}e^{-6u} - (z^2+2z+9)\right] + 2, \tag{3.14}$$

$$\frac{\dot{f}}{f} = \frac{g^2}{6}\left[(z-1)\left(3a^2-zb^2\right) - \frac{\tilde{\rho}^2}{2}e^{-6u} + (z^2+2z+9)\right] - z - 1. \tag{3.15}$$

Using these variables, the field equations are manifestly invariant under the rescaling (1.3). For given $z \geq 1$, there is a one parameter family of black brane solutions, labelled by $\tilde{\rho}$. A neutral black brane has $\tilde{\rho} = 0$ while the extremal limit is given by $|\tilde{\rho}| \to \sqrt{2(z^2+2z+9)}$.

### 3.2 Exact solutions

When $z = 1$ the terms involving $a$ and $b$ on the right hand side of the Einstein equations drop out. The equations then reduce to those of Einstein-Maxwell theory with a negative cosmological constant and one finds the AdS-RN solution describing charged black branes in $4+1$ dimensional asymptotically AdS spacetime,

$$f^2 = \frac{1}{g^2} = \left(1 - e^{-2u}\right)\left(1 + e^{-2u} - \frac{\tilde{\rho}^2}{12}e^{-4u}\right), \tag{3.16}$$

$$A_t = \frac{Lr_0\tilde{\rho}}{2}\left(1 - e^{-2u}\right). \tag{3.17}$$

At $z > 1$ there is a corresponding family of charged asymptotically Lifshitz black branes. In general these solutions can only be obtained numerically, but it turns out that in the special case $z = 6$ an isolated exact solution can be found [17, 26],

$$b = 1\,, \quad f^2 = \frac{1}{g^2} = a^2 = 1 - e^{-6u}, \quad A_t = \pm\sqrt{2}Lr_0^6\,(e^{3u} - 1). \tag{3.18}$$

We will primarily rely on numerical solutions in the following but the AdS-RN solution and the exact $z = 6$ solution are useful for checking the numerics.

### 3.3 Numerical solutions

The family of black brane solutions at generic $z > 1$ can be mapped out using numerical techniques similar to those of [16]. The numerical integration is started near the black



JHEP08(2010)027

hole, with suitable boundary conditions for a regular non-degenerate horizon at $u = 0$, and then proceeds outwards towards the asymptotic region. First of all, there should be a simple zero of $f^2$ and $g^{-2}$ at the horizon. Furthermore, the product $f\alpha$ must have a simple zero at the horizon in order for the gauge connection to be regular there. Similarly, the combination $ga$ on the right hand side of (3.13) should be regular at the horizon and it then follows from (3.12) that $b$ takes a finite value there. Putting all of this together we find that the near-horizon behavior can be parametrized as follows

$$f(u) = \sqrt{u}(f_0 + f_1 u + f_2 u^2 + \ldots), \tag{3.19}$$

$$g(u) = \frac{1}{\sqrt{u}}(g_0 + g_1 u + g_2 u^2 + \ldots), \tag{3.20}$$

$$\alpha(u) = \sqrt{u}(\alpha_0 + \alpha_1 u + \alpha_2 u^2 + \ldots), \tag{3.21}$$

$$a(u) = \sqrt{u}(a_0 + a_1 u + a_2 u^2 + \ldots), \tag{3.22}$$

$$b(u) = b_0 + b_1 u + b_2 u^2 + \ldots. \tag{3.23}$$

Inserting these near-horizon expansions into the equations of motion we obtain a two-parameter family of initial value data for any given $z$, parametrized for instance by $\tilde{\rho}$ and $b_0$. It turns out, however, that these two parameters cannot be varied independently but are restricted by the condition that the metric and Lifshitz vector approach the Lifshitz fixed point solution (1.2) and (2.10) sufficiently rapidly as $u \to \infty$ [16, 27, 28]. This means that for a given value of $z$ the parameter $\tilde{\rho}$ uniquely determines a charged black brane solution, up to overall scale.

### 3.4 Asymptotic behavior at large $u$

We now consider the asymptotic behavior of our fields as $u \to \infty$. The first observation is that the system of equations (3.11)–(3.15) only contains the combination $\frac{\dot{f}}{f}$ and therefore a uniform rescaling of $f$ is a symmetry of the equations. The symmetry is fixed, however, in an asymptotically Lifshitz solution for which $f \to 1$ as $u \to \infty$.[3]

We next observe that (3.15) can be used to eliminate $f$ from (3.12) – (3.14) leaving a closed system of first-order equations for $a$, $b$, and $g$. The large $u$ behavior can be obtained by linearizing around the Lifshitz fixed point $a = b = g = 1$. The corresponding problem for $d = 2$ was discussed in [16, 27] and we omit the details here. At large $u$, solutions of the full non-linear system approach a linear combination of the eigenmodes of the linearized system plus a universal mode coming from source terms involving $\tilde{\rho}^2$. The leading large $u$ behavior of the eigenmodes is $O(e^{\lambda_i u})$ with the eigenvalues $\lambda_i \in \{-3-z, \frac{1}{2}\left(-3-z \pm \sqrt{9z^2-26z+33}\right)\}$ while the universal mode falls off as $O(e^{-6u})$ independent of $z$.

Figure 1 shows the three eigenvalues as a function of $z$. The eigenmode that belongs to the largest eigenvalue is problematic [16, 27, 28]. For $z \geq 3$ it is non-negative and a solution that contains it fails to be asymptotically Lifshitz. For $1 < z < 3$ it is a negative

[3]When solving the equations numerically, it is convenient to initially put $f_0 = 1$ in the near-horizon expansion (3.19) when setting up the numerical integration and then rescale $f$ at the end of the day so that $f \to 1$ as $u \to \infty$.



JHEP08(2010)027

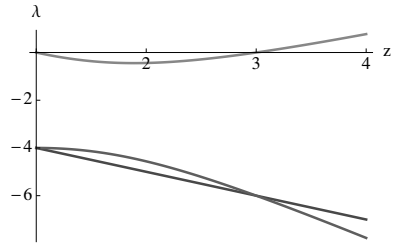


**Figure 1**. Eigenvalues of the linearized problem for $\{g, b, a\}$ as a function of $z$ for $d = 3$.



mode but the falloff at large $u$ is too slow to give finite energy. This mode is eliminated in our black hole solutions by fine-tuning the value of $b$ at the black hole horizon. For $z < 3$ the universal $e^{-6u}$ mode is sub-leading compared to the two remaining eigenmodes of the linearized system but at $z > 3$ it dominates the asymptotic behavior. In the dividing $z = 3$ case the linearized system is degenerate and the asymptotic behavior includes powers of $u$ on top of the $e^{-6u}$ falloff.

Finally, we turn to equation (3.11) for the Maxwell field. In the Lifshitz background with $f = g = 1$ it has the solution

$$\alpha = \begin{cases} \tilde{\mu}\, e^{-zu} + \frac{\tilde{\rho}}{(z-3)} e^{-3u} & \text{if} \quad z \neq 3\,, \\ \tilde{\mu}\, e^{-3u} + \tilde{\rho}\, u\, e^{-3u} & \text{if} \quad z = 3\,. \end{cases} \tag{3.24}$$

The non-vanishing component of the vector potential in a coordinate frame is then

$$A_t = \begin{cases} \mu + \frac{L\rho}{(z-3)} r^{z-3} & \text{if} \quad z \neq 3\,, \\ \mu + L\rho \log\left(\frac{r}{r_0}\right) & \text{if} \quad z = 3\,, \end{cases} \tag{3.25}$$

with $\mu = L\tilde{\mu}\, r_0^z$. Once again the qualitative behavior of solutions changes at $z = 3$. For low $z$ values, in the range $1 < z < 3$, the term involving the chemical potential $\mu$ dominates compared to the term involving the charge density $\rho$ at large $r$, while at $z \geq 3$ it is the charge density term that is leading [29].

In general, we are not working with Lifshitz background itself but with solutions of the full non-linear system of equations that are only asymptotically Lifshitz. It turns out, however, the leading large $u$ behavior of $\alpha$ carries over from the Lifshitz background to more general case as long as the value of $z$ isn't too high.[4]

## 4 Black brane thermodynamics

So far, we have set up the holographic model and considered charged black brane geometries that are conjectured to provide a dual description of a strongly coupled 3+1 dimensional system near a quantum critical point with dynamical critical exponent $z \geq 1$. These black

[4] At $z \geq 9$ we expect non-linear effects to give rise to additional terms in (3.24) with a falloff in between that of the charge density and chemical potential terms. We will not keep track of such terms here since all systems of physical interest that we are aware of have $z < 9$.

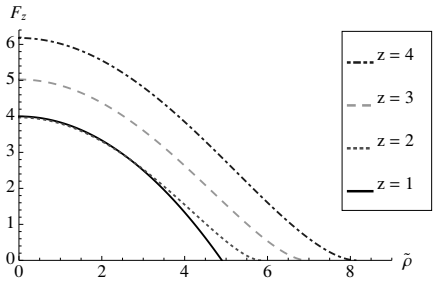


**Figure 2**. Temperature function $F_z(\tilde{\rho})$ for several $z$ values. The $z = 1$ curve plots the exact result (4.10) while the $z > 1$ curves are obtained from numerical black hole solutions.

branes turn out to have interesting thermodynamics. At high temperature the thermodynamic behavior is governed by the underlying Lifshitz symmetry, but collective effects come into play as the temperature is lowered and modify the thermodynamics. To see this, we use a combination of analytic and numerical arguments to compute the specific heat of the system as a function of temperature. Our starting point is the following expression for the Hawking temperature of a black brane,[5]

$$T_H = \frac{r_0^z}{4\pi}\,\frac{f_0}{g_0}\,, \tag{4.1}$$

which is obtained in the standard way by requiring the Euclidean metric of the black brane to be smooth at the horizon at $r = r_0$. The coefficients $f_0$ and $g_0$ are taken from the near-horizon expansions (3.19) and (3.20) in the scale invariant variable $u$ and only depend on the value of $\tilde{\rho}$. The temperature can therefore be expressed as follows,

$$T_H = \frac{r_0^z}{4\pi}\,F_z(\tilde{\rho})\,, \tag{4.2}$$

with $F_z(\tilde{\rho}) \equiv \frac{f_0}{g_0}$ for different values of $z$ shown in figure 2.

The specific heat at fixed volume in the boundary theory is then

$$C = T\,\frac{dS}{dT} = T\frac{(dS/dr_0)}{(dT/dr_0)}\,, \tag{4.3}$$

where $S = \frac{1}{4}r_0^3$ is the Bekenstein-Hawking entropy density of the black brane and $T$ in the boundary system is identified with the Hawking temperature (4.2). We have to make a choice whether to work at fixed charge density $\rho$ or fixed chemical potential $\mu$ in the boundary theory when calculating thermodynamic quantities. For the field theory problem that we wish to model it is natural to keep the charge density fixed since the net density of charge carriers is given by the density of dopants, which is fixed in a given sample [29]. In this case

$$\frac{d}{dr_0} = \frac{\partial}{\partial r_0} - \frac{3\tilde{\rho}}{r_0}\frac{\partial}{\partial\tilde{\rho}}\,, \tag{4.4}$$

[5]From here on we fix the characteristic length scale as $L = 1$. Explicit factors of $L$ can be reintroduced into the formulas by dimensional analysis.



JHEP08(2010)027

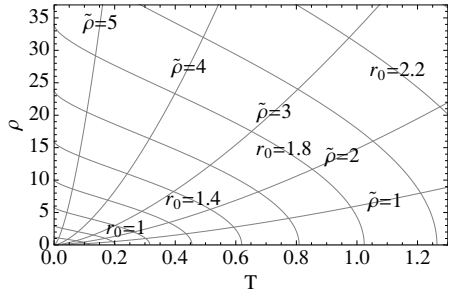


**Figure 3**. Contour map expressing $r_0$ and $\tilde{\rho}$ in terms of $T$ and $\rho$ at $z = 2$.

and we find

$$\frac{C}{T} = \frac{3\pi r_0^{3-z}}{zF_z(\tilde{\rho}) - 3\tilde{\rho}F_z'(\tilde{\rho})}. \tag{4.5}$$

If we instead were to keep the chemical potential $\mu$ fixed then

$$\frac{d}{dr_0} = \frac{\partial}{\partial r_0} - \frac{z\tilde{\mu}}{r_0}\left(\frac{d\tilde{\mu}}{d\tilde{\rho}}\right)^{-1}\frac{\partial}{\partial\tilde{\rho}}, \tag{4.6}$$

with $d\tilde{\mu}/d\tilde{\rho}$ obtained from the asymptotic behavior of the Maxwell field (3.24) in the numerical black brane solution, and then the remaining steps in the calculation of the specific heat are parallel to those at fixed charge density.

The variables $r_0$ and $\tilde{\rho}$ on the right hand side of equation (4.5) refer to the 4+1 dimensional black brane geometry while it is $T$ and $\rho$ that have direct interpretation in the dual field theory. The latter variables are expressed in terms of the former via the definition $\tilde{\rho} = \rho/r_0^3$ and equation (4.2) for the Hawking temperature. We can numerically invert these relations in order to express the specific heat (4.3) in terms $T$ and $\rho$. Figure 3 shows the map between brane variables and physical variables for $z = 2$ and similar maps are obtained for other $z$ values.

### 4.1 Scaling at high temperature

Below, we present numerical results for $C/T$ obtained via the above procedure for several values of $z$ but some information can be obtained by analytic arguments. In particular, we can extract a scaling relation for the specific heat at high temperature. The argument is the same for any number of spatial dimensions $d$. Writing $\tilde{\rho} = \rho/r_0^d$, the expression (4.1) for the temperature remains the same except that the detailed shape of the function $F_z(\tilde{\rho})$ depends on $d$. The limit of high temperature at fixed $\rho$ corresponds to large $r_0$ and $\tilde{\rho} \to 0$. The field equations depend on $\tilde{\rho}^2$ in a smooth way so we expect $F_z(\tilde{\rho})$ to be a smooth even function of $\tilde{\rho}$ (this is also evident from the graphs in figure 2) and the denominator in the $d$ dimensional version of equation (4.5) reduces to $zF_z(0)$. As a result the temperature and the entropy density, and their first derivatives, depend only on the overall scale $r_0$ in the high-temperature limit and the electric charge carried by the black brane does not affect



JHEP08(2010)027

the dynamics to leading order,

$$T \approx \frac{F_z(0)}{4\pi}\, r_0^z\,, \qquad S = \frac{1}{4} r_0^d\,. \tag{4.7}$$

The high-temperature behavior of the specific heat then immediately follows from the general expression (4.3),

$$C \sim r_0^d \sim T^{d/z}, \tag{4.8}$$

which reduces, in particular, to $C \sim T^{3/z}$ when $d = 3$. It is straightforward to go a step further and integrate both sides of (4.3) with respect to $T$ to obtain the following relation between energy and entropy of the system in the high-temperature limit,

$$E = \frac{d}{d+z} T\, S\,, \tag{4.9}$$

recovering the result found previously for electrically neutral black branes in [30]. The scaling behavior can be traced to the underlying Lifshitz symmetry of the quantum critical theory. It is easy to see that a generic statistical mechanical system in three spatial dimensions with a dispersion relation of the form $\omega \sim k^z$ exhibits the same scaling behavior [30].

### 4.2 Low-temperature behavior

At low temperature, the black brane thermodynamics exhibits interesting behavior due to collective effects in the dual field theory and the simple scaling that is seen at high temperature no longer applies. The behavior is qualitatively different in conformal systems with $z = 1$ as compared to Lifshitz systems with $z > 1$ and we consider these cases in turn.

At $z = 1$ we have the exact AdS-RN black brane solution (3.17) for which the Hawking temperature is easily determined. One finds

$$F_1(\tilde{\rho}) = 4 - \frac{\tilde{\rho}^2}{6}\,, \tag{4.10}$$

and the specific heat at fixed $\rho$ is given by

$$\frac{C}{T} = \frac{18\pi r_0^2}{24 + 5\tilde{\rho}^2}. \tag{4.11}$$

At low temperature the charge on the black brane approaches the extremal limit, $\tilde{\rho} \to \sqrt{24}$ and the specific heat depends linearly on temperature,

$$\frac{C}{T} \to \frac{\pi \rho^{2/3}}{16 \cdot 3^{1/3}} \quad \text{as} \quad T \to 0. \tag{4.12}$$

A weakly-coupled Fermi liquid has a specific heat that is linear in $T$ at low temperatures and it is interesting to see the same behavior emerge in the low-temperature limit of a black brane in Einstein-Maxwell theory without having made any reference to specific matter fields in the calculation. This result was obtained previously in [18] where it was taken as evidence for the existence of a Fermi surface in the dual field theory. Spectral functions of probe fermions coupled to the $z = 1$ system computed in [19, 20, 22] also



JHEP08(2010)027

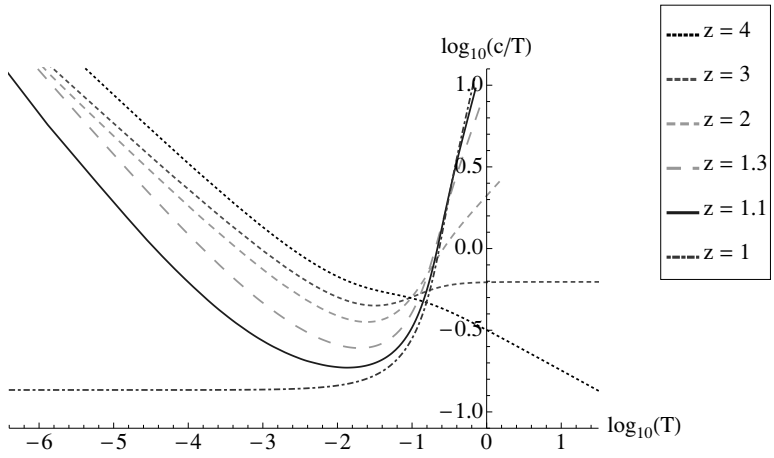


**Figure 4**. Black brane specific heat divided by temperature for several $z$ values calculated at fixed charged density $\rho = 1$. The $z = 1$ curve is obtained from the exact result (4.11).

strongly suggest the presence of a Fermi surface. Having a specific heat that is linear in $T$ and a Fermi surface does not imply that the system consists of weakly coupled fermions. Indeed, the scaling behavior of excitations near the Fermi surface differs from that of a Landau Fermi liquid in the probe fermion analysis of [19, 20] and the zero-temperature conductivity computed in [18] was found to be diffusive rather than ballistic, suggesting that disorder plays a role.

At $z > 1$ we do not have explicit analytic black brane solutions except the isolated $z = 6$ solution (3.18) and our results for the specific heat in $z > 1$ systems are therefore based on numerical black brane solutions with non-vanishing Lifshitz vector field. The key qualitative difference compared to the $z = 1$ case can be seen in figure 2. The function $F_1(\tilde{\rho})$ goes to zero in a linear fashion in the extremal limit $\tilde{\rho} \to \sqrt{24}$ but for $z > 1$ both $F_z(\tilde{\rho})$ and its first derivative go to zero in the extremal limit $\tilde{\rho} \to \sqrt{2(z^2 + 2z + 9)}$. It then follows from equation (4.5) that the ratio $C/T$ diverges in the $T \to 0$ limit for $z > 1$. The growth in $C/T$ towards lower temperatures is evident in the $z > 1$ curves in figure 4.[6] This trend is in qualitative agreement with the measured specific heat of certain heavy fermion alloys [4]. The high $T$ behavior of the specific heat curves in the figure, on the other hand, matches the scaling law (4.8).

## 5 Discussion

In this paper we have employed a relatively simple holographic description of a strongly coupled 3+1 dimensional quantum critical point with asymmetric scaling to model the anomalous specific heat found at low temperature in many heavy fermion compounds.

[6] Finite numerical precision limits how far the curves for $z > 1$ in figure 4 can be extended towards low $T$.



JHEP08(2010)027

The calculation is performed entirely within the context of black hole thermodynamics and the nature of the low-lying spectrum of excitations is thus investigated without introducing any specific matter probes. It would be very interesting to complement the results obtained here by a study of spectral functions for probe fermions, generalizing the $z = 1$ work of [19, 20, 22], and a calculation of conductivities. This requires us to extend existing gravitational techniques for obtaining spectral functions and transport coefficients to models exhibiting Lifshitz scaling with non-trivial dynamical critical exponent $z > 1$, and our work in this direction is in progress.

One limitation of the present work concerns the non-vanishing black hole area in the extremal limit, which corresponds to having non-vanishing entropy at zero temperature in the dual system. This can for instance be remedied by coupling the system to a scalar field and include the back-reaction to the scalar hair carried by the black hole at very low temperatures. In this case the area of the black hole horizon shrinks as the temperature is lowered and the system no longer has finite zero-temperature entropy. This was shown in [31] for asymptotically AdS black holes with hair and we have obtained analogous results in our $z > 1$ model with scalar matter included [32]. The scalar hair corresponds to having a charged superfluid condensate in the dual theory and the instability to developing superfluidity bears out the general expectation that scale invariant quantum critical matter is never found as the true ground state of a system. A further study of the interplay between the heavy fermion physics and superfluidity in these holographic models is an interesting avenue for further work.

We find it intriguing that experimentally measured deviations from Fermi liquid behavior in critically doped heavy fermion alloys can be qualitatively reproduced by holographic duals with Lifshitz symmetry. The curves for $z > 1$ in figure 4 suggest a power law for $C/T$ at low temperature rather than a logarithm. The experimental data vary from one material to another and both logarithmic and power law fits are used [4]. The fact that our curves for $z > 1$ approach straight lines at low $T$ should not be over interpreted but it is encouraging to see the right trend coming from simple gravitational models with Lifshitz scaling.


## Acknowledgments

This work was supported in part by the Göran Gustafsson foundation, the Swedish Research Council (VR), the Icelandic Research Fund, the University of Iceland Research Fund, and the Eimskip Research Fund at the University of Iceland. We thank E. Ardonne, H. Hansson, and P. Kakashili for useful discussions.


## References


[1] H.v. Löhneysen et al., *Non-Fermi liquid behavior in a heavy-fermion alloy at a magnetic instability*, *Phys. Rev. Lett.* **72** (1994) 3262.

[2] H.v. Löhneysen, M. Sieck, O. Stockert and M. Waffenschmidt, *Investigation of non-Fermi-liquid behavior in $CeCu_{6-x}Au_x$*, *Physica* **B 223** 471 (1996).

[3] G.R. Stewart, *Heavy-fermion systems*, *Rev. Mod. Phys.* **56** (1984) 755 [SPIRES].




JHEP08(2010)027

[4] G.R. Stewart, *Non-Fermi-liquid behavior in d- and f-electron metals*, *Rev. Mod. Phys.* **73** (2001) 797 [SPIRES].

[5] H.v. Lohneysen, A. Rosch, M. Vojta and P. Wolfle, *Fermi-liquid instabilities at magnetic quantum phase transitions*, *Rev. Mod. Phys.* **79** (2007) 1015 [SPIRES].

[6] P. Coleman and A.J. Schofield, *Quantum criticality*, *Nature* **433** (2005) 226 [cond-mat/0503002].

[7] S.A. Hartnoll, *Lectures on holographic methods for condensed matter physics*, *Class. Quant. Grav.* **26** (2009) 224002 [arXiv:0903.3246] [SPIRES].

[8] C.P. Herzog, *Lectures on holographic superfluidity and superconductivity*, *J. Phys.* **A 42** (2009) 343001 [arXiv:0904.1975] [SPIRES].

[9] G.T. Horowitz, *Introduction to holographic superconductors*, arXiv:1002.1722 [SPIRES].

[10] J. McGreevy, *Holographic duality with a view toward many-body physics*, arXiv:0909.0518 [SPIRES].

[11] S. Sachdev, *Condensed matter and AdS/CFT*, arXiv:1002.2947 [SPIRES].

[12] J.M. Maldacena, *The large-N limit of superconformal field theories and supergravity*, *Adv. Theor. Math. Phys.* **2** (1998) 231 [*Int. J. Theor. Phys.* **38** (1999) 1113] [hep-th/9711200] [SPIRES].

[13] Q. Si, S. Rabello, K. Ingersent and J.L. Smith, *Locally critical quantum phase transitions in strongly correlated metals*, *Nature* **413** (2001) 804.

[14] S. Kachru, X. Liu and M. Mulligan, *Gravity duals of Lifshitz-like fixed points*, *Phys. Rev.* **D 78** (2008) 106005 [arXiv:0808.1725] [SPIRES].

[15] P. Koroteev and M. Libanov, *On existence of self-tuning solutions in static braneworlds without singularities*, *JHEP* **02** (2008) 104 [arXiv:0712.1136] [SPIRES].

[16] U.H. Danielsson and L. Thorlacius, *Black holes in asymptotically Lifshitz spacetime*, *JHEP* **03** (2009) 070 [arXiv:0812.5088] [SPIRES].

[17] E.J. Brynjolfsson, U.H. Danielsson, L. Thorlacius and T. Zingg, *Holographic superconductors with lifshitz scaling*, *J. Phys.* **A 43** (2010) 065401 [arXiv:0908.2611] [SPIRES].

[18] S.-J. Rey, *String theory on thin semiconductors: holographic realization ofFermi points and surfaces*, *Prog. Theor. Phys. Suppl.* **177** (2009) 128 [arXiv:0911.5295] [SPIRES].

[19] H. Liu, J. McGreevy and D. Vegh, *Non-Fermi liquids from holography*, arXiv:0903.2477 [SPIRES].

[20] T. Faulkner, H. Liu, J. McGreevy and D. Vegh, *Emergent quantum criticality,Fermi surfaces and AdS2*, arXiv:0907.2694 [SPIRES].

[21] M. Taylor, *Non-relativistic holography*, arXiv:0812.0530 [SPIRES].

[22] M. Cubrovic, J. Zaanen and K. Schalm, *String theory, quantum phase transitions and the emergent Fermi-liquid*, *Science* **325** (2009) 439 [arXiv:0904.1993] [SPIRES].

[23] S.S. Gubser, I.R. Klebanov and A.M. Polyakov, *Gauge theory correlators from non-critical string theory*, *Phys. Lett.* **B 428** (1998) 105 [hep-th/9802109] [SPIRES].

[24] E. Witten, *Anti-de Sitter space and holography*, *Adv. Theor. Math. Phys.* **2** (1998) 253 [hep-th/9802150] [SPIRES].

JHEP08(2010)027

[25] S.A. Hartnoll and P. Kovtun, *Hall conductivity from dyonic black holes*, *Phys. Rev.* **D 76** (2007) 066001 [arXiv:0704.1160] [SPIRES].

[26] D.-W. Pang, *On charged lifshitz black holes*, *JHEP* **01** (2010) 116 [arXiv:0911.2777] [SPIRES].

[27] G. Bertoldi, B.A. Burrington and A. Peet, *Black holes in asymptotically Lifshitz spacetimes with arbitrary critical exponent*, *Phys. Rev.* **D 80** (2009) 126003 [arXiv:0905.3183] [SPIRES].

[28] S.F. Ross and O. Saremi, *Holographic stress tensor for non-relativistic theories*, *JHEP* **09** (2009) 009 [arXiv:0907.1846] [SPIRES].

[29] S.A. Hartnoll, J. Polchinski, E. Silverstein and D. Tong, *Towards strange metallic holography*, *JHEP* **04** (2010) 120 [arXiv:0912.1061] [SPIRES].

[30] G. Bertoldi, B.A. Burrington and A.W. Peet, *Thermodynamics of black branes in asymptotically Lifshitz spacetimes*, *Phys. Rev.* **D 80** (2009) 126004 [arXiv:0907.4755] [SPIRES].

[31] G.T. Horowitz and M.M. Roberts, *Zero temperature limit of holographic superconductors*, *JHEP* **11** (2009) 015 [arXiv:0908.3677] [SPIRES].

[32] E.J. Brynjolfsson, U.H. Danielsson, L. Thorlacius and T. Zingg, *Holographic models with anisotropic scaling*, arXiv:1004.5566 [SPIRES].

JHEP08(2010)027

# Paper III

# Holographic models with anisotropic scaling

**E J Brynjolfsson[1], U H Danielsson[2], L Thorlacius[1,3] and T Zingg[1,3]**

[1] University of Iceland, Science Institute, Dunhaga 3, IS-107 Reykjavik, Iceland

[2] Institutionen för fysik och astronomi, Uppsala Universitet, Box 803, SE-751 08 Uppsala, Sweden

[3] NORDITA, Roslagstullsbacken 23, SE-106 91 Stockholm, Sweden

E-mail: erlingbr@hi.is ulf.danielsson@physics.uu.se lth@nordita.org zingg@nordita.org

**Abstract.** We consider gravity duals to d+1 dimensional quantum critical points with anisotropic scaling. The primary motivation comes from strongly correlated electron systems in condensed matter theory but the main focus of the present paper is on the gravity models in their own right. Physics at finite temperature and fixed charge density is described in terms of charged black branes. Some exact solutions are known and can be used to obtain a maximally extended spacetime geometry, which has a null curvature singularity inside a single non-degenerate horizon, but generic black brane solutions in the model can only be obtained numerically. Charged matter gives rise to black branes with hair that are dual to the superconducting phase of a holographic superconductor. Our numerical results indicate that holographic superconductors with anisotropic scaling have vanishing zero temperature entropy when the back reaction of the hair on the brane geometry is taken into account.

## 1. Introduction

We consider $d+2$ dimensional gravity models that are dual to quantum critical points with anisotropic scaling in $d+1$ dimensions,

$$t \to \lambda^z t, \qquad \vec{x} \to \lambda \vec{x}\,, \tag{1}$$

with $z \geq 1$ and $\vec{x} = (x_1, \ldots, x_d)$. The $d+2$ dimensional bulk action consists of three parts,

$$S = S_{\text{Einstein-Maxwell}} + S_{\text{Lifshitz}} + S_{\text{matter}}\,. \tag{2}$$

The first term is the standard action of Einstein-Maxwell gravity with a negative cosmological constant,

$$S_{\text{Einstein-Maxwell}} = \int \mathrm{d}^{d+2}x\sqrt{-g}\,\left(R - 2\Lambda - \frac{1}{4}F_{\mu\nu}F^{\mu\nu}\right). \tag{3}$$

This is followed by a term involving a massive vector field,

$$S_{\text{Lifshitz}} = -\int \mathrm{d}^{d+2}x\sqrt{-g}\,\left(\frac{1}{4}\mathcal{F}_{\mu\nu}\mathcal{F}^{\mu\nu} + \frac{c^2}{2}\mathcal{A}_\mu\mathcal{A}^\mu\right), \tag{4}$$

whose sole purpose is to provide backgrounds with anisotropic scaling. This is a modified version of the holographic model of [1], which was formulated in four-dimensional spacetime and obtained

anisotropic scaling by including a pair of coupled two- and three-form field strengths.[1] Upon integrating out the three-form field strength, the remaining two-form becomes a field strength of a massive vector [3] and in this form the model is easily extended to general dimensions. Finite temperature corresponds to having a black hole in the higher-dimensional spacetime and with the Maxwell gauge field, added in [4], the black hole can carry electric charge, which is dual to a finite charge density in the lower-dimensional theory. Finally, we consider matter in the form of a scalar field, which is charged under the Maxwell gauge field but does not couple directly to the auxiliary massive vector field,

$$S_{\rm matter} = -\frac{1}{2}\int {\rm d}^{d+2}x\sqrt{-g}\,\left((\partial^\mu\phi^* + iqA^\mu\phi^*)\,(\partial_\mu\phi - iqA_\mu\phi) + m^2\phi^*\phi\right). \tag{5}$$

At low temperature there is an instability for charged black holes in the model to grow scalar hair, which corresponds to the superconducting phase of holographic superconductors with $z > 1$ asymmetric scaling [4], as described in Section 3 below.

The equations of motion obtained from the action (2) consist of the scalar field equation

$$(\nabla^\mu - iqA^\mu)\,(\nabla_\mu - iqA_\mu)\,\phi - m^2\phi = 0\,, \tag{6}$$

along with the Einstein equations, the Maxwell equations, and field equations for the auxiliary massive vector,

$$\begin{aligned} G_{\mu\nu} + \Lambda g_{\mu\nu} &= T^{\rm Maxwell}_{\mu\nu} + T^{\rm Lifshitz}_{\mu\nu} + T^{\rm matter}_{\mu\nu}\,, & (7)\\ \nabla_\nu F^{\nu\mu} &= j^\mu_{\rm matter}\,, & (8)\\ \nabla_\nu \mathcal{F}^{\nu\mu} &= c^2\mathcal{A}^\mu\,. & (9) \end{aligned}$$

The asymmetric scaling symmetry (1), sometimes referred to as Lifshitz scaling, is realized in a d+2 dimensional spacetime,

$$ds^2 = L^2\left(-r^{2z}dt^2 + r^2 d\vec{x}^2 + \frac{dr^2}{r^2}\right), \tag{10}$$

whose metric is invariant under the transformation

$$t \to \lambda^z t, \quad \vec{x} \to \lambda\vec{x}, \quad r \to \frac{r}{\lambda}\,. \tag{11}$$

Length dimensions are carried by the characteristic length $L$ while the coordinates $(t, r, \vec{x})$ are dimensionless. The scale invariant Lifshitz geometry (10) is a solution of the equations of motion when $L$ is related to the cosmological constant $\Lambda$ via

$$\Lambda = -\frac{z^2 + (d-1)z + d^2}{2L^2}\,, \tag{12}$$

and the mass of the auxiliary vector field is fine-tuned to $c = \sqrt{z\,d}/L$. In this solution the Maxwell field vanishes, $A_\mu = 0$, but the massive vector field has the background value

$$\mathcal{A}_t = \sqrt{\frac{2(z-1)}{z}}L\,r^z\,, \qquad \mathcal{A}_{x_i} = \mathcal{A}_r = 0\,. \tag{13}$$

[1] See also [2] for early work on gravitational backgrounds with anisotropic scaling.

## 2. Charged black branes

In order to study finite temperature effects in the dual strongly coupled field theory we look for static black brane solutions of the equations of motion (6) - (9) which are asymptotic to the Lifshitz fixed point solution given by (10) and (13). From now on we set $L = 1$ and consider a metric of the form

$$ds^2 = -r^{2z} f(r)^2 dt^2 + r^2 d\vec{x}^2 + \frac{g(r)^2}{r^2} dr^2 \,. \tag{14}$$

An asymptotically Lifshitz black brane with a non-degenerate horizon has a simple zero of both $f(r)^2$ and $g(r)^{-2}$ at the horizon, which we take to be at $r = r_0$, and $f(r)$, $g(r) \to 1$ as $r \to \infty$. It is straightforward to generalize this ansatz to include black holes with a spherical horizon or topological black holes with a hyperbolic horizon but it is the flat horizon case (14) that is of direct interest for the gravitational dual description of strongly coupled $d+1$ dimensional field theories. In a static electrically charged black brane background the Maxwell gauge field and the massive vector can be taken to be of the form

$$A_\mu = r^z f(r)\{\alpha(r), 0, \ldots, 0\}\,; \qquad \mathcal{A}_\mu = \sqrt{\frac{2(z-1)}{z}} r^z f(r)\{a(r), 0, \ldots, 0\}\,. \tag{15}$$

with $\alpha(r) \to 0$ and $a(r) \to 1$ as $r \to \infty$.

### *2.1. Field equations for static configurations*

For static configurations the equations of motion can be expressed as a first order system of ordinary differential equations. Introducing a scale invariant radial variable $u = \log(r/r_0)$ and writing $\dot{} \equiv \frac{d}{du}$, the scalar field equation becomes

$$\dot{\phi} = \chi\,, \tag{16}$$

$$\dot{\chi} + \left(\frac{\dot{f}}{f} - \frac{\dot{g}}{g}\right)\chi = -(d+z)\,\chi + \left(m^2 - q^2\alpha^2\right) g^2 \phi\,, \tag{17}$$

while the Maxwell equations and the equations of motion for the massive vector reduce to,

$$\dot{\alpha} + \frac{\dot{f}}{f}\alpha = -z\,\alpha + g\,\beta\,, \tag{18}$$

$$\dot{\beta} = -d\,\beta + q^2 g\,\phi^2 \alpha\,, \tag{19}$$

$$\dot{a} + \frac{\dot{f}}{f} a = -z\,a + z\,g\,b\,, \tag{20}$$

$$\dot{b} = -d\,b + d\,g\,a\,. \tag{21}$$

The functions $\chi$, $\beta$, and $b$ are defined via (16), (18), and (20), respectively. The Einstein equations can also be written in first order form,

$$\frac{\dot{g}}{g} + \frac{\dot{f}}{f} = (z-1)\left(g^2 a^2 - 1\right) + \frac{1}{2d}\left(\chi^2 + q^2 g^2 \alpha^2 \phi^2\right), \tag{22}$$

$$2d\,\frac{\dot{f}}{f} = d(1-d-2z) + \frac{\chi^2}{2} + g^2\Bigg[(z-1)\left(da^2 - zb^2\right) - \frac{\beta^2}{2} + \frac{1}{2}\left(q^2\alpha^2 - m^2\right)\phi^2 + z^2 + (d-1)z + d^2\Bigg]. \tag{23}$$

The field equations (16) - (23) are manifestly invariant under the scaling (11) and the Lifshitz fixed point solution is given by $f = g = a = b = 1$ and $\alpha = \beta = \phi = \chi = 0$.

In the absence of charged matter, the Maxwell equation (19) integrates to $\beta(u) = \tilde{\rho}\, e^{-du}$. The integration constant $\tilde{\rho} = \rho/r_0^d$ is proportional to the electric charge per unit $d$-volume of the black brane, which in turn corresponds to the charge density in the dual field theoretic system. For given $d$ and $z \geq 1$, the remaining field equations then have a one parameter family of black brane solutions, labelled by $\tilde{\rho}$. A neutral black brane without scalar hair has $\tilde{\rho} = 0$ while the extremal limit is given by $\tilde{\rho} \to \pm\sqrt{2(z^2 + (d-1)z + d^2)}$. A non-vanishing charged scalar field changes this picture as discussed below.

Equation (18) can easily be solved in the Lifshitz geometry (10) without matter, giving

$$\alpha(u) = \begin{cases} \tilde{\mu}\, e^{-zu} + \frac{1}{(z-d)}\tilde{\rho}\, e^{-du} & \text{if} \quad z \neq d\,, \\ \tilde{\mu}\, e^{-du} + \tilde{\rho}\, u\, e^{-du} & \text{if} \quad z = d\,, \end{cases} \tag{24}$$

where the integration constant $\tilde{\mu} = \mu/r_0^z$ corresponds to having non-vanishing chemical potential in the dual system. In general, we are not working with the Lifshitz background but with solutions that are only asymptotically Lifshitz as $u \to \infty$. However, as long as the value of $z$ isn't too high,[2] the asymptotic behavior of the gauge potential carries over from the Lifshitz background to the more general case, and one can read off the charge density and chemical potential in the dual field theory from the leading two terms in the expansion of $\alpha$ at large $u$. Calculations in this paper refer to fixed $\rho$, corresponding to a fixed density of charge carriers in the dual system, but one can also work at fixed chemical potential.

*2.2. Numerical solutions*

Black brane solutions at generic $z > 1$ can be obtained using numerical techniques similar to those of [5]. The field equations are integrated numerically starting near the black hole, with suitable initial conditions and proceeding out towards the asymptotic region. For a regular, non-degenerate horizon we require the functions that appear in the metric ansatz (14) to behave as

$$f(u) = \sqrt{u}(f_0 + f_1 u + \ldots), \quad g(u) = \frac{1}{\sqrt{u}}(g_0 + g_1 u + \ldots), \tag{25}$$

near $u = 0$. The appropriate near-horizon behavior of the remaining field variables can be worked out and then inserted into the equations of motion to generate initial value data for the numerical integration. For any given values of $d$ and $z$, we obtain a three parameter family of initial values, where for instance $\phi(0)$, $\beta(0)$, and $b(0)$ can be taken as the independent parameters. The condition that the metric and massive vector approach the Lifshitz fixed point solution (10) and (13) sufficiently rapidly as $u \to \infty$ restricts the solutions further [5, 6, 7]. As a result, $b(0)$ is fixed for given $\phi(0)$ and $\beta(0)$ and one has a two-parameter family of solutions. This means in particular that, in the absence of scalar hair, there is a unique (up to overall scale) asymptotically Lifshitz charged black brane solution for given $d$, $z$ and $\tilde{\rho}$.

The Hawking temperature is determined by the near-horizon behavior of the black brane metric,

$$T_H = \frac{r_0^z}{4\pi}\,\frac{f_0}{g_0}\,. \tag{26}$$

The full numerical solution of the field equations is required, however, to relate the coefficients $f_0$ and $g_0$ to the charge density $\rho$ and other physical variables of the dual field theory.

[2] At $z \geq 3d$ non-linear effects give rise to additional terms in (24) with a falloff in between that of the charge density and chemical potential terms.

*2.3. Conserved charge under radial evolution*

A conserved charge under radial evolution was found in [6] for electrically neutral black branes with $d = 2$ and arbitrary dynamical critical exponent $z$. Such a conserved charge is useful for matching solutions across the bulk geometry from the near-horizon region to the asymptotic large $u$ region and also provides a check on numerical solutions. The charge found in [6] generalizes to charged black branes with scalar hair in general spatial dimensions,

$$\begin{aligned} D_0 &= r_0^{z+d} e^{(z+d)u} f \left[ \frac{1}{2g}(\chi^2 - 2d(d+1)) - 2d(z-1)ab - d\,\alpha\beta \right. \\ &\quad \left. + g\left[ (z-1)(d\,a^2 - z\,b^2) + z^2 + (d-1)z + d^2 - \frac{1}{2}(\beta^2 + m^2\phi^2 - q^2\alpha^2\phi^2) \right] \right]. \end{aligned} \tag{27}$$

It is straightforward to check that $\frac{d}{du} D_0 = 0$ when the field equations (16) - (23) are satisfied. The conserved charge is related to thermodynamic state variables of the dual system in a simple way. Inserting a perturbative near-horizon expansion of the fields, one finds

$$D_0 = 2 r_0^{d+z} \frac{f_0}{g_0} = 32\pi S\, T, \tag{28}$$

where $T$ is the temperature (26) and $S = r_0^d/4$ is the Bekenstein-Hawking entropy density, which are identified with the temperature and entropy of the dual field theory.

*2.4. Exact solution*

As always, it is useful to have explicit analytic solutions to work with. Although Lifshitz black branes at $z > 1$ can in general only be obtained numerically, it turns out that for each value of $d$ an isolated $z = 2d$ exact solution can be found [4, 8],[3]

$$b = 1\,, \quad f^2 = \frac{1}{g^2} = a^2 = 1 - e^{-2du}, \quad f\alpha = \pm\sqrt{2} e^{-du}\,(1 - e^{-du}), \tag{29}$$

with $\phi = 0$ and $\tilde{\rho} = \pm\sqrt{2}d$. It is straightforward to continue the exact black brane metric inside the horizon and obtain the globally extended geometry [4]. Define a tortoise coordinate $u_*$ by

$$u_* = \frac{1}{2d\, r_0^{2d}} \log\left(1 - e^{-2du}\right), \tag{30}$$

and then transform the $(t, u)$ variables to a pair of null coordinates

$$V = \exp\left[d\, r_0^{2d}(u_* + t)\right], \quad U = -\exp\left[d\, r_0^{2d}(u_* - t)\right]. \tag{31}$$

In the new coordinate system the metric is given by

$$ds^2 = \frac{-dU\, dV}{d^2(1 + UV)^2} + \frac{r_0^2\, d\vec{x}^2}{(1 + UV)^{1/d}}\,, \tag{32}$$

and is manifestly non-singular at the horizon, which is located at $UV = 0$. There is a null curvature singularity at $UV \to \infty$, which corresponds to $r \to 0$ in the original coordinate system. The asymptotic region $r \to \infty$ corresponds to $UV \to -1$. By a further transformation

[3] The corresponding exact solutions for $d = 2$, $z = 4$ black holes with a spherical horizon and topological black holes with a hyperbolic horizon were also found in [4]. In the limit of vanishing electric charge these black hole solutions reduce to the previously discovered $z = 4$ black hole solution of [6].

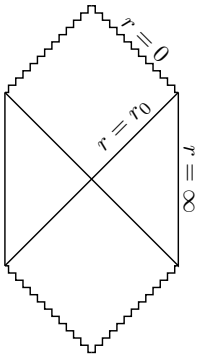


**Figure 1.** Global geometry of an asymptotically Lifshitz black hole. The null singularity at $r = 0$ is indicated by the jagged lines.

to new null variables $P, Q$, defined through $V = \tan\frac{\pi P}{2}$, $U = \tan\frac{\pi Q}{2}$, the global geometry can be represented by a simple diagram shown in Figure 1. Each point in the diagram represents an entire $d$-volume parametrized by $\vec{x}$. The global diagram in Figure 1 differs from standard Carter-Penrose conformal diagrams in that the boundary at $r \to \infty$ is not conformally flat. This is a consequence of the scaling asymmetry between $t$ and $\vec{x}$ and is readily apparent in the globally extended metric (32).

When $z = 1$ the auxiliary massive vector field $\mathcal{A}_\mu$ can be consistently set to zero and the field equations then reduce to those of Einstein-Maxwell gravity with a negative cosmological constant. In this case, there is a well known exact solution, the AdS-Reissner-Nordstrm black brane, which has a timelike curvature singularity inside an inner and an outer horizon. The interior geometry of the exact $z = 2d$ black brane is markedly different with a null curvature singularity at $r = 0$ and no smooth inner horizon.

### 3. Holographic superconductors with asymmetric scaling

We now consider charged black branes with hair. Static spherically symmetric solutions of the scalar field equation (6) have the asymptotic form $\phi(u) \to c_-(e^{-\Delta_- u} + \ldots) + c_+(e^{-\Delta_+ u} + \ldots)$, with

$$\Delta_\pm = \frac{d+z}{2} \pm \sqrt{\left(\frac{d+z}{2}\right)^2 + m^2}, \tag{33}$$

while the asymptotic behavior of the electromagnetic field field strength is

$$\beta(u) \approx \frac{\rho}{r_0^d} e^{-du} + \ldots . \tag{34}$$

Working at fixed charge density in the dual field theory, we read the radial location of the horizon off from the asymptotic behavior of $\beta(u)$ and then the temperature can be obtained from the numerical solution for $f(u)$ and $g(u)$ using (26).

In the following we set the scalar mass squared to $m^2 = \frac{1}{4} - \left(\frac{d+z}{2}\right)^2$, which is inside the range where there is a choice of two boundary theories [9]. This choice leads to convenient values, $\Delta_\pm = \frac{d+z}{2} \pm \frac{1}{2}$, for the dimensions of the operators $\mathcal{O}_\pm$ that are dual to the scalar field in each of the two boundary theories. Non-linear descendants of the leading scalar field modes are suppressed by $O(e^{-2u})$ at $u \to \infty$ and this choice of mass squared ensures that the first descendant of $\psi_-$ falls off faster than $\psi_+$.

In order to study holographic superconductivity, we first select some value for $d$, $z$ and the electric charge $q$ carried by the scalar field and then generate numerical black brane solutions for

a range of initial values $\beta(0)$ and $\phi(0)$. We then investigate the asymptotic large $u$ behavior of the scalar hair in the numerical solutions. A superconducting condensate corresponds to either

$$c_+ = 0, \quad \langle \mathcal{O}_- \rangle = c_- \neq 0, \qquad \text{or} \qquad c_- = 0, \quad \langle \mathcal{O}_+ \rangle = c_+ \neq 0, \tag{35}$$

depending on which of the two boundary theories is being considered [10, 11]. We look for a curve in the $\beta(0)$ *vs.* $\psi(0)$ plane of initial values at the horizon, for which the corresponding black brane solution has vanishing $c_+$ ($c_-$), and tabulate the value of $c_-$ ($c_+$) along this curve. The temperature is found from the same numerical solutions *via* (26) and (34). Figure 2 shows a plot of $c_-$ *vs.* $T$ obtained by this procedure for $d = 2$, $z = 2$, and $q = 1$. The results are expressed in terms of dimensionless ratios that are insensitive to the overall scale (set by the charge density $\rho$, which is held fixed at some finite value throughout).

These results demonstrate that a superconducting condensate can form in systems with anisotropic scaling but we have not touched on a number of interesting topics including the electric conductivity and magnetic properties of these holographic superconductors.

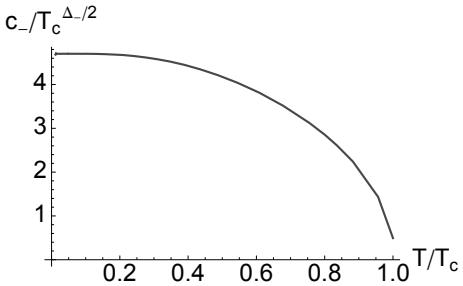


**Figure 2.** Scalar field condensate in a holographic superconductor at $z = d = 2$.

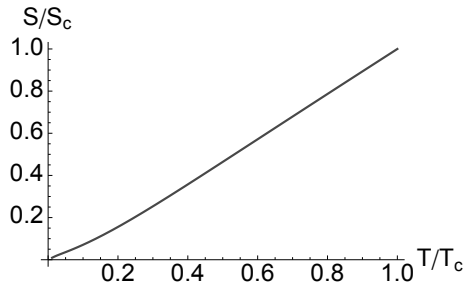


**Figure 3.** Entropy as a function of temperature in the superconducting phase of the holographic superconductor in Figure 2.

## 4. Zero temperature entropy vs. scalar hair

In the absence of charged matter, the charged black branes in our model have an extremal limit given by $\tilde{\rho} \to \pm\sqrt{2(z^2 + (d-1)z + d^2)}$. It then follows from $\tilde{\rho} = \rho/r_0^d$ that the radial location of the horizon $r_0$ has a finite value in the extremal limit for fixed charge density $\rho$. This in turn means that the entropy density $S = r_0^d/4$ remains finite in the zero temperature limit indicating a macroscopic groundstate degeneracy.

This conclusion is radically altered when the system is coupled to a charged scalar field. In this case the zero temperature limit is approached in the condensed phase and the black holes, that are dual to extreme low temperature states, have scalar hair. It is straightforward to keep track of the black brane entropy as the temperature is lowered below the critical value for forming the superconducting condensate. The result for the same $d = 2$, $z = 2$ holographic superconductor as was considered in the previous section is shown in Figure 3. Both the entropy density and the temperature are normalized to their values at the onset of condensation, $S_c$ and $T_c$ respectively.

Although the numerical calculations break down before absolute zero is reached, the numerical data strongly suggest that $S$ vanishes in the $T \to 0$ limit for a generic dynamical critical exponent $z$, which is consistent with a non-degenerate ground state in the dual field theory. The corresponding result for conformal systems with $z = 1$ was established in [12].

## 5. Summary

We have presented an overview of the construction of charged black brane solutions in gravity models that realize the anisotropic scaling symmetry that is characteristic of many interesting quantum critical points. The motivation for the study of these models comes from condensed matter theory, in particular from two- and three-dimensional systems involving strongly correlated electrons. The relevance of gravitational models to real world condensed matter systems remains highly speculative, but the gravitational approach continues to produce effects that are intriguingly similar to what is seen in experiments. A recent example from our own work [13] involves non-Fermi-liquid behavior in the specific heat of anisotropic black branes of the type considered in the present paper, which turns out to be qualitatively similar to the measured specific in certain heavy fermion metals near a quantum phase transition [14, 15]. While much of the work on gravitational modeling of strongly coupled field theories to date involves asymptotically AdS spacetime and an underlying conformal symmetry, it was crucial to the success of this particular application to have a non-trivial dynamical critical exponent $z > 1$. This provides impetus for further study of gravity models with anisotropic scaling.


## Acknowledgments

This work was supported in part by the Göran Gustafsson foundation, the Swedish Research Council (VR), the Icelandic Research Fund, the University of Iceland Research Fund, and the Eimskip Research Fund at the University of Iceland.


## References


[1] Kachru S, Liu X, and Mulligan M 2008 Gravity duals of Lifshitz-like fixed points *Phys. Rev.* D **78** 106005 (*Preprint* arXiv:0808.1725 [hep-th])

[2] Koroteev P and Libanov M 2008 On existence of self-tuning solutions in static braneworlds without singularities *J. High Energy Phys.* JHEP02(2008)104 (*Preprint* arXiv:0712.1136 [hep-th])

[3] Taylor M 2008 Non-relativistic holography (*Preprint* arXiv:0812.0530 [hep-th])

[4] Brynjolfsson E J, Danielsson U H, Thorlacius L and Zingg T 2010 Holographic superconductors with Lifshitz scaling *J. Phys. A: Math. Theor.* **43** 065401(*Preprint* arXiv:0908.2611 [hep-th])

[5] Danielsson U H and Thorlacius L 2009 Black holes in asymptotically Lifshitz spacetime," *J. High Energy Phys.* JHEP03(2008)070 (*Preprint* arXiv:0812.5088 [hep-th])

[6] Bertoldi G, Burrington B A and Peet A (2009) Black holes in asymptotically Lifshitz spacetimes with arbitrary critical exponent *Phys. Rev.* D **80** 126003 (*Preprint* arXiv:0905.3183 [hep-th])

[7] Ross S F and Saremi O (2009) Holographic stress tensor for non-relativistic theories *J. High Energy Phys.* JHEP09(2009)009 (*Preprint* arXiv:0907.1846 [hep-th])

[8] Pang D W 2010 On charged Lifshitz black holes *J. High Energy Phys.* JHEP10(2010)116 (*Preprint* arXiv:0911.2777 [hep-th])

[9] Klebanov I R and Witten E 1999 AdS/CFT correspondence and symmetry breaking *Nucl. Phys. B* **556** 89 (*Preprint* hep-th/9905104)

[10] Gubser S S 2008 Breaking an Abelian gauge symmetry near a black hole horizon *Phys. Rev.* D **78** 065034 (*Preprint* arXiv:0801.2977 [hep-th])

[11] Hartnoll S A, Herzog C P and Horowitz G T 2008 Building a Holographic Superconductor *Phys. Rev. Lett.* **101** 031601 (*Preprint* arXiv:0803.3295 [hep-th])

[12] Horowitz G T and Roberts M M 2009 Zero temperature limit of holographic superconductors *J. High Energy Phys.* JHEP11(2009)015 (*Preprint* arXiv:0908.3677 [hep-th])

[13] Brynjolfsson E J, Danielsson U H, Thorlacius L and Zingg T 2010 Black hole thermodynamics and heavy fermion metals (*Preprint* arXiv:1003.5361 [hep-th])

[14] Löhneysen H v, Pietrus T, Portisch G, Schlager H G, Schröder A, Sieck M, and Trappmann T 1994 Non-Fermi liquid behavior in a heavy-fermion alloy at a magnetic instability *Phys. Rev. Lett.* **72** 3262

[15] Stewart G R 2001 Non-Fermi-liquid behavior in d- and f-electron metals *Rev. Mod. Phys.* **73** 797 (Addendum-ibid. 2006 **78** 743)

# Paper IV

Published for SISSA by Springer

Received: *December 7, 2010*
Accepted: *January 10, 2011*
Published: *January 25, 2011*

# Holographic metals at finite temperature

**V. Giangreco M. Puletti,**[a] **S. Nowling,**[a] **L. Thorlacius**[a,b] **and T. Zingg**[a,b]

[a] *NORDITA,*
*Roslagstullsbacken 23, SE-106 91 Stockholm, Sweden*
[b] *University of Iceland, Science Institute,*
*Dunhaga 3, IS-107 Reykjavik, Iceland*

*E-mail:* valentina@nordita.org, nowling@nordita.org, larus@nordita.org, zingg@nordita.org

Abstract: A holographic dual description of a 2+1 dimensional system of strongly interacting fermions at low temperature and finite charge density is given in terms of an electron cloud suspended over the horizon of a charged black hole in asymptotically AdS spacetime. The electron star of Hartnoll and Tavanfar is recovered in the limit of zero temperature, while at higher temperatures the fraction of charge carried by the electron cloud is reduced and at a critical temperature there is a third order phase transition to a configuration with only a charged black hole. The geometric structure implies that finite temperature transport coefficients, including the AC electrical conductivity, only receive contributions from bulk fermions within a finite band in the radial direction.

Keywords: Holography and condensed matter physics (AdS/CMT), Gauge-gravity correspondence, Black Holes

ArXiv ePrint: 1011.6261



doi:10.1007/JHEP01(2011)117

JHEP01(2011)117

## Contents



JHEP01(2011)117

## 1 Introduction

There has been considerable recent interest in developing holographic models of strongly coupled physics in low dimensions with a view towards condensed matter systems (see [1–4] for reviews). This can be motivated both from the point of view of extending the gauge theory/gravity correspondence to include a variety of interesting field theoretic systems without supersymmetry, and also from the point of view of gaining a new theoretical handle on materials containing strongly correlated electrons.

In a recent paper Hartnoll and Tavanfar [5] considered a simple holographic model for strongly interacting fermions in 2+1 dimensions at zero temperature and finite charge density. In their approach, which builds on earlier work in [6, 7], the bulk Maxwell field, which is dual to the field theory current, is sourced by an ideal fluid consisting of charged free fermions. The combined Einstein, Maxwell, and fluid field equations in the bulk spacetime have planar solutions, referred to as electron stars in [5], where the charge and energy densities of the bulk fermion fluid have a non-trivial radial profile. The geometry is asymptotically AdS but deep in the electron star interior the metric exhibits Lifshitz scaling with a non-universal dynamical critical exponent that depends on the couplings of the model. Similar constructions were considered in [8, 9] for neutral and charged free fermion fluids supported by a degeneracy pressure.

In the present paper we extend the gravity dual description of [5] to include finite temperature configurations in the boundary field theory. We construct static solutions of the bulk field equations where an 'electron cloud' is suspended above the horizon of a charged black hole, or more precisely a black brane with a planar horizon. The electron cloud has both an outer and an inner edge. The outer edge is also found in the electron stars of [5] but the inner edge is a new feature, found only at finite temperature. At the inner edge the gravitational pull of the black brane on the electron fluid is balanced by electrostatic repulsion.

In the fluid description, observables in the boundary theory, such as the electric conductivity, only receive contributions from bulk fermions located within a band of finite

width in the radial direction. The sharpness of the edges is presumably an artifact of the classical perfect fluid description and we expect both quantum corrections and fluid interactions to give rise to tails in the bulk fermion profile that fall off towards the boundary and the black brane horizon, respectively.[1]

At the level of classical geometry, a finite temperature in the boundary theory is introduced by including a black hole in the bulk spacetime, with a non-vanishing Hawking temperature. Quantum effects in the bulk include thermal Hawking radiation, which comes to equilibrium with the bulk fermion fluid, but at weak gravitational coupling this thermalization in the bulk is suppressed and will not be considered here. This simplifies our analysis considerably as it allows us to use a zero temperature equation of state for the free fermions in the bulk to capture finite temperature effects in the boundary field theory.

At low temperatures in the boundary theory, the electric charge in the bulk geometry is partly carried by the electron cloud and partly by the charged black brane inside it. As the temperature is raised, the two edges of the electron cloud move towards each other and an ever larger fraction of the total electric charge in the bulk geometry resides inside the black brane. The two edges of the electron fluid meet at a finite critical temperature, above which there is only a black brane solution with no electron cloud present. We find that the system undergoes a third order phase transition at the critical point.[2]

As the temperature is lowered, on the other hand, the inner edge of the electron cloud approaches the black brane horizon, which in turn recedes towards vanishing area. In the zero temperature limit, one recovers the electron star geometry where there is no longer any black hole and all the charge is carried by the electron fluid. We confirm this by showing that the horizon recedes from the boundary, the geometry at low temperature encodes the dynamical exponent $z$, and by comparing free energy densities. We find that at low temperatures the free energy density of an electron cloud geometry smoothly goes over to that of an electron star. Furthermore, we compare the free energy densities between an electron cloud solution and an AdS-RN black brane solution at finite temperature. We find that, whenever a solution with an electron cloud exists, it is favored over an AdS-RN black brane.

The electrical conductivity at finite temperature can be obtained for this system using, by now, standard holographic techniques (see for instance [1, 2]). We find that the finite temperature conductivity smoothly interpolates between the AdS-RN and electron star results [5].

The same finite temperature solutions were found independently by Hartnoll and Petrov in [10]. Initially there was a discrepancy between their work and ours in the analysis of the phase transition, but after correcting an error in our expression for the free energy density, we now also find a third order phase transition.

[1] Such tails are, for instance, found in an alternative approach to including bulk fermions based on a single fermion wave equation [11].

[2] In an earlier preprint of this paper it was incorrectly stated that the phase transition was second order. The correct behavior was identified in [10].



JHEP01(2011)117

## 2 Field equations and electron cloud solutions

The Einstein-Maxwell equations with a negative cosmological constant and a charged perfect fluid are

$$R_{\mu\nu} - \frac{1}{2}g_{\mu\nu}R - \frac{3}{L^2}g_{\mu\nu} = \kappa^2(T^{\rm Maxwell}_{\mu\nu} + T^{\rm fluid}_{\mu\nu})\,, \qquad \nabla^\nu F_{\mu\nu} = e^2\, J^{\rm fluid}_\mu\,. \tag{2.1}$$

We adopt units where the characteristic AdS length scale is $L = 1$. The source terms are given by

$$T^{\rm Maxwell}_{\mu\nu} = \frac{1}{e^2}\left(F_{\mu\lambda}F_\nu{}^\lambda - \frac{1}{4}g_{\mu\nu}F_{\lambda\sigma}F^{\lambda\sigma}\right), \tag{2.2}$$

$$T^{\rm fluid}_{\mu\nu} = (\rho + p)u_\mu u_\nu + p\, g_{\mu\nu}\,, \tag{2.3}$$

$$J^{\rm fluid}_\mu = \sigma u_\mu\,, \tag{2.4}$$

where $\sigma$ is the charge density of the fluid, $\rho$ is its energy density, $p$ the pressure, and $u^\mu$ the four velocity, $u^\mu u_\mu = -1$. The justification and limitations of the perfect fluid description are discussed in detail in [5] and the same considerations apply here.

We look for static black brane solutions with planar symmetry,

$$ds^2 = -f(v)dt^2 + g(v)dv^2 + \frac{1}{v^2}(dx^2 + dy^2)\,, \qquad A = \frac{e}{\kappa}h(v)\,dt\,, \tag{2.5}$$

where the radial coordinate goes from $v \to 0$ at the asymptotic boundary to a constant value $v = v_0$ at the black brane horizon. We find it convenient to introduce a scale invariant variable $u = -\log(v/v_0)$, such that $u = 0$ at the horizon and $u \to \infty$ at the boundary, and work with rescaled fields,

$$\hat f = v_0^2 f, \quad \hat g = v_0^2 g, \quad \hat h = v_0 h, \quad \hat p = \kappa^2 p, \quad \hat\rho = \kappa^2\rho, \quad \hat\sigma = e\kappa\sigma\,. \tag{2.6}$$

The equations of motion (2.1) can then be expressed in a first order form, convenient for numerical evaluation,

$$\frac{d\hat f}{du} + \frac{\hat k^2}{2} + \hat f(1 - 3e^{-2u}\hat g) = e^{-2u}\hat f\hat g\hat p\,, \tag{2.7}$$

$$\frac{d\hat k}{du} + \hat k = e^{-2u}\left(\frac{1}{2}\hat h\hat k + \hat f\right)\frac{\hat g\hat\sigma}{\sqrt{\hat f}}\,, \tag{2.8}$$

$$\frac{1}{\hat f}\frac{d\hat f}{du} + \frac{1}{\hat g}\frac{d\hat g}{du} - 4 = e^{-2u}\frac{\hat g\hat h\hat\sigma}{\sqrt{\hat f}}\,, \tag{2.9}$$

where $\hat k \equiv d\hat h/du$. Following [5], we assume a free fermion equation of state defined via

$$\hat\sigma = \hat\beta\int_{\hat m}^{\hat\mu} d\varepsilon\,\varepsilon\sqrt{\varepsilon^2 - \hat m^2}\,, \qquad \hat\rho = \hat\beta\int_{\hat m}^{\hat\mu} d\varepsilon\,\varepsilon^2\sqrt{\varepsilon^2 - \hat m^2}\,, \qquad -\hat p = \hat\rho - \hat\mu\hat\sigma\,, \tag{2.10}$$

where $\hat\beta$ is a coupling dependent dimensionless constant, $\hat m$ is proportional to the electron mass, $\hat m^2 = \frac{\kappa^2}{e^2}m^2$, and the (rescaled) local chemical potential $\hat\mu$ is given by the background Maxwell gauge field in the tangent frame, $\hat\mu \equiv \hat h/\sqrt{\hat f}$.



JHEP01(2011)117

As discussed in [5], there is a range of parameters,

$$e^2 \sim \frac{\kappa}{L} \ll 1\,, \tag{2.11}$$

for which we can assume a classical bulk geometry with a non-trivial back-reaction due to the fermion fluid. If, at the same time, the Compton wavelength of the fermions is small compared to the AdS length scale,

$$mL \gg 1\,, \tag{2.12}$$

then we are also justified in taking spacetime to be locally flat in the fermion equation of state. These conditions amount to the dimensionless parameters in the equation of state (2.10) taking order one values [5],

$$\hat{\beta} \sim 1\,, \qquad \hat{m}^2 \sim 1\,. \tag{2.13}$$

The construction of the electron cloud geometry proceeds in a few steps. First we solve the vacuum equations, with $\hat{\sigma} = \hat{\rho} = \hat{p} = 0$, to find the charged AdS-RN black brane solution inside the cloud,

$$\hat{f} = e^{2u} + \frac{\hat{q}^2}{2} e^{-2u} - \left(1 + \frac{\hat{q}^2}{2}\right) e^{-u}\,, \qquad \hat{g} = \frac{e^{4u}}{\hat{f}}\,, \qquad \hat{h} = \hat{q}(1 - e^{-u})\,. \tag{2.14}$$

The dimensionless constant $\hat{q}$ is proportional to the charge carried by the black brane and we have used the freedom to rescale the time coordinate $t$ to fix the overall normalization of $\hat{f}$. When the charge parameter is in the range $\hat{q}^2 < 6$ the black brane is non-extremal with a non-degenerate horizon, where the local chemical potential $\hat{\mu}$ vanishes. As we move away from the horizon the chemical potential grows but remains too small to support a fermion fluid until

$$\hat{\mu}^2 = \frac{\hat{h}^2(u)}{\hat{f}(u)} > \hat{m}^2\,. \tag{2.15}$$

We will only consider non-vanishing fermion mass. For zero fermion mass the inner edge of the electron cloud reaches the horizon for all temperatures. The geometry, with the back-reaction from the fermion fluid included, is then harder to determine and we will not consider this case here.

The condition (2.15) is easily seen to be equivalent to

$$\hat{q}^2 > \frac{\hat{m}^2 e^u (e^{2u} + e^u + 1)}{e^u - 1 + \frac{\hat{m}^2}{2}} \equiv r(u)\,. \tag{2.16}$$

The right hand side is shown for two different values of $\hat{m}^2$ in figure 1. It can be read off from the figure that:

- There cannot be any fermion fluid outside a non-extremal black brane if $\hat{m}^2 \geq 1$, since in this case $r(u) > 6$ for all $u > 0$. This restriction on $\hat{m}$ was already seen in [5] as a condition for the existence of electron star solutions at zero temperature.



JHEP01(2011)117

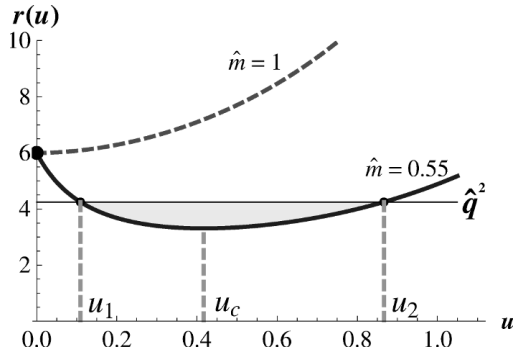


**Figure 1**. The auxiliary function $r(u)$ in (2.16), used in the construction of the electron cloud solution, is plotted for $\hat{m} = 1$ (dashed red) and $\hat{m} = 0.55$ (solid blue).

- For $\hat{m}^2 < 1$ and a near-extremal black brane with $\hat{q}^2 < 6$, the condition (2.16) is satisfied within a finite interval $u_1 < u < u_2$, indicated in the figure. The endpoints of the interval correspond to the inner and outer edges of the electron cloud in a "probe" approximation, where the back-reaction on the geometry due to the fermion fluid is ignored.

- For $\hat{m}^2 < 1$ and $\hat{q}^2$ below a critical value (which depends on $\hat{m}^2$), the condition (2.16) is not satisfied for any $u > 0$. This implies there is a critical temperature above which there is only a black brane and no electron fluid in the bulk.

The second step in the construction of an electron cloud solution with back-reaction included is to numerically integrate the field equations (2.7)–(2.9) starting from the inner edge of the electron cloud. The functions $\hat{f}$, $\hat{g}$, $\hat{h}$, and $\hat{k}$ are continuous at the matching point $u = u_1$ and thus we can generate initial values for the numerical integration using the exact AdS-RN solution (2.14) with $\hat{q}$ determined from (2.16) evaluated at $u = u_1$.

The local chemical potential $\hat{\mu}$ goes to zero in the asymptotic $u \to \infty$ region and the numerical integration is terminated at a point $u = u_s$ where the condition (2.16) is no longer satisfied. We find that the back-reaction of the fermion fluid on the geometry leads to $u_s > u_2$, and that this effect becomes more pronounced, $u_s \gg u_2$, at low temperature. Figure 2 shows numerical results for the fluid variables $\hat{\sigma}$, $\hat{\rho}$, and $\hat{p}$ for $\hat{m} = 0.55$, $\hat{\beta} = 10$, and $\hat{q}^2 = 4.49$.

The third and final step in the construction is to obtain the spacetime geometry outside the electron cloud by matching the numerical solution onto a charged black brane solution at $u = u_s$ in much the same way as is done for electron stars in [5]. The exterior solution has the general form

$$\hat{f} = c_s^2 e^{2u} + \frac{Q_s^2}{2} e^{-2u} - M_s e^{-u}\,, \qquad \hat{g} = \frac{c_s^2 e^{4u}}{\hat{f}}\,, \qquad \hat{h} = \mu_s - Q_s e^{-u}\,, \tag{2.17}$$



JHEP01(2011)117

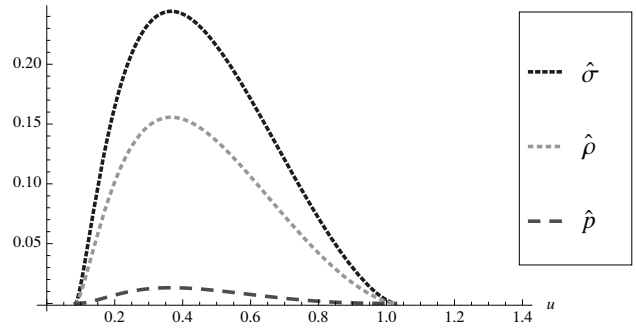


**Figure 2**. The radial profiles of the fluid variables $(\hat{\sigma}, \hat{\rho}, \hat{p})$ for $\hat{m} = 0.55$, $\hat{\beta} = 10$, and $\hat{q}^2 = 4.49$.

where the subscript $s$ on the various constant parameters is a reminder that they are determined by matching onto a numerical solution at $u = u_s$. We already fixed the overall scale of the time coordinate when writing the inside black brane solution in (2.14) so now there appears an extra parameter $c_s$ in $\hat{f}$. Also, since the external solution only extends to $u = u_s$ and not to an event horizon, we do not require the usual relationship between $M_s$, $Q_s$, and $\mu_s$ found for a vacuum AdS-RN black brane. The parameters in (2.17) are instead determined to be

$$c_s^2 = \hat{f}(u_s)\hat{g}(u_s)e^{-4u_s}\,, \tag{2.18}$$

$$Q_s = \hat{k}(u_s)e^{u_s}\,, \tag{2.19}$$

$$\mu_s = \hat{h}(u_s) + \hat{k}(u_s)\,, \tag{2.20}$$

$$M_s = \hat{f}(u_s)\hat{g}(u_s)e^{-u_s} + \frac{1}{2}\hat{k}^2(u_s)e^{u_s} - \hat{f}(u_s)e^{u_s}\,. \tag{2.21}$$

These parameters refer to the rescaled fields in (2.6) while the physical parameters appearing in an external AdS-RN solution with a canonically normalized time coordinate are given by

$$\mu = \frac{\mu_s}{c_s v_0}\,, \qquad Q = \frac{Q_s}{c_s v_0^2}\,, \qquad M = \frac{M_s}{c_s^2 v_0^3}\,. \tag{2.22}$$

Once the parameters of the external black brane solution have been determined for given values of $\hat{m}$, $\hat{\beta}$, and $\hat{q}$, standard methods can be used to obtain the free energy density as a function of temperature for these geometries. This will be carried out in section 3 below.

The next step is to determine the Hawking temperature of the electron cloud geometry, which is to be identified with the temperature in the boundary field theory. The Hawking temperature is easily obtained from the behavior of the Euclidean metric near the horizon. One finds

$$\frac{T}{\mu} = \frac{6 - \hat{q}^2}{8\pi\mu_s}\,, \tag{2.23}$$

where we have again divided by the physical chemical potential $\mu$ in order to have a dimensionless quantity to work with.



JHEP01(2011)117

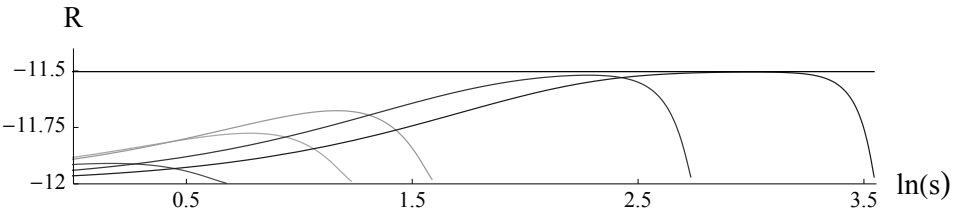


**Figure 3**. The curvature scalar $R$ versus the proper distance $s$ measured from the outer edge of the electron cloud for $\hat{m} = .55\,, \hat{\beta} = 10$ and for $T/\mu$ values $.55, .22, 9.4\times10^{-2}, 9\times10^{-4}$ and $1\times10^{-5}$. The curves extend further to the right with decreasing temperature. The value for $R$ in the Lifshitz region deep inside an electron star with the same $\hat{m}$ and $\hat{\beta}$ is shown as a horizontal line for reference.

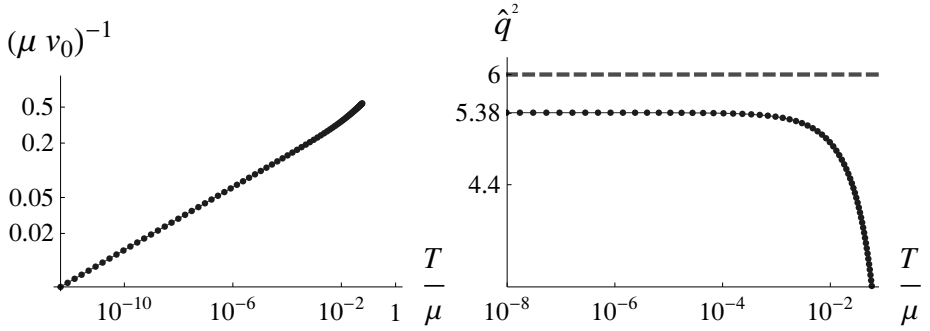


**Figure 4**. On the left we plot the horizon radius $v_0^{-1}$ as a function of the temperature, $T$. On the right we show the charge parameter of the inside black brane solution (2.14), $\hat{q}^2$, versus $T$ for $\hat{m} = .55$ and $\hat{\beta} = 10$. For reference we plot the extremal value $\hat{q}^2 = 6$.

In the limit of zero temperature we expect to recover the electron star geometry of [5]. In this case the radial coordinate extends to $u \to -\infty$ and the metric exhibits Lifshitz scaling in the deep interior.

In figure 3 one can see that the curvature scalar $R$ as a function of the proper distance $s$ measured from the outside of the electron cloud is approaching the expected asymptotic value for a Lifshitz geometry as we lower the temperature $T$ before plunging to $R = -12$ at the horizon. From $R$ evaluated on the solution and the metric, one confirms the correct dynamical exponent, e.g. $z = 5.75466$ when $\hat{m} = .55$ and $\hat{\beta} = 10$.

On the left in figure 4, we see that the horizon radius vanishes as the temperature is lowered indicating that the horizon recedes from the AdS boundary. Furthermore by fitting the low temperature data in the figure, we find that

$$\frac{T}{\mu} \propto \left(\frac{1}{\mu v_0}\right)^z \,, \tag{2.24}$$

where $z$ matches the appropriate expected Lifshitz exponent to a very high precision. This



JHEP01(2011)117

is further evidence that the anisotropic scaling found inside the electron star is recovered by our electron cloud solutions at low temperature.

The plot on the right in figure 4 shows that the zero temperature limit in the boundary theory is in fact not obtained by approaching an extremal interior black brane, which would have $\hat{q}^2 = 6$. This is at first sight counterintuitive but can ultimately be traced to the focusing effect that the electron fluid has on the geometry outside the black brane. If one were to try to construct an electron cloud solution starting with a value of $\hat{q}^2$ that is closer to 6, than what is seen in the figure the metric would collapse to a curvature singularity at a finite proper distance outside the horizon and the solution would never reach an asymptotic AdS region.

## 3 Free energy

Further evidence that the electron cloud solution is the proper finite temperature extension of an electron star comes from comparing free energy densities. We obtain the free energy by evaluating the on-shell Euclidean action of the bulk system, including the usual Gibbons-Hawking boundary term [12] and boundary counterterms required for regularization [13, 14]. A bulk action for the charged electron fluid also needs to be included, as described in [5]. The full bulk action turns out to be the integral of a total derivative, and when combined with the appropriate boundary terms, it gives a simple result for the free energy density,

$$F = M - \mu\, Q \, - sT \,, \tag{3.1}$$

where $s$ is the Bekenstein-Hawking entropy density.[3] This can be simplified by using the thermodynamic relation

$$\frac{3}{2} M - \mu\, Q - s\, T = 0 \,, \tag{3.2}$$

giving

$$F = -\frac{M}{2} \,. \tag{3.3}$$

The relation (3.1) follows from the radial conservation of the quantity

$$D = \frac{e^{3u}}{\sqrt{\hat{f}\hat{g}}} \left( -2\hat{h}\hat{k} - 2\hat{f} + \frac{d\hat{f}}{du} \right) . \tag{3.4}$$

By using the equations of motion (2.7)–(2.10), it is straightforward to check that $\frac{dD}{du} = 0$ and one then evaluates $D$ at the horizon and at the $u \to \infty$ boundary to obtain (3.2).

Using (2.22), the free energy density can be re-expressed in terms of output parameters from our numerical evaluation,

$$F = -\frac{1}{2} \frac{M_s}{c_s^2 v_0^3} \,. \tag{3.5}$$

[3] In an earlier version of the paper the $sT$ term was missing from the expression for the free energy density. This led to an incorrect characterization of the phase transition.



JHEP01(2011)117

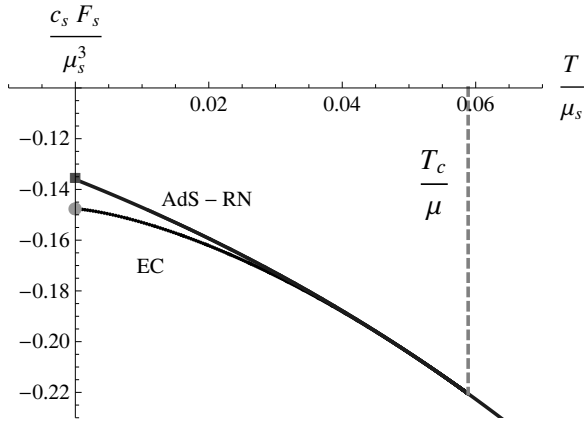


**Figure 5**. The free energy densities of AdS-RN black brane and electron cloud solutions for $\hat{\beta} = 10$ and $\hat{m} = .55$. In addition the free energy for an extremal black hole and the electron star solution of [5] are shown with a red box and a green dot, respectively.

The factor of $v_0^3$ in the denominator tells us that we should instead work with the dimensionless quantity

$$\frac{F}{\mu^3} = -\frac{1}{2}\frac{c_s M_s}{\mu_s^3}\,, \tag{3.6}$$

when comparing free energy densities.

In figure 5 we use these dimensionless variables to compare the free energy densities of various geometries for a typical case when $\hat{m} = .55$ and $\hat{\beta} = 10$, holding the chemical potential fixed. One readily sees that the electron cloud solution is preferred over the black brane solution up to the point where the local chemical potential is too low to support any fluid. Beyond this point the only solution is an AdS-RN black brane. At low temperatures, on the other hand, the free energy density of the electron cloud geometries approaches that of the corresponding electron star.

In addition to the low-temperature regime, it is also interesting to ask about the nature of the transition to the AdS-RN black brane solution at higher temperatures. To address this issue, we consider the difference in energy densities between an electron cloud solution just below the critical temperature $T_c$ and an AdS-RN black brane solution,

$$\Delta\left(\frac{F}{\mu^3}\right) \equiv \left(\frac{F}{\mu^3}\right)_{AdS-RN} - \left(\frac{F}{\mu^3}\right)_{EC}\,, \tag{3.7}$$

at the same value of $T/\mu$. Figure 6 shows a log-log plot of this difference near the critical point where one loses the cloud solution at $T_c/\mu = 0.058868$ for $\hat{m} = .55$ and $\hat{\beta} = 10$. The solid curve in figure 6 is a straight line of slope 3 giving numerical evidence of a third order phase transition where

$$\Delta\left(\frac{F}{\mu^3}\right) = \mathcal{O}\left(\frac{T_c - T}{\mu}\right)^3\,. \tag{3.8}$$



JHEP01(2011)117

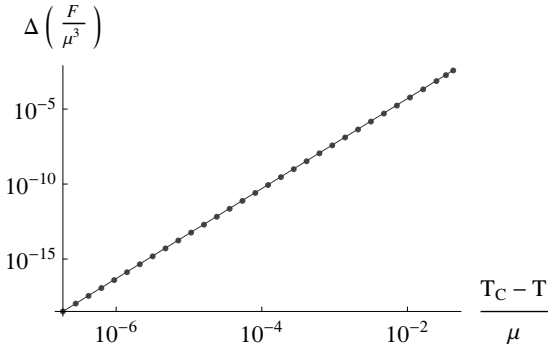


**Figure 6**. The difference between the black brane and electron cloud free energies near the phase transition temperature at $\hat{\beta} = 10$ and $\hat{m} = .55$.

This feature was observed numerically in [10], and those authors also gave a simple analytic argument for this behavior.

## 4 Electric conductivity

The finite temperature AC conductivity at zero momentum can be computed in an analogous way as was done for the zero temperature electron star in [5]. In fact, the finite temperature computation is more standard since in this case the ingoing boundary conditions [15] for the fluctuations in the gauge field are imposed at a smooth black brane horizon rather than at the (mildly) singular Lifshitz horizon inside an electron star.

The background is perturbed, assuming a time dependence of the form $e^{-i\omega t}$, and the resulting equations are linearized. To get a closed system of equations, the following perturbations are needed

$$\hat{A}_x = \delta\hat{A}_x(u)e^{-i\omega t}\,, \qquad \hat{g}_{tx} = \delta\hat{g}_{tx}(u)e^{-i\omega t}\,, \qquad \hat{u}_x = \delta\hat{u}_x(u)e^{-i\omega t}. \tag{4.1}$$

This leads to a system of four first order differential equations

$$\delta\hat{A}_x + \frac{\hat{h}}{\hat{f}}\,\delta\hat{g}_{tx} + e^{2u}\hat{\mu}\,\delta\hat{u}_x = 0, \tag{4.2}$$

$$\frac{d\delta\hat{g}_{tx}}{du} - 2\delta\hat{g}_{tx} + 2\,\frac{d\hat{h}}{du}\,\delta\hat{A}_x = 0, \tag{4.3}$$

$$e^u\frac{d\delta\hat{A}_x}{du} + \sqrt{\frac{\hat{g}}{\hat{f}}}\delta\hat{B}_x = 0, \tag{4.4}$$

$$e^u\,\frac{d\delta\hat{B}_x}{du} + \left[\frac{1}{\sqrt{\hat{f}\hat{g}}}\left(2e^{2u}\frac{d\hat{h}}{du}^2 - \omega_s^2\hat{g}\right) + \frac{\hat{f}\hat{\sigma}\sqrt{\hat{g}}}{\hat{h}}\right]\delta\hat{A}_x = 0, \tag{4.5}$$



JHEP01(2011)117

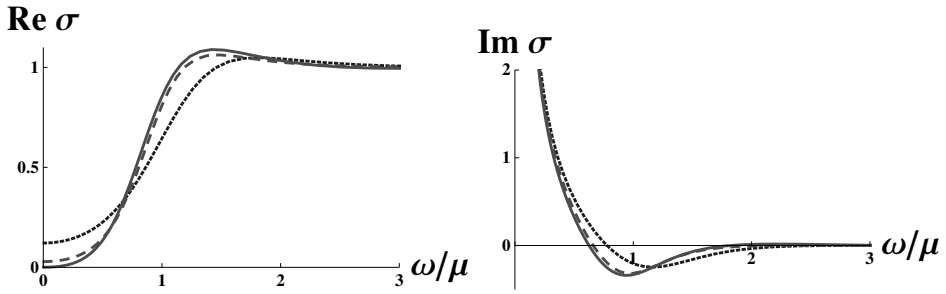


**Figure 7**. Real and Imaginary part of the conductivity for $\hat{m} = 0.55, \hat{\beta} = 10$. The curves blue dots, dashed green and solid red correspond to temperature value $T/T_C = 2, 1$ and 0.162, respectively. $T_C/\mu = 0.05887$ denotes the critical temperature where the phase transition occurs. Curves for lower values of $T$ are almost indistinguishable from the solid red curve.

JHEP01(2011)117

where $\omega_s$ is defined in terms of the canonical normalized frequency $\omega$ as $\omega_s = c_s\, v_0\, \omega$. Equation (4.4) can be regarded as the definition of the auxiliary function $\delta\hat{B}_x$. We note that (4.4) and (4.5) form a closed system involving only $\delta\hat{A}_x$ and $\delta\hat{B}_x$.

At the horizon, ingoing boundary conditions are imposed [15]. This implies $\delta\hat{A}_x \to u^{-\frac{i\omega}{4\pi T}}$ and $\delta\hat{B}_x \to i\omega u^{-\frac{i\omega}{4\pi T}}$ as $u \to 0$ and $T$ being the Hawking temperature of the AdS-RN black brane solution (2.14). At the AdS boundary, where the background is of the form (2.17), the behavior of those functions is

$$\delta\hat{A}_x = \hat{A}_x^{(0)} + \hat{A}_x^{(1)} e^{-u} + \cdots , \tag{4.6}$$

$$\delta\hat{B}_x = \hat{B}_x^{(0)} + \hat{B}_x^{(1)} e^{-u} + \cdots . \tag{4.7}$$

The coefficients $\hat{A}_x^{(i)}$ and $\hat{B}_x^{(i)}$ are connected, e.g. $\hat{B}_x^{(0)} = c_s \hat{A}_x^{(1)}$. This relation can be used to express the conductivity as

$$\sigma = -\frac{i}{\omega_s} \frac{\hat{B}_x^{(0)}}{\hat{A}_x^{(0)}} , \tag{4.8}$$

which is manifestly invariant under the rescaling described in the previous sections.

Our results for the conductivity are obtained by numerics. This is achieved by integrating out from the horizon in the background of an AdS-RN solution, as already indicated, until the inner edge of the electron shell is reached. There, $\delta\hat{A}_x$ and $\delta\hat{B}_x$ need to be continued smoothly into a solution of (4.4) and (4.5) with the electron cloud solution as background. At the outer edge, a second matching to the exterior solution must occur. Finally, the coefficients $\hat{A}_x^{(0)}$ and $\hat{B}_x^{(0)}$ can be read off at the boundary and plugged in to (4.8).

A plot of the conductivity can be seen in figure 7. The pole in the imaginary part, as usual, indicates the presence of a delta peak in the real part. The offset in the conductivity goes rather quickly to zero once the electron cloud is in place. This is also shown in figure 8. Parameterizing the real and imaginary part of the conductivity as

$$\mathrm{Re}\,\sigma \sim \sigma_0 + \sigma_2 \left(\frac{\omega}{\mu}\right)^2 , \qquad \mathrm{Im}\,\sigma \sim \sigma_{-1} \frac{\mu}{\omega} \tag{4.9}$$

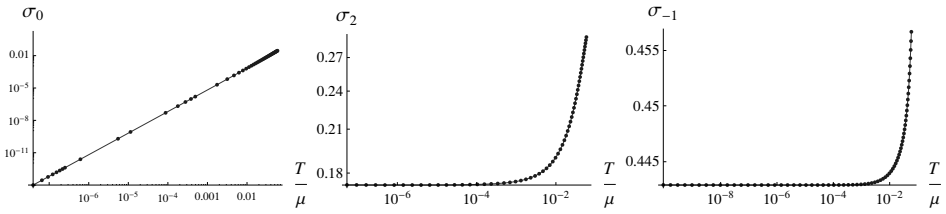


**Figure 8**. Numerical results for the coefficients $\sigma_0, \sigma_2$ and $\sigma_{-1}$ in the electrical conductivity in equation (4.9).

JHEP01(2011)117

for small $\omega$, it can be seen from our numerical data that $\sigma_2$ and $\sigma_{-1}$ level off for small temperatures and $\sigma_0$ decreases like $T^2$ in this limit. This is consistent with the zero-temperature result in [5], where $\sigma_0$ is not present, and with $\omega/T$ scaling at low temperatures. Above the critical temperature the background is an AdS-RN black brane and the calculation of the conductivity reduces to the one described in [2].

## 5 Discussion

One of the most interesting recent developments in holographic model building is the observation that at low temperatures it can be energetically favorable for black holes in AdS space to eject their charge in the form of matter "hair" [7, 16–19]. In the boundary theory this hair may give rise to many interesting features including spontaneous symmetry breaking [20], dynamical critical exponents [5] and non-fermi liquids [7, 21]. In general, this may allow one to use holographic techniques to study condensed matter systems not amenable to other theoretical tools.

In this paper we explored the finite boundary temperature generalization of the electron star configuration described in [5]. The electron star solution is a zero temperature model for a quantum phase transition displaying dynamical critical exponents as well as non-fermi liquid features. In the bulk the configuration is that of a zero temperature ideal charged fermion fluid. In the deep interior this fluid has an asymptotic Lifshitz scaling symmetry. As one approaches the boundary, the gauge potential is screened by the charged fluid. Eventually, the local chemical potential falls below the fermion mass causing the fluid density to vanish. In the asymptotic region one is left with an AdS-RN geometry.

At finite boundary temperatures there is instead a cloud-like configuration, with the electron fluid hovering outside an AdS-RN black brane geometry. This configuration is only possible when the fluid and black brane have same sign charges such that electrostatic repulsion balances gravitational attraction. Within the fluid and its exterior, the electron cloud solution is similar to the electron star. The gauge field is screened and eventually the fluid can no longer be supported. We found that as one lowers the temperature, for fixed chemical potential one smoothly obtains the free energy of the electron star solution at zero temperature.

In the other extreme, beyond a critical temperature the local chemical potential is always lower than the fermion mass and no fermion fluid is supported. In this case we are left with an AdS-RN black brane geometry. We studied the transition numerically and found that it is a third order phase transition, as pointed out in [10].

We can summarize the phase diagram as follows, in the high temperature regime there is an AdS-RN black brane. As one lowers the temperature it is favorable for the black brane to expel some of its charge in the form of an electron cloud hovering over the horizon. As one cools the system further, the interior black brane carries less and less charge and has shrinking area. Finally, at zero temperature the black brane is gone and the fluid takes the form of an electron star.

In addition to studying electron cloud thermodynamics we also computed the conductivity, finding that it is nicely consistent with the electron star results of [5] at low temperature and with the AdS-RN black brane at high temperature.

In [21] it was argued that if the fluid in an electron star experiences a local temperature and magnetic field, it is possible to detect a Fermi surface evidenced by Kosevich-Lifshitz oscillations. It should also be possible to see such oscillations in electron clouds.

A major challenge for the construction we are working with is how to interpret the electron fluid directly in terms of operators in the boundary field theory. It would be interesting to see how the work of [8] may be extended for charged fluids in order to further characterize the nature of the underlying quantum critical point.

## Acknowledgments

We thank S. A. Hartnoll and K. Schalm for helpful discussions. This work was supported in part by the Icelandic Research Fund and by the University of Iceland Research Fund.

## References

[1] C.P. Herzog, *Lectures on holographic superfluidity and superconductivity*, *J. Phys.* **A 42** (2009) 343001 [arXiv:0904.1975] [SPIRES].

[2] S.A. Hartnoll, *Lectures on holographic methods for condensed matter physics*, *Class. Quant. Grav.* **26** (2009) 224002 [arXiv:0903.3246] [SPIRES].

[3] J. McGreevy, *Holographic duality with a view toward many-body physics*, *Adv. High Energy Phys.* **2010** (2010) 723105 [arXiv:0909.0518] [SPIRES].

[4] S. Sachdev, *Strange metals and the AdS/CFT correspondence*, *J. Stat. Mech.* (2010) P11022 [arXiv:1010.0682] [SPIRES].

[5] S.A. Hartnoll and A. Tavanfar, *Electron stars for holographic metallic criticality*, arXiv:1008.2828 [SPIRES].

[6] J. de Boer, K. Papadodimas and E. Verlinde, *Holographic neutron stars*, *JHEP* **10** (2010) 020 [arXiv:0907.2695] [SPIRES].

[7] S.A. Hartnoll, J. Polchinski, E. Silverstein and D. Tong, *Towards strange metallic holography*, *JHEP* **04** (2010) 120 [arXiv:0912.1061] [SPIRES].



JHEP01(2011)117

[8] X. Arsiwalla, J. de Boer, K. Papadodimas and E. Verlinde, *Degenerate stars and gravitational collapse in AdS/CFT*, arXiv:1010.5784 [SPIRES].

[9] V. Parente and R. Roychowdhury, *A study on charged neutron star in $AdS_5$*, arXiv:1011.5362 [SPIRES].

[10] S.A. Hartnoll and P. Petrov, *Electron star birth: a continuous phase transition at nonzero density*, arXiv:1011.6469 [SPIRES].

[11] M. Čubrović, J. Zaanen and K. Schalm, *Constructing the AdS dual of a Fermi liquid: AdS black holes with Dirac hair*, arXiv:1012.5681 [SPIRES].

[12] G.W. Gibbons and S.W. Hawking, *Action integrals and partition functions in quantum gravity*, *Phys. Rev.* **D 15** (1977) 2752 [SPIRES].

[13] M. Henningson and K. Skenderis, *The holographic Weyl anomaly*, *JHEP* **07** (1998) 023 [hep-th/9806087] [SPIRES].

[14] V. Balasubramanian and P. Kraus, *A stress tensor for anti-de Sitter gravity*, *Commun. Math. Phys.* **208** (1999) 413 [hep-th/9902121] [SPIRES].

[15] D.T. Son and A.O. Starinets, *Minkowski-space correlators in AdS/CFT correspondence: recipe and applications*, *JHEP* **09** (2002) 042 [hep-th/0205051] [SPIRES].

[16] S.A. Hartnoll, C.P. Herzog and G.T. Horowitz, *Holographic superconductors*, *JHEP* **12** (2008) 015 [arXiv:0810.1563] [SPIRES].

[17] S.S. Gubser and A. Nellore, *Low-temperature behavior of the Abelian Higgs model in anti-de Sitter space*, *JHEP* **04** (2009) 008 [arXiv:0810.4554] [SPIRES].

[18] G.T. Horowitz and M.M. Roberts, *Zero temperature limit of holographic superconductors*, *JHEP* **11** (2009) 015 [arXiv:0908.3677] [SPIRES].

[19] J.P. Gauntlett, J. Sonner and T. Wiseman, *Holographic superconductivity in M-theory*, *Phys. Rev. Lett.* **103** (2009) 151601 [arXiv:0907.3796] [SPIRES].

[20] S.S. Gubser, *Breaking an Abelian gauge symmetry near a black hole horizon*, *Phys. Rev.* **D 78** (2008) 065034 [arXiv:0801.2977] [SPIRES].

[21] S.A. Hartnoll, D.M. Hofman and A. Tavanfar, *Holographically smeared Fermi surface: quantum oscillations and Luttinger count in electron stars*, arXiv:1011.2502 [SPIRES].

JHEP01(2011)117

# Paper V

Prepared for submission to JHEP

# Thermodynamics of dyonic Lifshitz black holes

**T. Zingg**[a,b]

[a] *Science Institute, University of Iceland,*
*Dunhaga 3, IS-107 Reykjavik, Iceland*
[a] *NORDITA,*
*Roslagstullsbacken 23, SE-106 91 Stockholm, Sweden*

*E-mail:* zingg@nordita.org

Abstract: Black holes with asymptotic anisotropic scaling are conjectured to be gravity duals of condensed matter system close to quantum critical points with non-trivial dynamical exponent $z$ at finite temperature. A holographic renormalization procedure is presented that allows thermodynamic potentials to be defined for objects with both electric and magnetic charge in such a way that standard thermodynamic relations hold. Black holes in asymptotic Lifshitz spacetimes can exhibit paramagnetic behavior at low temperature limit for certain values of the critical exponent $z$, whereas the behavior of AdS black holes is always diamagnetic.

Keywords: field theories in lower dimensions, quantum critical points, gauge-gravity correspondence, black holes

ArXiv ePrint: 1107.3117

## Contents



## 1 Introduction

Taking the AdS/CFT correspondence [1] as a guideline, geometries with an anisotropic scaling have been presented in [2] as candidates for gravitational duals for quantum critical condensed matter systems that are invariant under Lifshitz scaling

$$t \to \lambda^z t,\, x \to \lambda x\ , \tag{1.1}$$

with a dynamical exponent $z > 1$. A detailed understanding of quantum critical metals poses a challenge in theoretical physics [3]. Using gravitational duals to shed new light on these and other condensed matter problems continues to be an active field of research (for reviews see e.g. [4–6]). While the validity of this formalism is still a matter of debate, it is important to develop these holographic duals further in order to be able to test them against experimental results. This paper provides a prescription for defining thermodynamic quantities for dyonic Lifshitz black branes that satisfy the expected thermodynamic relations. Such a prescription allows to investigate duals of systems with anisotropic scaling in the presence a magnetic field - along the same lines as e.g. AdS/CFT duality has been used to obtain a holographic description of the Hall conductivity [7].

The paper is structured as follows. In section 2, the effective action of the holographic model is introduced. It consists of an Einstein-Hilbert term coupled to a Proca field and a $U(1)$ gauge field, which is known to give rise to charged Lifshitz black brane solutions. Building on previous analysis [8–11], the model with both electric and magnetic fields present is investigated with an emphasis on holographic renormalization and thermodynamics. The focus will be on 3+1 dimensions, i.e. a strongly interacting field theory dual in 2+1 dimensions. This setup is relevant for a holographic description of materials where the charge carriers are confined to layers orthogonal to a magnetic field. Another benefit of working in this dimension is the duality between magnetic and electric fields, which simplifies the following analysis.

In section 3, counterterms are introduced such that the action and its functional derivatives are well-defined and finite on-shell. This extends the analysis in [11], where no gauge-field was considered, and allows to renormalize the action for values $z \geq 2$, which goes beyond the parameter range considered in [12]. The prescription presented here is based on a new approach to identify the degrees of freedom of the system. Within the space of solutions, Lifshitz-spacetimes form a subset which is disconnected from other classes of solutions. Thus, on-shell variations must be constrained such that they do not lead away from that subspace.

The renormalization procedure is then used in section 4 to define the internal energy and Helmholtz free energy of the black brane solutions. These obey the same relations as in standard thermodynamics. This extends the work of [12, 13] and gives further justification that the thermodynamic description of black holes, which is known to be valid in the AdS-case, is also applicable for non-relativistic holography.

## 2 The holographic model

The effective action used is of the form introduced in [8] with a Maxwell term added,

$$S_{bulk} = S_{EH} + S_{Proca} + S_{Maxwell} \, . \tag{2.1}$$

In the above,

$$S_{EH} = \frac{1}{2\kappa L^2} \int_M (R - 2\Lambda) v_M \, , \tag{2.2}$$

$$S_{Proca} = -\frac{1}{4\kappa L^2} \int_M (dP \wedge *dP + c\, P \wedge P) \, , \tag{2.3}$$

$$S_{Maxwell} = -\frac{1}{4\kappa L^2} \int_M F \wedge F \, , \tag{2.4}$$

where $P$ is a 1-form on the manifold $M$ and $F = dA$ the Maxwell-tensor. Variation with respect to the metric $g_{\mu\nu}$ gives the Einstein equations

$$G_{\mu\nu} + \Lambda g_{\mu\nu} = T^P_{\mu\nu} + T^{EM}_{\mu\nu} \, . \tag{2.5}$$

The energy tensors $T^P_{\mu\nu}$ and $T^{EM}_{\mu\nu}$ are defined as

$$T^P_{\mu\nu} = \frac{1}{2}\left(P_\mu P_\nu + [dP]_{\mu\lambda}[dP]_\nu{}^\lambda - \frac{1}{2}P_\lambda P^\lambda g_{\mu\nu} - \frac{1}{4}[dP]_{\lambda\kappa}[dP]^{\lambda\kappa}g_{\mu\nu}\right) , \tag{2.6}$$

$$T^{EM}_{\mu\nu} = \frac{1}{2}\left(F_{\mu\lambda}F_\nu{}^\lambda - \frac{1}{4}F_{\lambda\kappa}F^{\lambda\kappa}g_{\mu\nu}\right) . \tag{2.7}$$

Variation with respect to $P$ and $A$ leads to the equations of motion

$$d * dP = -c * P , \tag{2.8}$$

$$d * F = 0 . \tag{2.9}$$

Equations (2.5), (2.8) and (2.9) are known to have asymptotic Lifshitz solutions with dynamical exponent $z$ if

$$\Lambda = -\frac{z^2 + (d-1)z + d^2}{2L^2} , \tag{2.10}$$

$$c = \frac{dz}{L^2} , \tag{2.11}$$

where $d$ is related to the dimension of $M$ by $d + 2 = \dim M$.

For concreteness, the case $\dim M = 4$, i.e. $d = 2$, is used in the following. This is partly motivated by previous investigations [10, 14, 15], where results so far indicated that the qualitative behavior of the system is mainly characterized by the ratio $d/z$ rather than $d$ itself. Thus, using general $d$ would merely clutter notation without being much more instructive. Beyond that, the duality between electric and magnetic field strength in $3+1$ dimensions allows for some further simplification.

### 2.1 Dyonic black branes

For the black branes, an ansatz of a static and stationary metric is chosen via the tetrad

$$e_0 = L\frac{fg}{r^z}\,dt , \tag{2.12}$$

$$e_1 = L\frac{1}{r}\,dx , \tag{2.13}$$

$$e_2 = L\frac{1}{r}\,dy , \tag{2.14}$$

$$e_3 = -L\frac{1}{rg}\,dr . \tag{2.15}$$

The metric is then given by $g_{\mu\nu} = \eta^{AB}e_{A\mu}e_{B\nu}$. The tetrad has been introduced for later convenience. Furthermore, the orientation on the manifold $M$ is chosen to be

$$v_M = e_3 \wedge e_1 \wedge e_2 \wedge e_0 . \tag{2.16}$$

The Proca-field and gauge potential are parametrized as

$$P = \sqrt{\frac{2}{z}}Lr^{-z}afg^2\,dt , \tag{2.17}$$

$$A = Lr^{-z}\phi fg^2\,dt + LB_0 x\,dy . \tag{2.18}$$

Here, $B_0$ is the constant field strength of a magnetic field perpendicular to the $xy$-plane. For later convenience, $dP$ and $F$ are parametrized as

$$dP = -\sqrt{2z}Lr^{-z-1}bf\,dr\wedge dt\,, \tag{2.19}$$

$$F = Lr^{-z+1}f\rho_0\,dr\wedge dt + LB_0\,dx\wedge dy\,, \tag{2.20}$$

where the constant $\rho_0$ describes the charge density in the system. The above defined ansatz will solve the equations of motion (2.5), (2.8) and (2.9) provided the following system of first order ODEs holds

$$rf' = f\left(z-1-a^2\right)\,, \tag{2.21}$$

$$rg' = \frac{g}{2}\left(3+a^2\right) + \frac{1}{2g}\left(\Lambda + \frac{\rho_0^2+B_0^2}{4}r^4 + \frac{z}{2}b^2\right)\,, \tag{2.22}$$

$$ra' = -2a - \frac{1}{g^2}\left[zb + a\left(\Lambda + \frac{\rho_0^2+B_0^2}{4}r^4 + \frac{z}{2}b^2\right)\right]\,, \tag{2.23}$$

$$rb' = 2b-2a\,, \tag{2.24}$$

$$r\phi' = -2\phi + \frac{1}{g^2}\left[\rho_0 r^2 - \phi\left(\Lambda + \frac{\rho_0^2+B_0^2}{4}r^4 + \frac{z}{2}b^2\right)\right]\,. \tag{2.25}$$

A straightforward calculation shows that the quantity

$$\begin{aligned} D_0 = \frac{f}{r^{z+2}}\Big(&-\Lambda - \frac{\rho_0^2+B_0^2}{4}r^4 - \frac{1}{2}zb^2 - 3g^2 \\ &+a^2g^2 - 2abg^2 + \frac{\rho_0^2+B_0^2}{\rho_0}r^2g^2\Phi\Big) \end{aligned} \tag{2.26}$$

is a first integral. This quantity will prove useful in deriving an equation of state in section 4.

The system (2.21)-(2.25) has the asymptotic Lifshitz fixed point $f=f_\infty, g=1, a=b=\sqrt{z-1}, \phi=0$. It is however not the only fixed point, as there would also be the possibility $f\sim r^{z-1}, g=\sqrt{\frac{4+z+z^2}{6}}, a=b=\phi=0$, which corresponds to an asymptotic AdS solution. The system can be solved in the asymptotic region $r\to 0$ by first linearizing around the Lifshitz fixed point, which gives the asymptotic modes of the solution, and then iteratively calculating the descendants of these modes. The expansion up to the orders that are relevant for this paper can be found in appendix A. A crucial result of this expansion (up to a choice of sign) is

$$P = \left(\sqrt{\frac{2(z-1)}{z}} + \xi\right)e_0\,, \tag{2.27}$$

where $\xi$ is a scalar function that vanishes asymptotically for asymptotic Lifshitz solutions. This will play an important role in the calculation of the on-shell variation in the next section.

## 3 Renormalization

Using the equations of motion (2.21)-(2.25), the bulk action can be shown to reduce to a surface term on-shell,

$$S_{bulk}^{on-shell} = \frac{1}{2\kappa L^3}\int_{\partial M} g\left(2 - \frac{b_0^2 r^2 \phi}{\rho_0}\right) v_{\partial M} \ . \tag{3.1}$$

In the above expression, $v_{\partial M}$ is the induced volume form on the surface, i.e. $v_{\partial M} = e_1 \wedge e_2 \wedge e_0$. Plugging in the expansion from appendix A shows that the integrand diverges at the boundary as $r \to 0$. Thus, the action needs to be renormalized before the standard thermodynamic gauge-gravity dictionary can be applied. This can be done as for asymptotic AdS solutions [16], that is by confining the integration domain to $r > \varepsilon$ and defining a series of counterterms on the boundary $\partial M_\varepsilon$, such that the limit $\varepsilon \to 0$ is well-defined on-shell. It should be noted that the following analysis is also made under the condition $\Xi_1 = 0$, where $\Xi_1$ is a coefficient in the expansion from appendix A. For $z \geq 2$ ($z \geq d$) this would anyway be a necessary condition, as otherwise there would be a non-renormalizable mode in the solution, while for $z < 2$ ($z < d$), this choice greatly simplifies the definition of an energy, as it vastly reduces the number of required counterterms to cancel all divergent contributions[1]. Furthermore, it will also be assumed that $z < 6$ ($z < d + 4$). With this, it will be sufficient to consider counterterms which are at most quadratic in $F$ and $A$, which simplifies the analysis. At the same time, most known quantum critical systems in experimental physics have a dynamical exponent in the range $1 < z < 3$, which is well within the range considered. It can be expected, however, that the final result for the thermodynamic quantities in section 4 remains the same for higher values of $z$, but an explicit expression for the renormalized action would involve terms which are quartic[2] and higher order in $F$ and $A$. Finally, the normalization $f_\infty = 1$ is used throughout. This is not a real restriction, as another value would simply correspond to a different choice of the time scale, which could easily be reintroduced by multiplying expressions with the appropriate power of $f_\infty$.

The final form of the action is thus given by

$$S = S_{bulk} + S_{reg} + S_{ct} \ . \tag{3.2}$$

$S_{reg}$ is a regulating term necessary to have a well defined variation in the presence of a boundary,

$$2\kappa L^2 S_{reg} = 2\int_{\partial M_\varepsilon} K v_{\partial M_\varepsilon} - \int_{\partial M_\varepsilon} A \wedge *F - \frac{L}{(2-z)}\int_{\partial M} \mathfrak{L}_{e_3} A \wedge *F \ . \tag{3.3}$$

The first term is the usual Gibbons-Hawking term which ensures that the variation with respect to the metric is well defined. $K$ is the trace of the intrinsic curvature $K_{\mu\nu} = \nabla_{(\mu} n_{\nu)}$, which in the given setup can be calculated as $K_{\mu\nu} = \frac{g}{2L}\frac{\partial}{\partial r} h_{\mu\nu}$, where $h_{\mu\nu} = g_{\mu\nu} - n_\mu n_\nu$ is

[1] Similar conclusions were drawn in [11].

[2] There won't be any terms with odd powers as the equations of motion are invariant under charge conjugation $A \to -A$.

the induced metric on $\partial M_\varepsilon$. The second term accounts for working in a background with fixed charged density, i.e. $\imath_{e_3}\delta F$, on the boundary instead of a fixed chemical potential.[3] This choice comes from the consideration that the holographic field theoretic problem in mind for this setup is a sample with 2-dimensional (semi-)conducting layers in a constant magnetic field with a fixed number of dopants rather than a given chemical potential. In the third term, $\mathfrak{L}_{e_3}$ is the Lie derivative with respect to $e_3$, which can be interpreted as the normal derivative on the boundary. This last term is required to cancel a divergent contribution of the preceding term that occurs for $z > 2$. Introducing $\star$ to denote the induced Hodge-Star on the boundary and decomposing the Maxwell tensor as

$$F^e = \imath_{e_3} F \,, \tag{3.4}$$

$$F^m = F\Big|_{\partial M} \,, \tag{3.5}$$

the regulating term (3.3) can also be written as

$$2\kappa L^2 S_{reg} = 2\int_{\partial M_\varepsilon} K v_{\partial M_\varepsilon} - \int_{\partial M_\varepsilon} A \wedge \star F^e - \frac{L}{(2-z)} \int_{\partial M} \mathfrak{L}_{e_3} A \wedge \star F^e \,. \tag{3.6}$$

This makes it more manifest that the last two terms correspond to a Legendre transformation. In the standard dictionary, a bulk gauge field $A$ will source a current $\mathcal{J}$ in the dual field theory on the boundary. In that theory, $F^e$ has an interpretation as the response, i.e. $\langle \mathcal{J} \rangle \sim \frac{\delta S}{\delta A} \sim F^e$. For $z > 2$, it can be read off from (A.5) that the mode with $\mathcal{Q}\nu$ will grow faster than the mode involving $\mathcal{Q}$. Thus, the latter needs to be canceled and it is actually $A + \frac{L}{(2-z)}\mathfrak{L}_{e_3} A$ that becomes the source for the dual current.[4] The Legendre transformation then interchanges the role of $A + \frac{L}{(2-z)}\mathfrak{L}_{e_3} A$ as source and $F^e$ as response.

Finally, $S_{ct}$ is a counterterm that cancels all remaining divergences from the bulk action. It is given by

$$\begin{aligned} 2\kappa L^2 S_{ct} = {} & \frac{2(z+1)}{L} \int_{\partial M} v_{\partial M} + \frac{\sqrt{2z(z-1)}}{L} \int_{\partial M_\varepsilon} \xi v_{\partial M} \\ & + \frac{L}{2(2-z)} \int_{\partial M} \mathfrak{L}_{e_3} A \wedge \star \mathfrak{L}_{e_3} A + \frac{L}{2(2-z)} \int_{\partial M} F^m \wedge \star F^m \,, \end{aligned} \tag{3.7}$$

where $\xi$ was introduced in (2.27). The first term in (3.7) is simply a boundary cosmological constant. The second term cancels a divergence with exponent $z_2$ coming from $\Xi_2$ having a non-vanishing value (cf. appendix A).[5] For $1 < z < 2$ these two terms would actually suffice, for $z \geq 2$ there are however further divergences occurring due to the electric and magnetic fields not falling off fast enough. This is cured by adding the terms in the second line of (3.7) involving $\mathfrak{L}_{e_3} A$ and $F^m$.

Two issues might need some clarification. First, the attentive reader may have noticed that there is a certain redundancy in the notation as $\mathfrak{L}_{e_3} A = F^e$. This is done on purpose

[3] This point is explained in e.g. [5].

[4] This works analogous to the discussion in [17].

[5] It is worth noting that the $\xi$-term also cancels the divergence proportional to $z_1$ when $\Xi_1 \neq 0$. To renormalize the action, however, terms with higher powers in $\xi$ would also need to be included.

to make the conceptual difference between those two terms manifest. $\mathfrak{L}_{e_3}A$ is defined through $A$, which is the field that enters the bulk action (2.1). The field $F^e$ is introduced by performing a Legendre transformation. In the logical order, this transformation is done after the action has been renormalized. Therefore, the counterterm (3.7) is written in terms of $\mathfrak{L}_{e_3}A$ and without any explicit dependence on $F^e$.

Second, the first two terms in (3.7) which cancel all divergent contributions when $A = 0$ are different from the terms proposed in [11], where

$$2\kappa L^2 \tilde{S}_{ct} = \frac{4}{L}\int_{\partial M} v_{\partial M} + \frac{\sqrt{2z(z-1)}}{L}\int_{\partial M_\varepsilon}\sqrt{\langle P,P\rangle}v_{\partial M}\ . \tag{3.8}$$

However, by using (2.27), a short calculation reveals

$$\begin{aligned} 4+\sqrt{2z(z-1)}\sqrt{\langle P,P\rangle} &= (z+3) - \frac{z}{2}\langle P,P\rangle + O(\xi^2) \\ &= 2(z+1) + \sqrt{2z(z-1)}\,\xi + O(\xi^2)\ . \end{aligned} \tag{3.9}$$

Thus, when $\xi^2 v_{\partial M}$ vanishes for $r \to 0$, which is indeed the case in the parameter range considered here, the first line of (3.7) would give exactly the same contribution as (3.8).

Energy and momentum can also be calculated along the lines of [16]. The procedure differs, however, in the following two ways. First, as was already pointed out in [11], the dual theory is not relativistic and thus it is less convenient to work with the metric and the stress energy tensor $T^{\mu\nu} = \frac{2}{\sqrt{-h}}\frac{\delta S}{\delta h_{\mu\nu}}$, but more useful to work with a tetrad and $\tau_A$, where

$$*\,\tau_A = \eta_{AB}\frac{\delta S}{\delta e_B}\ . \tag{3.10}$$

Energy, momentum, energy flux and stress are then encoded in the components of $\tau_A$. A second, and more subtle difference is the way the variations are calculated. The aim is to consider gravity duals to systems with anisotropic scaling, but, as was noted earlier, in addition to the Lifshitz fixed point there also exists an AdS fixed point. In fact, the asymptotic Lifshitz spacetimes form an isolated subset of the space of solutions that is disconnected from the subset of asymptotic AdS spacetimes. Thus, in the same fashion as the covariant derivative on a surface embedded in $\mathbb{R}^N$ is basically the derivative of the embedding space constrained to be evaluated on curves that do not lead away from the surface, the variations must be constrained to 'curves' that stay inside the subspace of asymptotic Lifshitz solutions. These 'curves' are defined by (2.27), which is a direct consequence of making an ansatz that has asymptotic anisotropic scaling. Hence, the variation must be performed under the constraint that it is not $P$, but the scalar $\xi$ which

is a degree of freedom of the system.[6] Using this relation, (3.10) becomes

$$\begin{aligned}
2\kappa L^2\tau_0 = {} & 2K\cdot e_0 - 2Ke_0 + \left(\sqrt{\frac{2(z-1)}{z}}+\xi\right)\imath_{e_3}dP \\
& -(\langle A,F^e\rangle e_0 - \langle A,e_0\rangle F^e - \langle F^e,e_0\rangle A) \\
& -\frac{L}{2-z}\left(\langle \mathfrak{L}_{e_3}A,F^e\rangle e_0 - \langle \mathfrak{L}_{e_3}A,e_0\rangle F^e - \langle F^e,e_0\rangle \mathfrak{L}_{e_3}A\right) \\
& +\frac{2(z+1)}{L}e_0 + \frac{\sqrt{2z(z-1)}}{L}\xi e_0 \\
& +\frac{L}{2(2-z)}\left(\langle \mathfrak{L}_{e_3}A,\mathfrak{L}_{e_3}A\rangle e_0 - 2\langle \mathfrak{L}_{e_3}A,e_0\rangle \mathfrak{L}_{e_3}A\right) \\
& +\frac{L}{2(2-z)}\left(\langle F^m,F^m\rangle e_0 + 2F^m\cdot F^m\cdot e_0\right)\ . \qquad (3.11)
\end{aligned}$$

In the expression above, $M\cdot\omega$ denotes the contraction $M_\mu{}^\nu\omega_\nu$ for a 2-tensor $M$ and a 1-form $\omega$. $\tau_1$ and $\tau_2$ are given by similar expressions, but without the terms involving $\xi$. However, only $\tau_0$ will be relevant when defining the energy in the next section.

For when considering differentials of thermodynamic quantities later on, it is also useful to note the relation

$$2\kappa L^2\frac{\delta S}{\delta F^e} = -*\left[A+\frac{L}{2-z}\mathfrak{L}_{e_3}A\right]\ . \qquad (3.12)$$

### 3.1 A note about $z=2$

For $z=2$, and more generally $z=d$, the asymptotic expansions (see appendix A) become anomalous and contain logarithmic terms. Furthermore (3.6), (3.7) (3.11), and (3.12) are not well-defined due to the factor of $(2-z)$ in the denominator. In this special case these need to be modified,

$$2\kappa L^2 S_{reg} = 2\int_{\partial M_\varepsilon} Kv_{\partial M_\varepsilon} - \int_{\partial M_\varepsilon} A\wedge\star F^e - L\int_{\partial M}\ln r\,\mathfrak{L}_{e_3}A\wedge\star F^e\ , \qquad (3.13)$$

$$\begin{aligned}
2\kappa L^2 S_{ct} = {} & \frac{2(z+1)}{L}\int_{\partial M} v_{\partial M} + \frac{\sqrt{2z(z-1)}}{L}\int_{\partial M_\varepsilon}\xi v_{\partial M} \\
& +\frac{L}{2}\int_{\partial M}\ln r\,\mathfrak{L}_{e_3}A\wedge\star\mathfrak{L}_{e_3}A + \frac{L}{2}\int_{\partial M}\ln r\,F^m\wedge\star F^m\ , \qquad (3.14)
\end{aligned}$$

[6] Making this statement simply based on the expansion (A.1)-(A.5) might appear ad hoc. For the purpose of this paper it could just be thought of as a mere working assumption, but an investigation of the PDE-system (2.5), (2.8) and (2.9) via a Fefferman-Graham like expansion (cf. [18]) reveals that the actual degrees of freedom are not the components of $P$ but are defined via projections to $e_0, e_1, e_2$. These more general results will be reported on elsewhere [19].

$$
\begin{aligned}
2\kappa L^2\tau_0 \;=\; & 2K\cdot e_0 - 2K e_0 - \left(\sqrt{\frac{2(z-1)}{z}}+\xi\right)\imath_{e_3}dP \\
& -\left(\langle A,F^e\rangle e_0 - \langle A,e_0\rangle F^e - \langle F^e,e_0\rangle A\right) \\
& -L\ln r\,\left(\langle \mathfrak{L}_{e_3}A,F^e\rangle e_0 - \langle \mathfrak{L}_{e_3}A,e_0\rangle F^e - \langle F^e,e_0\rangle \mathfrak{L}_{e_3}A\right) \\
& +\frac{2(z+1)}{L}e_0 + \frac{\sqrt{2z(z-1)}}{L}\xi e_0 \\
& +\frac{L}{2}\ln r\,\left(\langle \mathfrak{L}_{e_3}A,\mathfrak{L}_{e_3}A\rangle e_0 - 2\langle \mathfrak{L}_{e_3}A,e_0\rangle \mathfrak{L}_{e_3}A\right) \\
& +\frac{L}{2}\ln r\,\left(\langle F^m,F^m\rangle e_0 + 2F^m\cdot F^m\cdot e_0\right)\;, \qquad (3.15)\\
2\kappa L^2\frac{\delta S}{\delta F^e} \;=\; & -*\left[A + L\ln r\,\mathfrak{L}_{e_3}A\right]\;. \qquad (3.16)
\end{aligned}
$$

## 4 Thermodynamics

A temperature is introduced in the dual theory by considering black brane solutions with an event horizon at some finite value $r = r_0$. At the horizon, $f \to f_0, a \to a_0, b \to b_0, \phi \to \phi_0$ while $g^2 \to g_0^2(1 - r/r_0)$. As the form of the equations is invariant under the rescaling $r \to \lambda r, B_0 \to \lambda^{-2}B_0, \rho_0 \to \lambda^{-2}\rho_0$, the horizon can be assumed to be at $r_0 = 1$. The dependence of the solutions on $r_0$ can then be introduced by using the rescaling backwards. With this simplification, the relation between the constants at the horizon is given by

$$
\begin{aligned}
g_0^2 \;=\; & -\Lambda - \frac{z}{2}b_0^2 - \frac{\rho_0^2+B_0^2}{4}\;, \qquad (4.1)\\
a_0 \;=\; & \frac{zb_0}{g_0^2}\;, \qquad (4.2)\\
\phi_0 \;=\; & -\frac{\rho_0}{g_0^2}\;. \qquad (4.3)
\end{aligned}
$$

Thermodynamic quantities can now be assigned using the same prescription as for the $AdS$ case (see e.g. [4]). The value of $\kappa$ is associated with the number of flavors $N$ in the dual field theory through $\frac{1}{\kappa} = \frac{\sqrt{2}N^{\frac{3}{2}}}{3\pi}$. The chemical potential $\mu$, magnetic field strength $\mathfrak{b}$ and the charge density $\mathfrak{q}$ can be read off from the asymptotic expansion in appendix A,

$$
\mu = \frac{\mathcal{Q}\nu}{L}\;, \mathfrak{b} = \frac{\mathcal{B}}{L^2}\;, \mathfrak{q} = \frac{\mathcal{Q}}{2\kappa L^2} = \frac{\sqrt{2}N^{\frac{3}{2}}\mathcal{Q}}{6\pi L^2}\;. \qquad (4.4)
$$

As $B_0$ and $\rho_0$ enter in a symmetric fashion in the equations of motion (2.21)-(2.25), the magnetization density is given by

$$
\mathfrak{m} = -\frac{\mathcal{B}\nu}{2\kappa L} = -\frac{1}{4\kappa^2}\frac{\mathfrak{b}\mu}{\mathfrak{q}}\;. \qquad (4.5)
$$

This relation will become more clear in the discussion in subsection 4.2. Reintroducing the scaling in $r_0$ reveals that $\mathfrak{m}, \mu \propto r_0^{-z}$ and the values of $\mathfrak{b}$ and $\mathfrak{q}$ are related to the variables at the horizon via

$$
\mathfrak{b} = \frac{B_0}{L^2 r_0^2}\;, \mathfrak{q} = \frac{\rho_0}{2\kappa L^2 r_0^2}\;. \qquad (4.6)
$$

A temperature is defined via Wick rotating time and then compactifying on the thermal circle, the result is

$$T = \frac{f_0 g_0^2}{4\pi r_0^z L} \,. \tag{4.7}$$

The value of $r_0$ also defines the entropy density,

$$\mathfrak{s} = \frac{2\pi}{\kappa L^2 r_0^2} \,. \tag{4.8}$$

The evaluation of the conserved quantity (2.26) at the horizon and in the region $r \to 0$ relates $T$ and $\mathfrak{s}$ with the variables in appendix A.

$$2\kappa L^3 \mathfrak{s} T = \begin{cases} -\frac{2\sqrt{z-1}(z^2-4)\mathcal{M}}{z} - (\mathcal{B}^2+\mathcal{Q}^2)\frac{\mu}{\mathcal{Q}} & z \neq 2 \,, \\ -4\mathcal{M} - \frac{1}{4}(\mathcal{B}^2+\mathcal{Q}^2) - (\mathcal{B}^2+\mathcal{Q}^2)\frac{\mu}{\mathcal{Q}} & z = 2 \,. \end{cases} \tag{4.9}$$

### 4.1 Thermodynamic potential and equation of state

By the standard prescription, the grand canonical potential is associated with the the value of the renormalized Euclidean on-shell action. However, in the case at hand (3.2) contains the term $-\int_{\partial M_\varepsilon} \left(A + \frac{L}{(2-z)} \pounds_{e_3} A\right) \wedge \star F^e$ which has been added to the action to allow for a setup with fixed charge density. This terms is not part of the renormalization to cancel divergences, but it changes the thermodynamic potential by the value $\mu\mathfrak{q}$, resulting in the canonical ensemble. Thus, from the on-shell value of the action (3.2),

$$\mathfrak{a}\mathcal{V} = T S^{Eucl,on-shell} \,, \tag{4.10}$$

where $\mathcal{V}$ is the volume of the system and $\mathfrak{a}$ is the Helmholtz free energy density. Plugging in the parametrization presented in section 2.1 and using the asymptotic expansion from appendix A leads to

$$2\kappa L^3 \mathfrak{a} = \begin{cases} 2(z-2)\sqrt{z-1}\mathcal{M} + \frac{\mathcal{B}^2\mu}{\mathcal{Q}} + \mathcal{Q}\mu & z \neq 2 \,, \\ 2\mathcal{M} + \frac{1}{4}(\mathcal{B}^2+\mathcal{Q}^2) + \frac{\mathcal{B}^2\mu}{\mathcal{Q}} + \mathcal{Q}\mu & z = 2 \,. \end{cases} \tag{4.11}$$

An internal energy can be defined by working in the spirit of the AdS/CFT correspondence and considering the on-shell action (3.2) as a generating functional for the dual field theory with the boundary values of the fields interpreted as sources for their dual operators. In [16] the dual stress energy tensor $T^{\mu\nu}$ was considered as the operator that is sourced by the boundary metric $h_{\mu\nu}$. As already indicated in section 3, instead of $T^{\mu\nu}$, the quantities $\tau_A$ defined in (3.10) will now be used for this purpose. With $\partial_t$ being the Killing vector that generates time translation invariance the internal energy density $\mathfrak{e}$ is associated to $\tau_0$, given in (3.11), through

$$L\mathfrak{e} = \tau_0(\partial_t)\Big|_{sources=0} \,. \tag{4.12}$$

The subscript $sources = 0$ reminds of the fact that according to the standard description, the right hand side of (4.12), which comes from a functional derivative of the on-shell action, must be evaluated with all sources, i.e. independent boundary values, set equal to zero. To account for this, $\tau_0(\partial_t)$ must be evaluated at the point where the explicit

dependence on the source $F^e$ is set equal to zero. Formulated quantitatively, this means that the term $-\int_{\partial M_\varepsilon}\left(A+\frac{L}{(2-z)}\mathfrak{L}_{e_3}A\right)\wedge\star F^e$ in (3.6) will not contribute to the internal energy. This is also sensible, as this term would give a contribution coming from having a nonzero chemical potential in the system, whereas the internal energy by definition should just account for the mass of the black brane that causes the curvature of spacetime. The result is

$$2\kappa L^3\mathfrak{e}=\begin{cases}-\frac{4(z-2)\sqrt{z-1}\mathcal{M}}{z} & z\neq 2\,,\\ -2\mathcal{M} & z=2\,.\end{cases} \tag{4.13}$$

Now (4.9), (4.11) and (4.13) can be combined to

$$\mathfrak{a}=\mathfrak{e}-\mathfrak{s}T\,, \tag{4.14}$$

which is indeed the correct expression for the density of the Helmholtz free energy. Furthermore, from the above calculations an equation of state can be derived,

$$\frac{z+2}{2}\mathfrak{e}=\begin{cases}\mathfrak{s}T-\mathfrak{m}\mathfrak{b}+\mu\mathfrak{q} & z\neq 2\,,\\ \mathfrak{s}T-\mathfrak{m}\mathfrak{b}+\mu\mathfrak{q}+\frac{L}{8\kappa}\mathfrak{b}^2+\frac{\kappa L}{2}\mathfrak{q}^2 & z=2\,.\end{cases} \tag{4.15}$$

The first line is in accord with the findings in [13] and [12]. The appearance of $\mathfrak{b}^2$ and $\mathfrak{q}^2$ in the equation of state for $z=2$ is an artifact of an ambiguity in defining a counterterm for this particular value of the dynamical critical exponent. The approach presented in section 3 was a minimal one, i.e. just taking the counterterms which are required to cancel all divergences. This results in the coefficients in (4.15). As a matter of fact, for $z=2$ it would be possible to add the terms $2\int_{\partial M}\mathfrak{L}_{e_3}A\wedge\star F^e-\int_{\partial M}\mathfrak{L}_{e_3}A\wedge\star\mathfrak{L}_{e_3}A$ and $\int_{\partial M}F^m\wedge\star F^m$ with arbitrary coefficients to the action. This would leave (4.14) unchanged, but would alter the coefficients of $\mathfrak{b}^2$ and $\mathfrak{q}^2$ in (4.15). In particular, it would be possible to cancel these coefficients, making the second line of (4.15) identical to the first. It is unclear, what argument should be used to single out this choice and fix the ambiguity.

### 4.2 The differential of the Helmholtz free energy

In thermodynamics, $\mathfrak{a}$ satisfies

$$d\mathfrak{a}=-\mathfrak{s}\,dT-\mathfrak{m}\,d\mathfrak{b}+\mu\,d\mathfrak{q}\,. \tag{4.16}$$

This corresponds to the three relations

$$\left.\frac{\partial\mathfrak{a}}{\partial T}\right|_{\mathfrak{b},\mathfrak{q}}=-\mathfrak{s}\,, \tag{4.17}$$

$$\left.\frac{\partial\mathfrak{a}}{\partial\mathfrak{b}}\right|_{T,\mathfrak{q}}=-\mathfrak{m}\,, \tag{4.18}$$

$$\left.\frac{\partial\mathfrak{a}}{\partial\mathfrak{q}}\right|_{T,\mathfrak{b}}=\mu\,. \tag{4.19}$$

These can easily be verified for dyonic AdS black branes in the case of $z=1$, where an exact solution is known. What will be shown in the following is that they also hold for $z>1$.

First of all, (4.19) is a direct consequence of (3.12) when taking the limit $r \to 0$. From this, (4.16) will follow if it can be shown that any of the relations (4.17)-(4.19) implies the other two. To proceed with the proof of this, it is useful to note that in the equations of motion (2.21)-(2.25) as well as (4.11), the values of $B_0$ and $\rho_0$ only occur in the combination

$$\eta = B_0^2 + \rho_0^2 \,. \tag{4.20}$$

Furthermore, as the dependence of $r_0$ just enters in the form of a rescaling of the final expression, all so far introduced thermodynamic quantities must be of the form $\frac{\Omega(\eta)}{r_0^s}$ with $s$ being some scaling exponent and $\Omega$ a function of a single variable.[7] Therefore, let the functions $\mathcal{F}$ and $\mathcal{G}$ be defined via

$$T = \frac{\mathcal{F}(\eta)}{4\pi L r_0^z} \,, \tag{4.21}$$

$$\frac{1}{2\kappa}\frac{\mu}{\mathfrak{q}} = -2\kappa\frac{\mathfrak{m}}{\mathfrak{b}} = \frac{L\mathcal{G}(\eta)}{r_0^{z-2}} \,. \tag{4.22}$$

Imposing the conditions $r_0 = 1$ and $\Xi_1 = 0$ on the ODE system (2.21)-(2.25) results in a one-parameter family of solutions, the parameter being $\eta$. Hence, $\mathcal{F}$ and $\mathcal{G}$ are not independent and must satisfy a non-trivial relation. This relation turns out to be

$$4\mathcal{F}' - (z-2)\mathcal{G} + 4\eta\mathcal{G}' = 0 \,. \tag{4.23}$$

The validity of this will follow as a corollary to what will be proved in the following, namely that (4.23) is equivalent to each of (4.17)-(4.19).

First of all, the differentials of $T$, $\mathfrak{b}$ and $\mathfrak{q}$ are

$$dT = -\frac{z\mathcal{F}}{4\pi L r_0^{z+1}} dr_0 + \frac{2\mathcal{F}'}{4\pi L r_0^z}(B_0\, dB_0 + \rho_0\, d\rho_0) \,, \tag{4.24}$$

$$d\mathfrak{b} = -\frac{2B_0}{L^2 r_0^3} dr_0 + \frac{1}{L^2 r_0^2} dB_0 \,, \tag{4.25}$$

$$d\mathfrak{q} = -\frac{\rho_0}{\kappa L^2 r_0^3} dr_0 + \frac{1}{2\kappa L^2 r_0^2} d\rho_0 \,. \tag{4.26}$$

From this, at constant $\mathfrak{b}$ and $\mathfrak{q}$,

$$dT\Big|_{\mathfrak{b},\mathfrak{q}} = \frac{1}{4\pi L r_0^{z+1}} \left(-z\mathcal{F} + 4\eta\mathcal{F}'\right) dr_0 \,, \tag{4.27}$$

$$d(\mathfrak{s}T)\Big|_{\mathfrak{b},\mathfrak{q}} = \frac{1}{2\kappa L^3 r_0^{z+3}} \left[-(z+2)\mathcal{F} + 4\eta\mathcal{F}'\right] dr_0 \,, \tag{4.28}$$

$$d\left(\frac{\mu}{\mathfrak{q}}\right)\Big|_{\mathfrak{b},\mathfrak{q}} = \frac{2\kappa L}{r_0^{z-1}} \left[-(z-2)\mathcal{G} + 4\eta\mathcal{G}'\right] dr_0 \,. \tag{4.29}$$

[7] Of course, $\mathfrak{q}$, $\mu$, $\mathfrak{b}$ and $\mathfrak{m}$ are not exactly of this form, they however differ only by a factor of $\mathfrak{q}$ or $\mathfrak{b}$ respectively.

Therefore,

$$\begin{aligned}
\left.\frac{\partial \mathfrak{a}}{\partial T}\right|_{\mathfrak{b},\mathfrak{q}} &= \frac{\partial}{\partial T}\left[-\frac{z}{z+2}T\mathfrak{s} + \frac{2}{z+2}\frac{\mathfrak{b}^2+4\kappa^2\mathfrak{q}^2}{4\kappa^2}\frac{\mu}{\mathfrak{q}}\right]\Bigg|_{\mathfrak{b},\mathfrak{q}} \\
&= -\frac{2\pi}{\kappa L^2 r_0^2\,(z\mathcal{F}-4\eta\mathcal{F}')}\left[z\mathcal{F} - \frac{4z}{z+2}\eta\mathcal{F}' - \frac{2(z-2)}{z+2}\eta\mathcal{G} + \frac{8}{z+2}\eta^2\mathcal{G}'\right] \\
&= -\frac{2\pi}{\kappa L^2 r_0^2} - \frac{4\pi\eta[4\mathcal{F}'-(z-2)\mathcal{G}+4\eta\mathcal{G}']}{(z+2)\kappa L^2 r_0^2\,(z\mathcal{F}-4\eta\mathcal{F}')} \\
&= -\mathfrak{s}\,. \qquad (4.30)
\end{aligned}$$

The last equality follows from (4.23). This establishes the equivalence of (4.23) and (4.17).

In an analogous way for constant $T$ and $\mathfrak{q}$,

$$\left.d\mathfrak{b}\right|_{T,\mathfrak{q}} = \frac{1}{2L^2 B_0 r_0^3 \mathcal{F}'}\left(z\mathcal{F}-4\eta\mathcal{F}'\right)\,dr_0\,, \qquad (4.31)$$

$$\left.d\mathfrak{s}\right|_{T,\mathfrak{q}} = -\frac{4\pi}{\kappa L^2 r_0^3}\,dr_0\,, \qquad (4.32)$$

$$\begin{aligned}
\left.d\left(\frac{\mu}{\mathfrak{q}}\right)\right|_{T,\mathfrak{q}} &= \frac{2\kappa L}{r_0^{z-1}\mathcal{F}'}\left[-(z-2)\mathcal{F}'\mathcal{G}+z\mathcal{F}\mathcal{G}'\right]\,dr_0 \\
&= \frac{\kappa L}{2r_0^{z-1}\eta\mathcal{F}'}\left[(z-2)(z\mathcal{F}-4\eta\mathcal{F}')\mathcal{G}-4z\mathcal{F}\mathcal{F}'\right]\,dr_0\,. \qquad (4.33)
\end{aligned}$$

In the last line, (4.23) was inserted. With this,

$$\begin{aligned}
\left.\frac{\partial \mathfrak{a}}{\partial \mathfrak{b}}\right|_{T,\mathfrak{q}} &= \frac{\partial}{\partial \mathfrak{b}}\left[-\frac{z}{z+2}T\mathfrak{s} + \frac{2}{z+2}\frac{\mathfrak{b}^2+4\kappa^2\mathfrak{q}^2}{4\kappa^2}\frac{\mu}{\mathfrak{q}}\right]\Bigg|_{T,\mathfrak{q}} \\
&= -\frac{z}{z+2}T\left.\frac{\partial \mathfrak{s}}{\partial \mathfrak{b}}\right|_{T,\mathfrak{q}} + \frac{1}{z+2}\frac{\mathfrak{b}\mu}{\kappa^2\mathfrak{q}} + \frac{2}{z+2}\frac{\mathfrak{b}^2+4\kappa^2\mathfrak{q}^2}{4\kappa^2}\frac{\mu}{\mathfrak{q}}\left.\frac{\partial}{\partial \mathfrak{b}}\left(\frac{\mu}{\mathfrak{q}}\right)\right|_{T,\mathfrak{q}} \\
&= \frac{1}{z+2}\frac{\mathfrak{b}\mu}{\kappa^2\mathfrak{q}} + \frac{z-2}{z+2}\frac{LB_0(\mathfrak{b}^2+4\kappa^2\mathfrak{q}^2)}{4\kappa r_0^{z-4}\eta}\mathcal{G} \\
&\quad + \frac{B_0 r_0^3}{L\kappa\,(z\mathcal{F}-4\eta\mathcal{F}')}\left[\frac{2z}{z+2}\frac{\mathcal{F}\mathcal{F}'}{r_0^{z+3}} - \frac{2z}{z+2}\frac{L^4(\mathfrak{b}^2+4\kappa^2\mathfrak{q}^2)\mathcal{F}\mathcal{F}'}{r_0^{z-1}\eta}\right] \\
&= \frac{\mathfrak{b}\mu}{4\kappa^2\mathfrak{q}} \\
&= -\mathfrak{m}\,. \qquad (4.34)
\end{aligned}$$

Again, as the equality holds if and only if (4.23) is assumed, the equivalence of that assumption to (4.18) is proved. Due to the symmetric appearance of $\mathfrak{b}$ and $\mathfrak{q}$, this must also be true for (4.19). As the validity of (4.19) has already been established, this concludes the proof of (4.16).

Unfortunately, the thermodynamic relations found so far are not sufficient to determine an explicit expression for $\mathcal{F}$ or $\mathcal{G}$. A few exact solutions are known (see appendix B), but in general numerical methods are needed to study these functions.

### 4.3 Susceptibility and magnetization

It is also possible to derive an expression for the density of the magnetic susceptibility,

$$\begin{aligned}\chi &= \left.\frac{\partial \mathfrak{m}}{\partial \mathfrak{b}}\right|_{T,\mathfrak{q}} \\ &= \frac{\mathfrak{m}}{\mathfrak{b}} + \mathfrak{b}\frac{\partial}{\partial \mathfrak{b}}\left(\frac{\mathfrak{m}}{\mathfrak{b}}\right)\Big|_{T,\mathfrak{q}} \\ &= \frac{\mathfrak{m}}{\mathfrak{b}} - \mathfrak{b}\frac{L^3 B_0}{4\kappa r_0^{z-4}\eta}\left[(z-2)\mathcal{G} - \frac{4z\mathcal{F}\mathcal{F}'}{z\mathcal{F}-4\eta\mathcal{F}'}\right] \\ &= \frac{1}{2(\mathfrak{b}^2+4\kappa^2\mathfrak{q}^2)}\left[(z\mathfrak{b}^2+8\kappa^2\mathfrak{q}^2)\frac{\mathfrak{m}}{\mathfrak{b}} - \frac{zL\mathfrak{b}^2\mathcal{F}}{4\kappa r_0^{z-2}\eta} + \frac{z^2 L\mathfrak{b}^2\mathcal{F}^2}{4\kappa r_0^{z-2}\eta(z\mathcal{F}-4\eta\mathcal{F}')}\right] . \end{aligned} \tag{4.35}$$

Using the specific heat at constant volume,

$$\frac{c_{\mathcal{V}}}{T} = \left.\frac{\partial \mathfrak{s}}{\partial T}\right|_{\mathfrak{b},\mathfrak{q}} = \frac{16\pi^2}{\kappa L r_0^{2-z}\,(z\mathcal{F}-4\eta\mathcal{F}')} , \tag{4.36}$$

as well as (4.8) and (4.21), (4.35) could also be written as

$$\chi = \frac{(z\mathfrak{b}^2+8\kappa^2\mathfrak{q}^2)}{2(\mathfrak{b}^2+4\kappa^2\mathfrak{q}^2)}\frac{\mathfrak{m}}{\mathfrak{b}} - \frac{zT\mathfrak{b}^2(2\mathfrak{s}-zc_{\mathcal{V}}T)}{4(\mathfrak{b}^2+4\kappa^2\mathfrak{q}^2)^2} . \tag{4.37}$$

As a consequence, in the limit of vanishing temperature, assuming $\mathfrak{s}$ and $c_{\mathcal{V}}T$ do not diverge in this limit[8],

$$\chi\Big|_{T=0} = \frac{(z\mathfrak{b}^2+8\kappa^2\mathfrak{q}^2)}{2(\mathfrak{b}^2+4\kappa^2\mathfrak{q}^2)}\frac{\mathfrak{m}}{\mathfrak{b}} , \tag{4.38}$$

and for vanishing magnetic field,

$$\chi\Big|_{\mathfrak{b}=0} = \lim_{\mathfrak{b}\to 0}\frac{\mathfrak{m}}{\mathfrak{b}} = -\frac{1}{4\kappa^2}\frac{\mu}{\mathfrak{q}} . \tag{4.39}$$

For $z = 1$ this identity can easily be checked for dyonic AdS black branes. That it also holds for $z > 1$ based on (4.16) is an intriguing result.

As was noted in [12], for $1 \leq z < 2$, the value of $\nu$ from appendix A can be expressed as

$$\nu = \int_0^1 r^{z-1} f dr . \tag{4.40}$$

Thus, because $f > 0$ outside the horizon, from (4.5) follows that $\mathfrak{m}$ has the opposite sign to $\mathfrak{b}$. As this also implies that $\chi$ will be negative, at least in the limits of low temperature and magnetic field strength, this means that the system exhibits diamagnetic behavior. In contrast, for $2 \leq z < 6$, an expression for $\nu$ is given by

$$\nu = \int_0^1 r^{z-1}(f-1)dr - \begin{cases} 0 & z = 2 , \\ \frac{1}{z-2} & 2 < z < 6 . \end{cases} \tag{4.41}$$

Here it is potentially possible to have a setup with $\mathfrak{m}$ and $\mathfrak{b}$ having the same sign and $\chi$ positive and thus modeling a paramagnetic material. In fact, the known exact solution for $z = 4$ (see appendix B.2) is such a case.

[8] Numerical investigations in [14] suggest that they remain finite.

### 4.4 Numerical results

Though the main results of this paper are derived analytically, it is instructive to also have a numerical check of certain equalities. As the qualitative features seemed to be rather indifferent to the particular value of $z$, numerical results are just presented for one value, $z = \frac{3}{2}$.

The information about thermodynamic quantities is encoded in the functions $\mathcal{F}$ and $\mathcal{G}$ (4.21) and (4.22). A plot of these functions can be seen in figure 1. The function $\mathcal{F}$

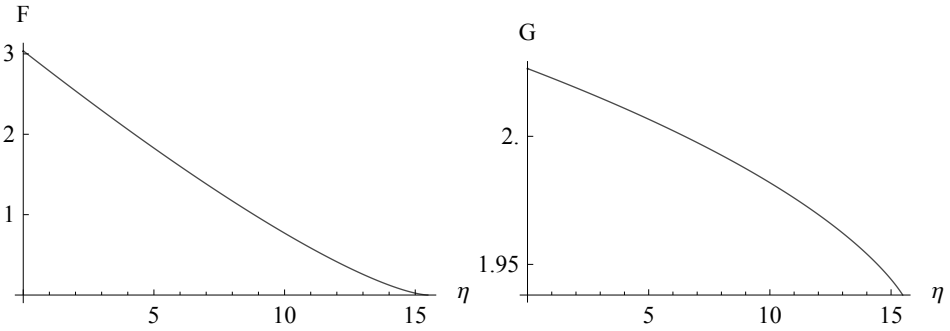


**Figure 1**. Plot of the functions $\mathcal{F}(\eta)$ (left) and $\mathcal{G}(\eta)$ (right). $\mathcal{F}$ vanishes for $\eta = \frac{31}{2}$, indicating that the black brane becomes extremal for this value.

can be seen to vanish sublinearly at the critical value $\eta = -4\Lambda = \frac{31}{2}$. As this happens at a finite value of $r_0$, this means that the black brane becomes extremal. A more detailed numerical investigation of the behavior of the system when approaching criticality can be found in [10].

The aim now is to check (4.23). To do this, define the functional

$$\tilde{\mathcal{F}} = \mathcal{F}_0 - \eta\mathcal{G} + \frac{z+2}{4}\int_0^\eta \mathcal{G}\ , \tag{4.42}$$

which is the general solution of (4.23) for given $\mathcal{G}$, and fix $\mathcal{F}_0$ such that $\tilde{\mathcal{F}}$ and $\mathcal{F}$ coincide at some value of $\eta$. Then (4.42) can be compared with the numerical value of $\mathcal{F}$ at other values of $\eta$. The relative error

$$\Delta_{rel}\mathcal{F} = 2\left|\frac{\mathcal{F}-\tilde{\mathcal{F}}}{\mathcal{F}+\tilde{\mathcal{F}}}\right| \tag{4.43}$$

is plotted in figure 2. For a better comparison with later plots, $\eta$ has been translated back into a value of temperature, normalized by the temperature at $\mathfrak{q} = \frac{1}{2\kappa}$. For temperatures of $O(1)$ and higher, the deviation can be seen to be lower than ten significant digits. When the temperature is lowered, the deviation increases. This can be attributed on the one hand to numerical values of $\mathcal{F}$ and $\mathcal{G}$ having lower precision at low temperatures and on the other hand to the accumulation of numerical errors when integrating (4.42).

As (4.23) was shown to be equivalent to (4.16), the above results give a good indication that the latter is indeed satisfied. It is however also be possible to make a more direct check.

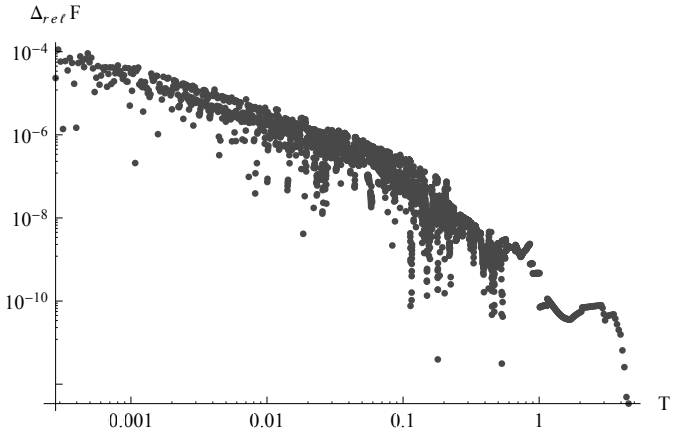


**Figure 2**. The relative error $\Delta_{rel}\mathcal{F}$ versus temperature normalized with the value at $\mathfrak{q} = \frac{1}{2\kappa}$. The loss of precision for lower temperatures is due to the numerical function values become less precise in that region and due to an accumulation of numerical errors from the integration.

For this purpose, the relative error

$$\Delta_{rel}\mathfrak{s} = 2\left|\frac{\frac{\partial \mathfrak{a}}{\partial T}\big|_{\mathfrak{b},\mathfrak{q}} + \mathfrak{s}}{\frac{\partial \mathfrak{a}}{\partial T}\big|_{\mathfrak{b},\mathfrak{q}} - \mathfrak{s}}\right| \tag{4.44}$$

is plotted in figure 3. Results here are less precise than for (4.43). This is mainly due

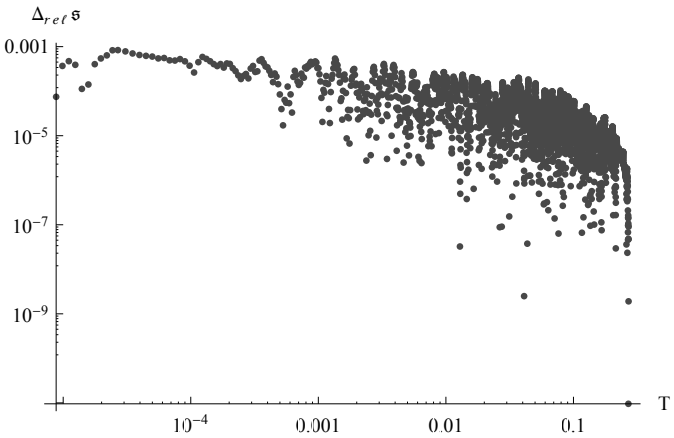


**Figure 3**. The relative error $\Delta\mathfrak{s}$ versus normalized temperature. The increase for lower values of temperature is due to the lower precision of the numerical data in that region.

to the fact that a numerical estimate of a derivative is in general more susceptible to the

precision of the input data than the estimate of an integral. Nevertheless, the numerics show an agreement to at least three significant digits – and even better agreement for higher temperatures, where the precision is better.

This section concludes with a numerical check of (4.39), which also was a consequence of (4.23). This identity allows to compare a second derivative of $\mathfrak{a}$ with quantities that can be read off from the asymptotics. Figure 4 shows the relative error

$$\Delta_{rel}\chi = 2\left|\frac{\frac{\partial^2\mathfrak{a}}{\partial\mathfrak{b}^2}\Big|_{T,\mathfrak{q}} - \frac{1}{4\kappa^2}\frac{\mu}{\mathfrak{q}}}{\frac{\partial^2\mathfrak{a}}{\partial\mathfrak{b}^2}\Big|_{T,\mathfrak{q}} + \frac{1}{4\kappa^2}\frac{\mu}{\mathfrak{q}}}\right| \tag{4.45}$$

at vanishing magnetic field. Also here an agreement of about three significant digits or

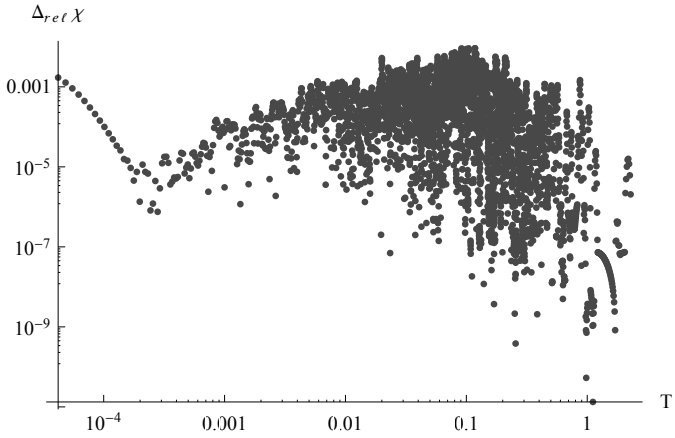


**Figure 4**. The relative error $\Delta_{rel}\chi$ versus normalized temperature for $\mathfrak{b} = 0$. As in the other plots, the error has a tendency to increase with lower values of $T$ due to precision issues in that region.

better can be seen.

The results presented here were as far as it was possible to go using numerics with reasonable computation time. The general trend was that the deviations presented above decreased when the precision was increased. It stands to reason that computations done with an even higher number of significant digits would further improve the numerical results.

## 5 Conclusions

In this paper, several results on of dyonic Lifshitz black branes were established.

Though the renormalization of the action presented in this paper is still work in progress, preliminary results for black branes with $d = 2$ and $z < 6$ can be obtained. The task of deriving an expression for general values of $d$, higher values of $z$ and even a

curved horizon seems straightforward, however, an implementation is expected to become more complicated when expansions up to higher order need to be taken into account.

A further result would be the evidence that this renormalization procedure gives expressions for the Helmholtz free energy and internal energy that are in agreement with standard thermodynamic relations. This bolsters the case for dyonic Lifshitz black branes as candidates for a holographic description of phenomena involving magnetism in quantum critical systems with a non-trivial dynamical exponent.

Finally, the magnetization and susceptibility of the dual theories were worked out using the gravitational description. For $1 \leq z < 2$, the low temperature limit is always diamagnetic, whereas paramagnetism can occur for $2 \leq z < 6$. The only known exact solution for $z = 4$ happens to be of the paramagnetic type, but it remains an open question whether paramagnetism is the rule in this region of parameter space.

## Acknowledgments

I would like to thank Lárus Thorlacius and Paata Kakashvili for interesting discussions and remarks during the process of writing this paper. This work was supported by the Icelandic Research Fund, the University of Iceland Research Fund and the Eimskip Research Fund at the University of Iceland.

## A Asymptotic Expansions

An expansion for generic $z$ for asymptotically Lifshitz solutions of (2.21)-(2.25) is as follows,

$$\begin{aligned} f = f_\infty\Bigg\{1 &- \frac{2\sqrt{z-1}(z_1-2)\Xi_1}{z(-2+2z+z_1)}r^{z_1} - \frac{\sqrt{z-1}(z_2-2)\Xi_2}{z(-2+2z+z_2)}r^{z_2} \\ &- \left[\frac{4\sqrt{z-1}\mathcal{M}}{2+z} + \frac{4\left(z^2-2z+2\right)\Xi_1\Xi_2}{z\left(z^2+3z+2\right)}\right]r^{2+z} \\ &- \frac{(z-1)(z-4)(\mathcal{B}^2+\mathcal{Q}^2)}{8(z-2)^2(z+1)}r^4 + \dots\Bigg\}\,, \end{aligned} \tag{A.1}$$

$$\begin{aligned} g = 1 &+ \frac{\sqrt{z-1}z_1\Xi_1}{z(-2+2z+z_1)}r^{z_1} + \frac{\sqrt{z-1}z_2\Xi_2}{z(-2+2z+z_2)}r^{z_2} \\ &+ \left[\sqrt{z-1}\mathcal{M} + \frac{\left(2z^3-5z^2+3z-2\right)\Xi_1\Xi_2}{2z^2(z+1)}\right]r^{2+z} \\ &- \frac{(2z-3)\left(\mathcal{B}^2+\mathcal{Q}^2\right)}{4(z-2)^2(z+1)}r^4 + \dots\,, \end{aligned} \tag{A.2}$$

$$\begin{aligned} a = \sqrt{z-1} &+ \frac{z_1(z_1-2)\Xi_1}{z(-2+2z+z_1)}r^{z_1} + \frac{z_2(z_2-2)\Xi_2}{z(-2+2z+z_2)}r^{z_2} \\ &+ \frac{(z-4)\sqrt{z-1}\left(\mathcal{B}^2+\mathcal{Q}^2\right)}{4(z-2)^2(z+1)}r^4 + 2\mathcal{M}r^{2+z} + \dots\,, \end{aligned} \tag{A.3}$$

$$\begin{aligned} b = \sqrt{z-1} &- \frac{2r^{z_1}z_1\Xi_1}{z(-2+2z+z_1)} - \frac{2r^{z_2}z_2\Xi_2}{z(-2+2z+z_2)} \\ &- \frac{(z-4)\sqrt{z-1}\left(\mathcal{B}^2+\mathcal{Q}^2\right)}{4(z-2)^2(z+1)}r^4 - \frac{4\mathcal{M}}{z}r^{2+z} + \dots\,, \end{aligned} \tag{A.4}$$

$$\phi = \mathcal{Q}\left[-r^z\nu + \frac{1}{2-z}r^2 + \dots\right]\,. \tag{A.5}$$

where $\dots$ indicate descendants of the previous listed modes. The Exponents $z_1$ and $z_2$ are given by

$$z_1 = \frac{1}{2}\left[z+2-\sqrt{(2+z)^2+8(z-1)(z-2)}\right]\,, \tag{A.6}$$

$$z_2 = \frac{1}{2}\left[z+2+\sqrt{(2+z)^2+8(z-1)(z-2)}\right]\,. \tag{A.7}$$

For $z > 2$, the exponent $z_1 > 0$ and thus, in order to be renormalizable, the solution must have $\Xi_1 = 0$. For the marginal case $z = 2$ with $z_1 = 0$ and $z_2 = 4$, there are logarithmic modes occurring. After discarding a growing mode, the expansions (A.1)-(A.5) are modified

to

$$f = f_\infty\Bigg\{1 + r^4\Bigg[\frac{32\mathcal{M} - 32\,\Xi_2 - \mathcal{B}^2 - \mathcal{Q}^2}{96} + \frac{8\mathcal{M} + \mathcal{B}^2 + \mathcal{Q}^2}{16}\ln r + \frac{\mathcal{B}^2 + \mathcal{Q}^2}{16}(\ln r)^2\Bigg] + \dots\Bigg\}\,, \tag{A.8}$$

$$g = 1 + r^4\Bigg[\frac{28\mathcal{M} + 32\,\Xi_2 + \mathcal{B}^2 + \mathcal{Q}^2}{96} + \frac{-16\mathcal{M} + 3(\mathcal{B}^2 + \mathcal{Q}^2)}{32}\ln r - \frac{\mathcal{B}^2 + \mathcal{Q}^2}{16}(\ln r)^2\Bigg] + \dots\,, \tag{A.9}$$

$$a = 1 + r^4\Bigg[-\frac{88\mathcal{M} - 64\,\Xi_2 + \mathcal{B}^2 + \mathcal{Q}^2}{96} - \frac{16\mathcal{M} + 3(\mathcal{B}^2 + \mathcal{Q}^2)}{16}\ln r - \frac{\mathcal{B}^2 + \mathcal{Q}^2}{8}(\ln r)^2\Bigg] + \dots\,, \tag{A.10}$$

$$b = 1 + r^4\Bigg[\frac{20\mathcal{M} - 32\,\Xi_2 - \mathcal{B}^2 - \mathcal{Q}^2}{48} + \frac{16\mathcal{M} + \mathcal{B}^2 + \mathcal{Q}^2}{16}\ln r + \frac{\mathcal{B}^2 + \mathcal{Q}^2}{8}(\ln r)^2\Bigg] + \dots\,, \tag{A.11}$$

$$\phi = \mathcal{Q}\left[r^2(-\nu + \ln r\,) + \dots\right]\,. \tag{A.12}$$

## B Exact solutions

### B.1 z=1 : dyonic AdS black holes

The solution of a dyonic black brane with a horizon at $r = 1$ is given by

$$f = 1, \quad g^2 = 1 - \left(1 + \frac{\rho_0^2 + B_0^2}{4}\right) r^3 + \frac{\rho_0^2 + B_0^2}{4} r^4, \quad a = b = 0, \quad \phi = \frac{\rho_0}{g^2}\left(-r + r^2\right)\,. \tag{B.1}$$

From this follow the thermodynamic quantities

$$\begin{aligned}
&\mathfrak{q} = \frac{\rho_0}{2\kappa L^2 r_0^2}\,, \quad \mu = \frac{\rho_0}{L r_0}\,, \quad \mathfrak{b} = \frac{B_0}{L^2 r_0^2}\,, \quad \mathfrak{m} = -\frac{B_0}{2\kappa L r_0}\,,\\
&T = \frac{12 - \rho_0^2 - B_0^2}{16\pi L r_0}\,, \quad \mathfrak{s} = \frac{2\pi}{\kappa L^2 r_0^2}\,, \quad \mathfrak{e} = \frac{4 + \rho_0^2 + B_0^2}{2\kappa L^3 r_0^3}\,,\\
&\mathfrak{a} = \frac{-4 + 3\rho_0^2 + 3B_0^2}{8\kappa L^3 r_0^3}\,, \quad \frac{c_\mathcal{V}}{T} = \frac{64\pi^2}{3\kappa L r_0\left(4 + \rho_0^2 + B_0^2\right)}\,,\\
&\chi = -\frac{L r_0\left(12 + 3\rho_0^2 + B_0^2\right)}{6\kappa\left(4 + \rho_0^2 + B_0^2\right)}\,.
\end{aligned} \tag{B.2}$$

### B.2 z=4

For $z = 4$, there is the special solution[9]

$$f = 1, \quad g^2 = 1 - r^4, \quad a = b = \sqrt{3}, \quad \Phi = -\frac{\rho_0 r^2}{2\,(r^2+1)}, \tag{B.3}$$

which solves (2.21)-(2.25) provided $\eta = B_0^2 + \rho_0^2 = 8$. As it is just an isolated solution at a single value of $\eta$, the thermodynamic quantities that involve differentiation can not be calculated. The ones obtainable are

$$\begin{aligned} \mathfrak{q} &= \frac{\rho_0}{2\kappa L^2 r_0^2}\,, \quad \mu = -\frac{\rho_0}{2L r_0^4}\,, \quad \mathfrak{b} = \frac{B_0}{L^2 r_0^2}\,, \quad \mathfrak{m} = \frac{B_0}{4\kappa L^2 r_0^4}\,, \\ T &= \frac{1}{\pi L r_0^4}\,, \quad \mathfrak{s} = \frac{2\pi}{\kappa L^2 r_0^2}\,, \quad \mathfrak{e} = 0\,, \quad \mathfrak{a} = -\frac{2}{\kappa L^3 r_0^6}\,. \end{aligned} \tag{B.4}$$

It might be worth noting that in this solution $\mathfrak{q}$ and $\mu$ have opposite sign and the internal energy $\mathfrak{e}$ is vanishing. It stands to reason that these features would be generic when generalizing this solution to $z = 2d$ along the lines of [20]. That the expression for the thermodynamical mass for the solutions presented there is nonzero is not a contradiction to the results here, as the calculation in [20] seems to have been done in a thermodynamic ensemble which does neither correspond the grand canonical nor the canonical one.

[9] This basically is the solution presented in [10], rotated on the $B_0\rho_0$ plane.

## References


[1] J. M. Maldacena, *The large N limit of superconformal field theories and supergravity*, *Adv. Theor. Math. Phys.* **2** (1998) 231–252, [hep-th/9711200].

[2] S. Kachru, X. Liu, and M. Mulligan, *Gravity Duals of Lifshitz-like Fixed Points*, *Phys. Rev.* **D78** (2008) 106005, [arXiv:0808.1725].

[3] P. Coleman and A. J. Schofield, *Quantum criticality*, *NATURE* **433** (Jan., 2005) 226–229, [cond-mat/0503002].

[4] S. A. Hartnoll, *Lectures on holographic methods for condensed matter physics*, *Class. Quant. Grav.* **26** (2009) 224002, [arXiv:0903.3246].

[5] J. McGreevy, *Holographic duality with a view toward many-body physics*, *Adv. High Energy Phys.* **2010** (2010) 723105, [arXiv:0909.0518].

[6] S. Sachdev, *Condensed matter and AdS/CFT*, arXiv:1002.2947.

[7] S. A. Hartnoll and P. Kovtun, *Hall conductivity from dyonic black holes*, *Phys. Rev.* **D76** (2007) 066001, [arXiv:0704.1160].

[8] M. Taylor, *Non-relativistic holography*, arXiv:0812.0530.

[9] G. Bertoldi, B. A. Burrington, and A. Peet, *Black Holes in asymptotically Lifshitz spacetimes with arbitrary critical exponent*, *Phys. Rev.* **D80** (2009) 126003, [arXiv:0905.3183].

[10] E. J. Brynjolfsson, U. H. Danielsson, L. Thorlacius, and T. Zingg, *Holographic Superconductors with Lifshitz Scaling*, *J. Phys.* **A43** (2010) 065401, [arXiv:0908.2611].

[11] S. F. Ross and O. Saremi, *Holographic stress tensor for non-relativistic theories*, *JHEP* **09** (2009) 009, [arXiv:0907.1846].

[12] M. H. Dehghani, R. B. Mann, and R. Pourhasan, *Charged Lifshitz Black Holes*, arXiv:1102.0578.

[13] G. Bertoldi, B. A. Burrington, and A. W. Peet, *Thermodynamics of black branes in asymptotically Lifshitz spacetimes*, *Phys. Rev.* **D80** (2009) 126004, [arXiv:0907.4755].

[14] E. J. Brynjolfsson, U. H. Danielsson, L. Thorlacius, and T. Zingg, *Black Hole Thermodynamics and Heavy Fermion Metals*, *JHEP* **08** (2010) 027, [arXiv:1003.5361].

[15] E. J. Brynjolfsson, U. H. Danielsson, L. Thorlacius, and T. Zingg, *Holographic models with anisotropic scaling*, arXiv:1004.5566.

[16] V. Balasubramanian and P. Kraus, *A stress tensor for anti-de Sitter gravity*, *Commun. Math. Phys.* **208** (1999) 413–428, [hep-th/9902121].

[17] S. A. Hartnoll, J. Polchinski, E. Silverstein, and D. Tong, *Towards strange metallic holography*, *JHEP* **04** (2010) 120, [arXiv:0912.1061].

[18] C. Fefferman and C. Robin Graham, *Conformal Invariants*, in *Elie Cartan et les mathématiques d'aujourd'hui*, Astérisque, pp. 95–116, Société Mathématique de France, Paris, June, 1985. hors série.

[19] T. Zingg, *in preparation*, .

[20] D.-W. Pang, *On Charged Lifshitz Black Holes*, *JHEP* **01** (2010) 116, [arXiv:0911.2777].